

Miguel Ângelo Canas Portela Costa

COMPUTATIONAL STUDIES FOR THE DISCOVERY OF NOVEL INHIBITORS OF METALLO-BETA-LACTAMASES AS THERAPEUTIC TARGETS FOR ANTIBIOTIC RESISTANCE

Tese de Mestrado em Design e Desenvolvimento de Fármacos, orientada pela
Prof. Doutora Maria Manuel da Cruz Silva e pela Prof. Doutora Gabriela Conceição Duarte Jorge da Silva

Janeiro de 2017



UNIVERSIDADE DE COIMBRA

Faculdade de Farmácia

Miguel Ângelo Canas Portela Costa

**COMPUTATIONAL STUDIES FOR THE DISCOVERY OF NOVEL INHIBITORS
OF METALLO-BETA-LACTAMASES AS THERAPEUTIC TARGETS
FOR ANTIBIOTIC RESISTANCE**

Tese de Mestrado em Design e Desenvolvimento de Fármacos, orientada pela
Prof. Doutora Maria Manuel da Cruz Silva e pela Prof. Doutora Gabriela Conceição Duarte Jorge da Silva

Janeiro de 2017



UNIVERSIDADE DE COIMBRA

Agradecimentos

Às minhas orientadoras, a Prof. Doutora Maria Manuel Silva e a Prof. Doutora Gabriela Jorge da Silva por toda a ajuda prestada e por colocarem ao meu alcance todos os meios necessários para poder aceitar este desafio e, com elas, desenvolver este tema.

À coordenadora do curso de mestrado, a Professora Doutora Maria Luisa Sá e Melo pela oportunidade de desenvolver este trabalho e pela disponibilização de todos os meios necessários para o fazer.

À Salete Batista, por tudo o que pacientemente me ensinou e pelas tarefas que se disponibilizou para realizar por mim em Milão, tendo para isso abdicado de tempo precioso para o seu próprio trabalho.

Aos meus pais, Miguel e Noémia, e às minhas irmãs, Mafalda e Mariana, por sempre me apoiarem e encorajarem a perseguir os meus objectivos.

À Joana, por ser sempre a minha fonte de inspiração e força. Por acreditar sempre, e incondicionalmente, em mim. Por me mostrar, todos os dias, que devemos sempre seguir os nossos sonhos. Por tornar tudo possível.

Abstract

Hydrolysis by β -lactamases (BL) is one of the major mechanisms that drive resistance to β -lactam antibiotics. The major strategy to overcome their activity is the use of inhibitors that have little to none antibiotic activity, but bind with greater affinity to BLs, allowing an effective antibiotic therapy. The metallo-BL (MBL), are a structurally distinct BL class that hydrolyse almost all classes of β -lactams and are not inhibited by any marketed inhibitor. They are increasingly produced by clinical bacteria and their prevalence will keep growing as some types of MBL are encoded in mobile genetic elements. It is thus, evident, the need for solutions that allow β -lactam antibiotics to keep their effectiveness.

The study of inhibitors for MBLs has highlighted some classes of compounds potentially useful for the design of a successful inhibitor in the future. However, none have yet entered further development stages.

In this study, we have developed a structure-based pharmacophore model to screen large compound databases (NCI, ZINC and DrugBank) for candidate ligands to IMP-I MBL, followed by molecular docking simulations of the compounds best fitting the pharmacophore, until a final collection of the 212 distinct molecules with the best docking fitness and the best 49 thiol compounds was reached. In the near future, these molecules will be screened *in vitro* for inhibitory activity against IMP-I.

Resumo

O principal mecanismo de resistência a β -lactâmicos é a hidrólise mediada por β -lactamases (BL). Assim, a principal estratégia para ultrapassar a acção destas enzimas é a terapêutica combinada com moléculas inibidoras que, apesar de terem pouca ou nenhuma actividade antimicrobiana, têm uma elevada afinidade com as BL, restabelecendo a eficácia da terapêutica antibiótica.

As metalo-BL (MBL) são uma classe estruturalmente distinta de BL, com um espectro hidrolítico que abrange a maioria dos antibióticos β -lactâmicos, não sendo inibidas eficazmente por nenhum inibidor. As MBL são cada vez mais isoladas em estirpes bacterianas responsáveis por infecções em humanos e a sua prevalência continuará a aumentar já que começam a ser codificadas por elementos genéticos móveis. É, assim, evidente a urgência do desenvolvimento de soluções que permitam restabelecer a eficácia aos antibióticos β -lactâmicos.

Nas últimas décadas, o estudo de inibidores de MBLs permitiu identificar algumas famílias de compostos com potencial para desenvolvimento de inibidores. Ainda não houve, no entanto, avanços que permitam o seu desenvolvimento clínico.

Neste estudo desenvolvemos um modelo farmacofórico para filtrar uma biblioteca de compostos construída a partir das bases de dados NCI, ZINC e DrugBank seleccionando moléculas candidatas a desenvolvimento como inibidores da MBL IMP-I. De seguida, realizámos simulações de *docking* dos compostos com melhores resultados no *screening* farmacofórico até obtermos um conjunto final com as moléculas com mais afinidade para o receptor (n=212) e um sub-grupo com os 49 melhores compostos com grupos tiol. Num futuro próximo, estas moléculas passarão por um processo de *screening in-vitro* que permita avaliar a actividade inibitória para a MBL IMP-I.

Contents

I	Introduction	13
1.1	History of antibiotics	13
1.2	History of antibiotic resistance	14
1.3	Development and spread of resistance in bacteria	15
1.4	Antibiotic classes and resistance mechanisms	16
1.4.1	Inhibitors of cell wall synthesis	16
1.4.2	Inhibitors of protein synthesis	18
1.4.3	Inhibitors of nucleic acid synthesis	27
1.5	General considerations on the bacterial cell wall	29
1.6	β -Lactam antibiotics	31
1.7	β -lactamases	37
1.7.1	Serine β -lactamases	37
1.7.1.1	Catalytic mechanism of Serine β -lactamases	39
1.7.1.2	Inhibitors of Serine β -lactamases	40
1.7.2	Metallo β -lactamases	43
1.7.2.1	Structure of metallo β -lactamases	43
1.7.2.2	Catalytic mechanism of metallo β -lactamases	46
1.7.2.3	Metallo- β -lactamase inhibitors	48
1.7.2.3.1	Sulfur containing inhibitors	48
1.7.2.3.2	Dicarboxylates	63
1.7.2.3.3	Heterocyclics	71
1.8	Structure-based drug design	78
1.8.1	Docking	78
1.8.2	Pharmacophore modelling	79
2	Aims	81
3	Methods	83
3.1	Preparation of the compound library	83
3.2	Selection and preparation of the target protein	84
3.3	Validation of reported IMP-I inhibitors	85

3.3.1	Molecular Docking	85
3.3.2	Pharmacophore modelling	90
3.4	Pharmacophore modelling runs	93
3.5	Docking calculations	95
4	Results	97
4.1	Generation of a structure-based pharmacophore model	97
4.2	IMP-I pharmacophore screening results	98
4.3	Molecular docking	101
5	Discussion	111
	Appendices	131
A	Molecules excluded from the result set	133
B	Molecule codes	137

List of Figures

I.1	Schematic representation of the mechanisms involved in bacterial cell wall synthesis that are antibiotic targets.	18
I.2	Chloramphenicol structure.	22
I.3	Tetracyclin structure.	22
I.4	Erythromycin structure.	23
I.5	Structure of streptogramins.	24
I.6	Fusidic acid structure.	24
I.7	Rifampicin structure.	25
I.8	Linezolid structure.	25
I.9	Lincomycin structure.	25
I.10	Daptomycin structure.	26
I.11	Surfactin structure.	26
I.12	Colistin structure.	27
I.13	Similarities of Sulfonamide and PABA structures.	28
I.14	Structure of trimethoprim, a diaminopyrimidine.	28
I.15	Structure of ciprofloxacin, norfloxacin and nalidixic acid.	29
I.16	Schematic representation of the mechanism of crosslinking of the peptides between the polysaccharide layers of the bacterial cell wall.	30
I.17	Cell wall composition of Gram-positive and Gram-negative bacteria.	30
I.18	Structure of Benzylpenicillin (Penicillin G).	31
I.19	Structure of Cephalosporin C.	33
I.20	Structure of monobactam aztreonam.	36
I.21	Proposed reaction mechanism for a penicillin β -lactam substrate and a Class A Serine β -lactamase.	39
I.22	Structure of Clavulanate, Sulbactam and Tazobactam.	40
I.23	Structure of Avibactam.	41
I.24	Structure of MK-7655.	41
I.25	Structure of RPX7009.	41
I.26	Structure of cyclobutanone inhibitor.	42
I.27	Structure of an O-aryloxycarboxyl hydroxamate.	42

I.28 Schematic representation of the three MBL subclasses with substrate selectivity, representative enzymes and catalytic properties.	44
I.29 Three dimensional representation of the structures of three MBLs.	44
I.30 Proposed catalytic mechanism of di-zinc MBLs.	47
I.31 Proposed catalytic mechanism of monozinc MBLs.	48
I.32 Mercaptoacetic acid.	49
I.33 Inhibitors synthesized by Hammond <i>et al.</i>	51
I.34 Inhibitors synthesized by Hammond <i>et al.</i> (cont.)	52
I.35 Structures of thiomandelic acid and analogues.	53
I.36 Thiomandelic acid and analogues inhibition of BclI.	54
I.37 Mercaptocarboxylates, and their non-sulfur counterparts (9-12), explored by Lié- nard <i>et al.</i>	54
I.38 Captopril co-crystalized with CphA MBL.	55
I.39 Captopril co-crystalized with LI MBL.	56
I.40 Mercaptophosphonate library of potential MBL inhibitors.	57
I.41 Activity of mercaptophosphonates as MBL inhibitors.	57
I.42 Thiomaltol structure.	58
I.43 Carbapenam derived IMP-I inhibitors, J-110,441 and J-111,225.	61
I.44 Thioxocephalosporins.	62
I.45 Sulfonyl hydrazone derivatives (part 1).	62
I.46 Sulfonyl hydrazone derivatives (part 2).	63
I.47 Sulfonyl hydrazone derivatives (part 3).	64
I.48 Thiophene-based inhibitors.	64
I.49 Substitutions on succinic acid and their inhibition of IMP-I.	65
I.50 Lead compounds selected after NCI chemical diversity set screening by Molough- ney <i>et al.</i>	66
I.51 ME1071, an MBL inhibitor derived from maleic acid.	66
I.52 Phthalic acid derivative.	67
I.53 Phthalic acid derivatives.	67
I.54 3-substituted phthalic acid derivatives.	68
I.55 3-alkyloxy phthalic acid derivatives.	69
I.56 3-amino phthalic acid derivatives.	70
I.57 Piperidine derivatives.	70
I.58 3,6-disubstituted phthalic acid derivatives.	71
I.59 Pyrrole derivatives with IMP-I inhibitory activity.	72
I.60 Biphenyltetrazole structure.	73
I.61 Biphenyltetrazole derivatives - 1998 series.	74
I.62 Biphenyltetrazole - unsubstituted parent compound.	75
I.63 Biphenyltetrazole derivatives - 1999 series.	75

1.64	N-heterocyclics synthesized and explored by Feng <i>et al.</i>	76
1.65	Steady-state inhibition studies of N-heterocyclics by Feng <i>et al.</i>	76
1.66	Compounds 5c and 7a from Hussein <i>et al.</i>	77
3.1	RMSD of the poses with the best fitness score and the lowest RMSD of all poses, both in relation to the original ligand pose.	85
4.1	Structure-based Pharmacophore generated from IMP-I MBL.	98
4.2	Pharmacophore feature: Hydrophobic.	98
4.3	Pharmacophore feature: Hydrogen-bond acceptors.	99
4.4	Pharmacophore feature: Hydrogen-bond donors.	99
4.5	Pharmacophore feature: Volume exclusion.	100
4.6	Screening summary.	102
4.7	Docking screening results: Nucleotides from the DrugBank subset.	103
4.8	Docking screening results: Nucleoside from the DrugBank subset.	103
4.9	Docking screening results: phenylalanine derivatives from the DrugBank subset.	104
4.10	Docking screening results: β -Lactams from the DrugBank subset.	104
4.11	Docking screening results: Gamma-glutamyl peptides from the DrugBank subset.	104
4.12	Docking screening results: Aliphatic molecules from the DrugBank subset.	104
4.13	Docking screening results: Molecules with indole and imidazole moieties from the DrugBank subset.	105
4.14	Docking screening results: Vitamin B6 derivatives from the DrugBank subset.	105
4.15	Docking screening results: Miscellaneous molecules from the DrugBank subset.	106
4.16	Docking screening results: Aminoacid derivatives with a free carboxylic group from the NCI subset.	107
4.17	Docking screening results: Catechin-like molecules from the NCI subset.	107
4.18	Docking screening results: Thymidine derivatives from the NCI subset.	107
4.19	Docking screening results: Diverse heterocyclic, polycyclic aromatic compounds from the NCI subset.	108
4.20	Docking screening results: Sulphate compounds from the NCI subset.	108
4.21	Docking screening results: Miscellaneous molecules from the NCI subset.	108
4.22	Docking screening results: Compounds with norburene moiety from the ZINC subset.	109
4.23	Docking screening results: Diverse compounds from the ZINC subset.	109
4.24	Docking screening results: Thioureas from the Thiol subset.	110
4.25	Docking screening results: Diverse compounds from the Thiol subset.	110
A.1	Docking screening results: Aldehydes from the DrugBank subset.	133
A.2	Docking screening results: Aldehydes from the NCI subset.	133
A.3	Docking screening results: Compounds with nitro groups from the NCI subset.	133

A.4	Docking screening results: Esters from the NCI subset.	134
A.5	Docking screening results: Esters from the ZINC subset.	134
A.6	Docking screening results: Compounds with nitro groups from the ZINC subset.	135
A.7	Docking screening results: Compounds with terminal alkenes from the ZINC subset.	135
A.8	Docking screening results: Ester from the Thiol subset.	135
A.9	Docking screening results: Compounds with nitro groups from the Thiol subset. .	136

List of Tables

1.1	Antibiotic classes and resistance mechanisms.	20
1.2	Antibiotic classes and resistance mechanisms.	21
1.3	Structure of several penicillins.	32
1.4	Structure of several cephalosporins.	34
1.5	Structure of several carbapenems.	35
1.6	Classification of β -lactamases	38
1.7	Metallo- β -lactamases from all subclasses.	45
1.8	Metallo- β -lactamases from all subclasses (cont.)	46
1.9	Residues usually coordinating Zn^{2+} ions in each MBL subclass.	46
1.10	Activity (K_i in μM) of inhibitors against IMP-I.	50
1.11	Activity of racemic thiomandelic acid inhibitor against subclasses B1, B2 and B3.	52
1.12	Activity of mercaptocarboxylates explored by Liénard <i>et al.</i>	55
1.13	Activity of D-captopril and captopril analogues against MBLs.	56
1.14	Inhibitory activities of 1,2,4-triazole-3-thiols against IMP-I.	59
1.15	Inhibitory activities of 1,2,4-triazole-3-thiols against IMP-I (cont.).	59
1.16	Inhibitory activities of selected compounds against IMP-I.	60
1.17	Combination effect of 3-substituted phthalic acid derivatives with biapenem against <i>P. aeruginosa</i>	69
3.1	Selection parameters for the NCI, ZINC and DrugBank databases.	83
3.2	Docking configurations for validation runs.	86
3.3	Literature validation results - Docking K_i	87
3.4	Literature validation results - Docking IC_{50}	88
3.5	Literature validation results - Docking % Inhibition.	89
3.6	Literature validation results - Pharmacophore modelling (K_i).	90
3.7	Literature validation results - Pharmacophore modelling (IC_{50}).	91
3.8	Literature validation results - Pharmacophore modelling (% Inhibition).	92
3.9	Screen Library configurations.	95
3.10	Docking protocols.	96

4.1	Pharmacophore screening summary. Number and percentage of positions that were fit into each feature.	100
4.2	First Docking screening results.	101
BI	Molecule identifiers.	137

Acronyms

6-APA 6-amino-penicillanic acid

BL β -lactamase

BLI β -lactamase inhibitor

BPT biphenyl tetrazole

CAMP cationic antimicrobial peptide

ESBL extended-spectrum β -lactamase

FDA Food and Drug Administration

LPS lipopolysaccharide

MBL metallo β -lactamase

MIC minimum inhibitory concentration

MMFF94 Merck Molecular Force Field

MRSA methicillin-resistant *Staphylococcus aureus*

NCI National Cancer Institute

OM outer membrane

PABA para-aminobenzoic acid

PBP penicillin binding protein

PDB protein data bank

RMSD root mean square deviation

SBL serine β -lactamase

SDF structure data format

UPGMA Unweighted Pair Group Method with Arithmetic mean

UTI urinary tract infection

Chapter I

Introduction

The discovery of antibiotics is one of the biggest hallmarks of medicine, saving countless lives from infectious diseases. However, antimicrobial resistance has developed in nature and evolved alongside the use of antibiotics, increasing in incidence and spreading among species.

The general awareness on antibiotic resistance has been increasing in recent years as many diseases are once more becoming difficult to treat due to the selective pressure exerted by the generalized use of antibiotics in human medicine and in the environment.

Without discovering novel antibiotic classes since the 1980's, investment on antibiotic research has been greatly reduced by the big pharmas, with only some companies maintaining active research on this topic. The continued research on antibiotics has since largely been based on the modification of existing molecules, producing incremental advances that may regain some activity, but that will likely not be enough to meet the challenge of antimicrobial resistance at hand.

Given the low return on investment the big pharmas were faced with, antibiotic discovery research was relegated to smaller companies and academia that, with limited resources and R&D capacity, cannot take up such a challenge alone. For this reason, industry/public funding initiatives have been created to foster the development of new drugs and strategies to fight antimicrobial resistance, such as COMBACTE [1].

I.1 History of antibiotics

Understanding the history of antibiotic and antimicrobial resistance development is essential to fully understand the threat of antibiotic resistance.

The most famous discovery of antimicrobial properties is that of penicillin by Alexander Fleming in the 1930's. However, antimicrobial properties of natural products have been known for centuries, even if the basis of these properties was not understood at the time, like the use of cinchona bark extract to treat malaria since the 17th century (we now know that the antimicrobial

properties are those of quinine) and ipecacuanha root (emetine) to treat amoebic dysentery. In early 1900's Ehrlich and Shiga realised that trypanrot caused the death of trypanosomes [2] and in 1909 Ehrlich and Hata found that arsphenamine could be used to cure syphilis [3].

Important as they were, these discoveries were only modestly effective. In 1929, Alexander Fleming noticed that *staphylococcus* sp. colonies around a contaminating colony of *Penicillium notatum* appeared to be undergoing lysis and isolated penicillin for the first time. He was not able to purify enough drug to be of use and it would not be until 1940 that the therapeutic value of penicillin was duly noted [4] and only by 1943 were the yields high enough for commercial use.

In 1935, Domagk *et al.* showed that prontosil red (a dye with a sulfonamide group, synthesized in 1932 by a group of scientists from Bayer) was effective against haemolytic *streptococci* sp. infections in mice [5]. Its activity was explained in 1935 and attributed to the sulfanilamide that was originated by the *in vivo* split of the dye [6]. This discovery prompted the synthesis and modification of sulfonamides, leading to more effective and safer molecules.

In the few decades following the discovery of sulfonamides and penicillin, almost all classes of antibiotics were discovered: streptomycin [7], gramicidin (the first antibiotic active against Gram-positive bacteria) [8], chlortetracycline, chloramphenicol, nalidixic acid, that was the precursor of the fluoroquinolones [2] and oxazolidinones [9]. Thereafter, no new antibiotic classes have been discovered, with antibiotic research providing only chemical modifications of existing drugs and class combinations to improve efficiency and avoid resistance.

1.2 History of antibiotic resistance

Evidence suggests that resistant microorganisms were found in nature long before the dawn of antibiotic use [10, 11], where it was useful as a defence mechanism from other microorganisms that produced harmful substances, and it was observed right from the beginning of antimicrobial research in resistant trypanosomes [3] or penicillin-resistant *Escherichia coli* [12]. While it was recognized from the beginning, it was not immediately perceived as a threat as, for example, penicillin resistance was not immediately observed in *Staphylococcus* or *Streptococcus* species [12]. However, resistance to penicillin among *Staphylococcus aureus* in hospitals grew from less than 1% incidence by the time penicillin started being used to 14% in 1946, to 38% in 1947, and to more than 90% today [3].

A steep rise in resistance to sulfonamides was also evident, to 80% resistant isolates after being widely used to treat *Shigella* sp. infections in Japan after World War II [3]. The switch to other antibiotics (tetracycline, chloramphenicol, and streptomycin) quickly spurred the appearance of multiresistant *Shigella* sp. strains. This quick rise in resistance meant a period of only 30 years of sulfonamides effectiveness to treat meningococcal disease [13] and illustrates the seriousness of this threat. The current resistance trends point to the return of deadly diseases that have been

uncommon since the pre-antibiotic era [9, 10, 14].

1.3 Development and spread of resistance in bacteria

Bacteria can develop resistance through gene mutations [14] and horizontal gene transfer [15]. Both mechanisms can be driven by the selective pressure of antimicrobials that are effective against the susceptible individuals, reducing the competition for the resistant population.

Mutational resistance is caused by a series of point mutations in chromosomes or plasmids that may lead to resistant traits with various degrees of efficacy [16, 17]. Mutations may affect many resistance mechanisms: alteration of the target protein (e.g.: mutation of DNA topoisomerases in quinolone resistance, mutations in ribosomes in aminoglycoside resistance and mutation of rRNA in macrolide resistance); enzymatic inactivation of the drug (e.g.: continued appearance of β -lactamases to degrade new β -lactam antibiotics); target bypassing (e.g.: a mutation in the pathway to build the cell wall in vancomycin resistance); and inhibition of drug access (e.g.: mutation of porins or a mutation that inactivates the expression of all porins, reducing the influx of antibiotic) [18].

The major mechanism of spreading resistance is, however, horizontal gene transfer. This mechanism is unsurprisingly effective since most antimicrobials are derived from natural products, which means that the potential for resistance already exists in nature in some species and will be spread quickly, as soon as antimicrobials are introduced, as a consequence of selective pressure [15]. These mechanisms are so fast that widespread resistance to a new antimicrobial agent can happen in a period as short as three years [19, 20], and this speed may be increasing [15].

Horizontal gene transfer occurs by several mechanisms: transformation, transduction and conjugation. Transformation is the natural uptake and integration of DNA from the environment and is very important among streptococci, being particularly well studied in *S. pneumoniae* and *Neisseria* species (it is noteworthy that even non-pathogenic species like *N. flavescens* and *N. cinerea* carry resistance genes and play a role in the dissemination of resistance [15]). Transduction is the transfer of genetic material by means of a bacteriophage, being particularly important among staphylococci and is thought to be the mechanism responsible for the development of resistance in methicillin-resistant *Staphylococcus aureus* (MRSA) [15]. Finally, conjugation is the direct, cell-to-cell transfer of plasmids by means of a sexual *pilus* and by far the most common mechanism for spreading resistance determinants. Almost all classes of antimicrobials have resistance genes encoded in plasmids, e.g.: aminoglycosides, fluoroquinolones, macrolides, and β -lactams, and this number seems to be increasing, as genes are being transferred from chromosomes to mobile genetic elements at an increasing rate [21] and also from plasmid into chromosomes by mobile genetic elements such as transposons, insertion sequences, and integrons. Additionally, resistance genes to different classes of antibiotics are usually found in the same plasmids [16], facilitating the spread of multiresistance

by the exchange of a single mobile genetic element, and even preserving resistance to antibiotics that may not be currently in use [15].

1.4 Antibiotic classes and resistance mechanisms

In general, antibiotics can be grouped in three major categories: Inhibitors of cell wall synthesis; inhibitors of protein synthesis; and inhibitors of nucleic acid synthesis. Table 1.1 summarizes the antibiotic classes in clinical use, grouped by major inhibition groups.

The selectivity of antibiotics stands on the differences between eukaryotic and prokaryotic cells. However, differences amongst prokaryotic cells confer intrinsic resistance of some species to some kinds of antibiotics (e.g.: mycoplasmas are naturally resistant to β -lactams as they lack the peptidoglycan layer that is the target of β -lactams and the outer membrane of Gram-negative bacteria confers increased resistance to many antibiotics due to decreased permeability and the presence of efflux pumps).

Acquired resistance mechanisms (i.e.: resistance developed through mutation or gene acquisition) are frequently intimately related to the molecular structure of antibiotics as they target the antibiotic molecule directly (e.g.: hydrolysis, phosphorylation, acetylation, nucleotidylation, monooxygenation, glycosilation, etc) or change the target structure slightly, reducing the affinity of the antibiotic to its target molecule (e.g.: altered target). Other resistance mechanisms however, are transversal to almost all classes (e.g.: increase of drug efflux or decrease of drug influx) or related with the mechanism of action of the antibiotic (while not directly with the molecule or the target themselves), like the reprogramming of the peptidoglycan biosynthesis responsible for vancomycin resistance.

1.4.1 Inhibitors of cell wall synthesis

There are several groups of inhibitors of cell wall synthesis (Table 1.1). The bacterial cell wall is a very interesting target for antimicrobial intervention as it is exclusive of prokaryotic cells, enabling the development of drugs that combine efficacy with an excellent toxicity profile. Moreover, the cell wall synthesis involves many steps that can be targeted by different antibiotic classes (Figure 1.1).

β -lactams

The β -lactam class includes penicillins, cephalosporins, carbapenems and monobactams (not exactly a β -lactam, but they have the same mechanism of action and a similar structure) and target

the penicillin binding proteins (PBPs) that are responsible for cross-linking the strands of peptidoglycan in the bacterial cell wall. The disruption of the activity of these proteins destabilizes the cell wall that is then easily ruptured or suffers autolysis [3].

Resistance to β -lactams is majorly mediated by β -lactamases (BLs), a family of hydrolases that disrupt the β -lactam ring, rendering them inactive. Similar in structure to the PBPs, BLs are encoded in chromosomes, mobile genetic elements [3] and plasmids, and the production of AmpC (a BL) can be induced by the presence of β -lactams [22].

In order to extend their activity spectrum and to escape the resistance conferred by these enzymes, several generations of β -lactams have been designed over the years and resistance to all of them has emerged through BLs. Clavulanic acid, sulbactam and tazobactam are part of a subgroup of β -lactams that, despite presenting only residual antibiotic activity, bind irreversibly to the BLs, inhibiting their activity and restoring activity to β -lactams, enabling successful treatment of several infections. There are, however, BLs resistant even to these inhibitors, becoming increasingly difficult to eliminate.

Glycopeptides

The glycopeptides bind acyl-D-alanyl-D-alanine, a peptide necessary for cell wall synthesis, forming very stable complexes that inhibit, by steric hindrance, the transpeptidation step required for the formation of the glycopeptide chains [23]. Being very large molecules (e.g.: vancomycin is 1.4kD), these molecules are only active against Gram-positive organisms as they are excluded from Gram-negatives by the outer membrane [24]. A recent work has developed lipophilic cationic vancomycin analogues able to penetrate the outer membrane of Gram-negative organisms, overcoming the intrinsic non-susceptibility of these pathogens to glycopeptides and showing potent activity [25].

The principal mechanism of resistance to glycopeptides is the development of an alternate cell wall synthesis pathway that uses D-alanyl-D-lactate or D-alanyl-D-serine instead, reducing the binding affinity of glycopeptides [24]. Another mechanism to reduce susceptibility to glycopeptides appears to be an increase in the number of peptidoglycan precursors in the cell wall, binding the glycopeptides before they can reach their targets in the cytoplasmic membrane [24, 26].

N-acetylmuramic acid (NAM) synthesis inhibitors

The first step of the bacterial cell wall synthesis takes place in the cytosol, where UDP-GlcAc and UDP-MurNAc-L-Ala-D-Glu-meso-Dap-D-Ala-D-Ala (cell wall precursors) are synthesized. NAM synthesis inhibitors, such as Fosfomicin, block this stage by inhibiting the conversion of UDP-N-acetylglucosamine by UDP-GlcNAc-3-enol-pyruvyltransferase [27].

D-ala-D-ala ligase/Alanine racemase inhibitors

Cycloserine inhibits the production of D-alanyl-D-alanine peptide by inhibiting the D-ala-D-ala ligase and the Alanine racemase that produces D-alanine from L-alanine [27–29].

Bactoprenol inhibitors

Bacitracin prevents phosphorylation of bactoprenol, a transport protein carrying peptidoglycan components outside the cell membrane [30], a process essential for bacterial cell wall formation. Two mechanisms of bacitracin resistance are known:

1. Efflux protein, BcrABC, pumps bacitracin out of the cell [31];
2. BacA protein provides active phosphorylated bactoprenol from a different synthetic pathway [32].

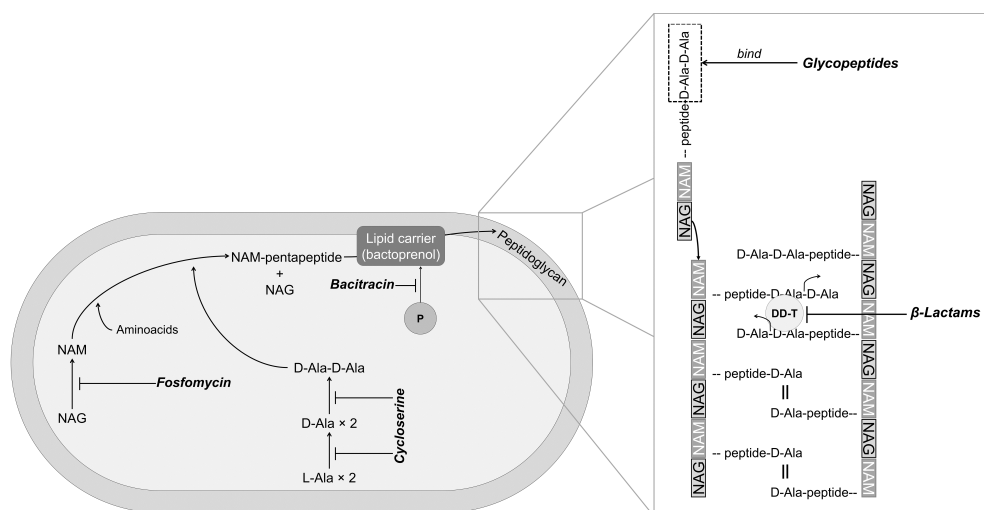


Figure I.1. Schematic representation of the mechanisms involved in bacterial cell wall synthesis that are antibiotic targets. Adapted from Greenwood, 2007

I.4.2 Inhibitors of protein synthesis

Inhibitors of protein synthesis exploit the differences between bacterial and eukaryotic ribosomes to achieve their selective toxicity. Inhibitors of bacterial protein synthesis include aminoglycosides, tetracyclines, macrolides, lincosamides, streptogramins, oxazolidinones, phenicols, rifamycins, fusidic acid, mupirocin, lipopeptides and cationic peptides.

Aminoglycosides

Aminoglycoside antibiotics generally consist of a linked ring system composed of aminosugars and an aminosubstituted cyclic polyalcohol (aminocyclitol) and can be divided in three major groups: streptomycins, neomycins, and kanamycins. These drugs enter the cells through quinones (active

transport), that are absent in anaerobes and *streptococci* sp., species that are, consequently, non-susceptible to aminoglycosides [3].

Streptomycins bind to the 30S ribosomal subunit, while kanamycins and neomycins bind to both 50S and 30S subunits (different site from streptomycins) [3]. The exact mode of action of aminoglycosides is still a subject of study, but several effects have been noted, including codon misreading, synthesis of defective proteins that may affect membrane integrity; formation of non-functioning initiation complexes; and inhibiting the translocation step in polypeptide synthesis [3].

There are three general mechanisms of aminoglycoside resistance: (1) reduction of the intracellular concentration of the drug within the cell, usually via efflux by dedicated or general efflux pumps; (2) alteration of the molecular target of the antibiotic, as result of a spontaneous mutation or enzymatic alteration; and (3) enzymatic inactivation of the drug by acetylation, phosphorylation and adenylation [33].

Table I.1. Antibiotic classes and resistance mechanisms. Adapted from Medical Microbiology, 4th edition.

Inhibitors of	Antibiotic class	Examples	Target	Resistance mechanisms
Cell wall synthesis	β -lactam	Penicillins, cephalosporins, carbapenems, monobactams	Peptidoglycan biosynthesis	Hydrolysis, efflux, altered target
	Glycopeptides	Vancomycin, teicoplanin	Peptidoglycan biosynthesis	ReproGramming peptidoglycan biosynthesis
	NAM synthesis inhibitors	Fosfomicin, fosmidomycin	N-acetylmuramic acid synthesis	Diminished uptake
	DADAL/AR inhibitors	Cycloserine	Inversion of L-Alanine and dimerization of D-Alanine	Overexpression of target
	Bactoprenol inhibitors	Bacitracin	Phosphorylation of bactoprenol	ReproGramming peptidoglycan biosynthesis, efflux
Protein synthesis	Aminoglycosides	Gentamicin, streptomycin, spectinomycin	Translation	Phosphorylation, acetylation, nucleotidylation, efflux, altered target
	Tetracyclines	Minocycline, tigecycline	Translation	Monooxygenation, efflux, altered target
	Macrolides	Erythromycin, azithromycin	Translation	Hydrolysis, glycosilation, phosphorylation, efflux, alteration of target
	Lincosamides	Clindamycin	Translation	Nucleotidylation, efflux, altered target
	Streptogramins	Synercid	Translation	C-O lyase (type B streptogramins), acetylation (type A streptogramins), efflux, altered target
	Oxazolidinones	Linezolid	Translation	Efflux, altered target

Table 1.2. Antibiotic classes and resistance mechanisms. Adapted from Medical Microbiology, 4th edition. (cont.)

Inhibitors of	Antibiotic class	Examples	Target	Resistance mechanisms
Protein synthesis	Phenicol	Chloramphenicol	Translation	Acetylation, efflux, altered target
	Rifamycins	Rifampin	Transcription	ADP-ribosylation, efflux, altered target
	Steroid antibacterials	Fusidic acid	Translation	Altered target
	Lipopeptides	Daptomycin, surfactin	Cell membrane	Altered target
	Cationic peptides	Colistin	Cell membrane	Altered target, efflux
Nucleic acid synthesis	Quinolones	Ciprofloxacin	DNA Replication	Acetylation, efflux, altered target
	Pyrimidines	Trimethoprim	Folic acid synthesis	Efflux, altered target
	Sulfonamides	Sulfamethoxazole	Folic acid synthesis	Efflux, altered target

Chloramphenicol

Chloramphenicol (Figure 1.2) prevents peptide bond formation by inhibiting the peptidyl transferase reaction on the bacterial ribosome. This large spectrum drug is effective on most Gram-positive and Gram-negative bacteria, chlamydiae and rickettsiae, and strictly intracellular bacteria that cause various infections, such as trachoma, psittacosis, and typhus. Resistance usually occurs by acetylation of the two hydroxyl groups by bacterial enzymes [27].

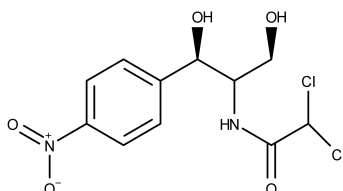


Figure 1.2. Chloramphenicol structure.

Tetracyclines

Tetracyclines comprise a linear fused tetracyclic nucleus (rings designated A, B, C, and D) with a variety of functional groups attached (Figure 1.3). The simplest tetracycline to display detectable antibacterial activity is 6-deoxy-6-demethyltetracycline (Figure 1.3) and so this structure may be regarded as the minimum pharmacophore [34].

This antibiotic family inhibits protein synthesis by preventing the association of aminoacyl t-RNA with the prokaryote ribosome [35, 36] by binding to the 30S subunit [35, 37].

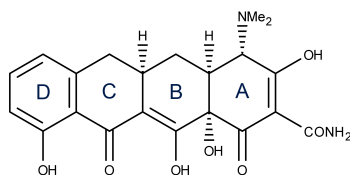


Figure 1.3. Tetracyclin structure.

Resistance to the tetracyclines occurs via three mechanisms:

1. Production of a membrane efflux pump that removes the drug as rapidly as it enters. There are several genes encoding these pumps;
2. Several ribosome protection proteins act to prevent tetracycline from binding to the ribosome;
3. A protein found only in *Bacteroides* spp. enzymatically inactivates tetracycline [38–40].

Macrolides

Macrolides are macrocyclic lactones that share a similar molecular structure characterized by a 14-, 15-, or 16-membered lactone ring substituted with some sugars such as cladinose and desosamine (Figure 1.4).

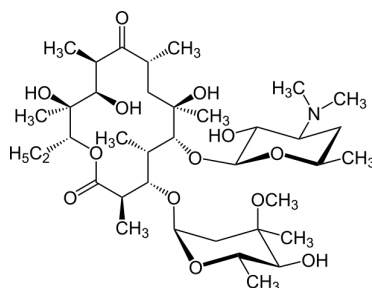


Figure 1.4. Erythromycin structure - a macrolide.

These antibiotics are thought to act by dissociating the peptide chain from the ribosome during the translocation step in bacterial protein synthesis, through dissociation of the tRNA. They have antistaphylococcal and antistreptococcal activity, acting also on chlamydiae, *Mycoplasma pneumoniae*, legionellae, and some mycobacteria. Conversely, they are not active against enterobacteria and *Pseudomonas aeruginosa*. Resistance is common among staphylococci, but less so in streptococci. However, resistant *Streptococcus pyogenes* strains are increasing in prevalence [27].

There are two major mechanisms of macrolide resistance:

1. Drug efflux from the cell by an efflux pump;
2. Modification of the ribosome by methylation of a nucleotide on the binding site [41].

Streptogramins

The streptogramin class comprises two types (A and B) of structurally different drugs that act synergistically by binding different sites on the 50S ribosomal subunit. Type A drugs (Figure 1.5 - A) block substrate binding at two sites on the 50S subunit, while type B drugs (Figure 1.5 - B) cause release of incomplete peptide chains. The synergy is the result of a conformational change induced by the binding of type A drugs that significantly increases the affinity for type B drugs [42].

Resistance to streptogramin antibiotics can be found in efflux pumps for both type A and B streptogramins; virginiamycin acetyl-transferases that inactivate type A streptogramins and several enzymes that can inactivate type B streptogramins; and alteration of bacterial ribosomal proteins or RNA such as the mutation in the ribosome that gives rise to macrolide resistance that is also effective against streptogramins [42].

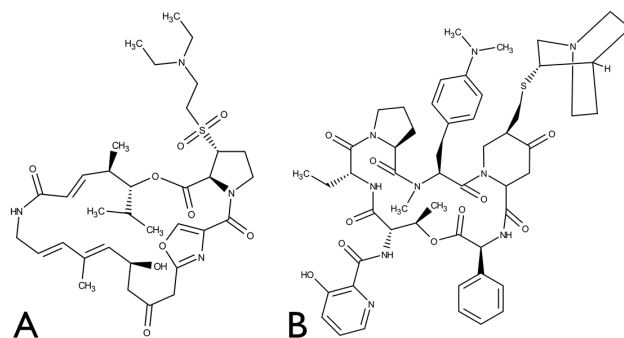


Figure I.5. Structure of streptogramins. **A.** Streptogramin Type A - Dalfopristin. **B** Streptogramin type B - Quinupristin.

Fusidic acid

Fusidic acid inhibits translocation of the growing polypeptide chain by inhibiting elongation factor G. Point mutations in the *fusA* gene lead to altered structures of the elongation factor, resulting in the cell becoming resistant [27].

This bacteriostatic has a steroid-like structure (Figure I.6) and although usually seen as an anti-staphylococcal agent, it is active against Gram-positive and Gram-negative cocci, *Mycobacterium tuberculosis*, *Nocardia asteroides*, and many anaerobes. Gram-negative bacilli are naturally resistant due to the cell wall [27].

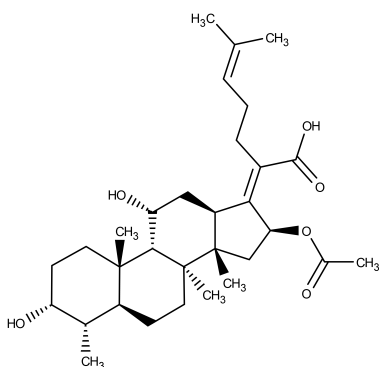


Figure I.6. Fusidic acid structure.

Rifamycins

Rifampicin (Figure I.7) acts by binding to the β -subunit of RNA polymerase, hindering the DNA transcription process.

Resistance to rifampicin is invariably the result of a structural alteration in the *rpo* gene that encodes the β -subunit of RNA polymerase [3].

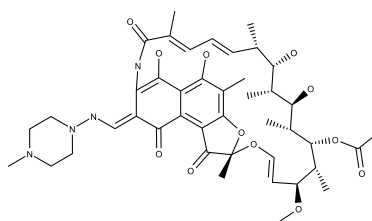


Figure 1.7. Rifampicin structure.

Oxazolidinones

Linezolid (Figure 1.8) inhibits protein synthesis at the stage of ribosomal assembly. Ribosomal mutations can lead to linezolid resistance in both staphylococci and enterococci. Linezolid resistance is currently very rare in *Staphylococcus aureus* and is only occasionally seen in enterococci, usually associated with prolonged therapy and failure to remove or drain a focus of infection [3].

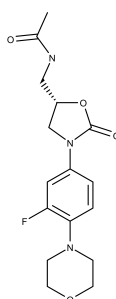


Figure 1.8. Linezolid structure.

Lincosamines

Lincosamines block peptide bond formation [43] by binding to the 50S ribosomal subunit and reducing the accessibility of phylogenetically conserved bases in the peptidyl transferase loop of 23S rRNA. Mutations on the peptidyl transferase can confer lincomycin (Figure 1.9) resistance in tobacco chloroplast [44] and clindamycin resistance in *E.coli* [45, 46].

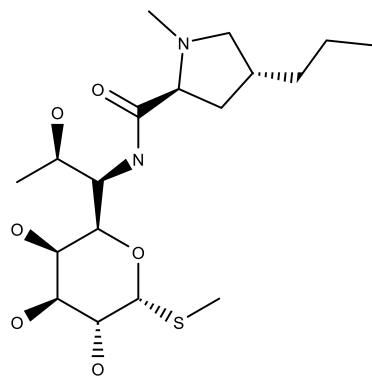


Figure 1.9. Lincomycin structure.

Lipopeptides

Daptomycin is structurally and functionally related to cationic antimicrobial peptides (CAMPs) produced by the innate immune system. This molecule consists of a cyclic polypeptide core of 13 aminoacids attached to a lipophilic tail (a decanoyl fatty acid) (Figure I.10) [47] that is active against Gram-positive bacteria.

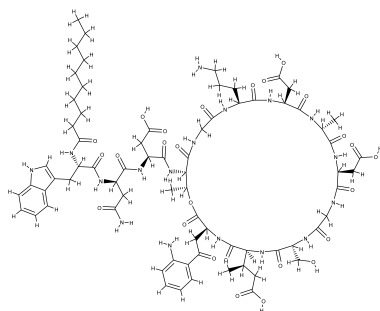


Figure I.10. Daptomycin structure.

The mechanism of action of daptomycin is unclear, but some effects have been found:

1. Rapid depolarization of *Bacillus* spp. cells;
2. Inhibition of the active transport of aminoacids;
3. Inhibition of peptidoglycan and/or lipoteichoic acid synthesis through still unclear mechanisms [47].

Resistance to Daptomycin seems to come from the development of an alternate pathway for synthesis of lipoteichoic acid [47], a major constituent of the cell wall of Gram-positive bacteria.

Surfactin consists of a cyclic heptapeptide moiety closed to a lactone ring by a fatty acid, produced by *Bacillus subtilis* (Figure I.11). Surfactin possesses hemolytic [48], anti-viral [48,49], anti-bacterial [50,51], and anti-tumor [52] activity, probably resulting from its capability of permeabilizing cellular membranes and viral envelopes [53].

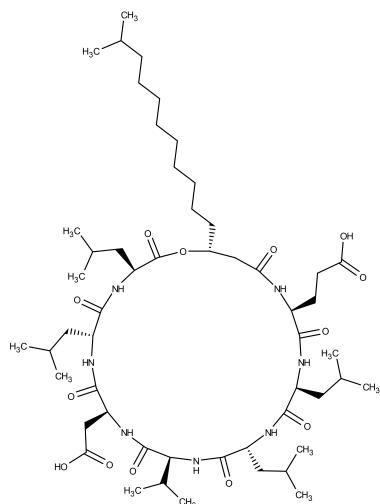


Figure I.11. Surfactin structure.

Resistance mechanisms to surfactin are not established although the molecule is known to be unstable in the soil, suggesting that some mechanisms are present for its degradation. Hoefler *et al.* identified an enzyme of *Streptomyces* sp. MgI with affinity for hydrolysing surfactin, some affinity for plipastatin and no affinity for other lipopeptides and macrocyclic substrates such as daptomycin and amphotericin B [54].

Cationic peptides

Colistin (polymyxin E), a polypeptide antibiotic of the polymyxin family consists of a cyclic heptapeptide with a tripeptide side chain acylated at the N terminus by a fatty acid tail (Figure 1.12).

Isolated in 1947 from soil bacterium *Bacillus polymyxa colistinus*, colistin was available from 1959 for treating Gram-negative infections, although with high rates of toxicity that prompted its replacement with newer antibiotics such as gentamicin and carbenicillin [55].

The rise of multidrug resistant Gram-negative bacteria renewed the interest in colistin as many of these microorganisms, such as *P. aeruginosa*, *Acinetobacter baumannii* and *Klebsiella pneumoniae* remained susceptible to polymyxins [56, 57] until the recent discovery of *mcr-1*, the first plasmid-mediated colistin resistance mechanism [58]. Thus far, the polymyxins remained one of the last classes of antibiotics with no known cell-to-cell resistance spread, with resistance being restricted to the alteration of the polymyxin target: lipopolysaccharide (LPS) A.

Colistin binds to the lipid A portion of the LPS by displacing calcium and magnesium ions from the outer cell membrane due to its cationic structure, leading to permeability changes in the cell envelope [55, 59]. Thus, modification of lipid A or total loss of the LPS reduces affinity for polymyxins [58].

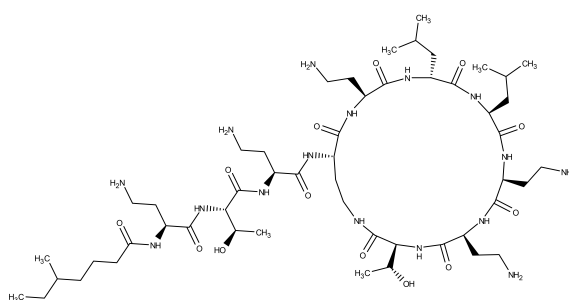


Figure 1.12. Colistin structure.

1.4.3 Inhibitors of nucleic acid synthesis

Given the role of nucleic acid as the basis of life, it is surprising that so many antimicrobial agents have been discovered that selectively interfere with the functions of DNA and RNA. Some, like the sulphonamides and diaminopyrimidines, achieve their effect indirectly by interrupting metabolic

pathways that lead to the manufacture of nucleic acids; others, of which the quinolones and nitroimidazoles are prime examples, exert a more direct action [3].

Sulfonamides and Diaminopyrimidines

Sulfonamides and diaminopyrimidines inhibit folate synthesis (in different steps), a coenzyme necessary for the synthesis of purines and pyrimidines, essential components of the nucleotides.

Sulfonamides are analogs of para-aminobenzoic acid (PABA) (Figure 1.13), an essential component in folate synthesis, while diaminopyrimidines (e.g.: trimethoprim, Figure 1.14) inhibit dihydrofolate reductase, the enzyme that catalyses the final step in folate synthesis [3]. Both drugs are effective on their own but they have a synergistic effect when used in combination.

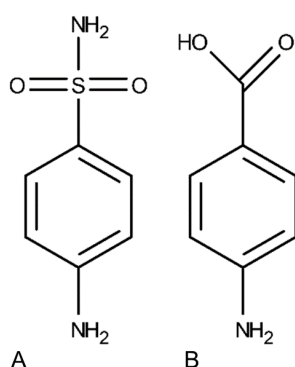


Figure 1.13. Similarities of Sulfonamide (A) and PABA (B) structures.

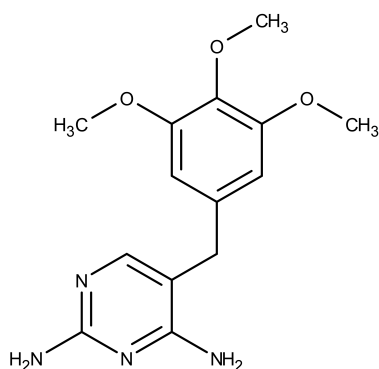


Figure 1.14. Structure of trimethoprim, a diaminopyrimidine.

Resistance to sulfonamides arises by overproduction of PABA or by production of an altered dihydropteroate synthetase that has a much lower affinity for sulfonamides than for PABA [60]. Trimethoprim resistance results from over-production of dihydrofolate reductase or from the production of an altered form [60].

Quinolones

Quinolones such as ciprofloxacin, norfloxacin and nalidixic acid (Figure 1.15) inhibit bacterial growth by acting on DNA gyrase and topoisomerase IV, which are necessary for correct func-

tioning of supercoiled DNA [3]. Despite usually targeting both enzymes, the primary target is topoisomerase IV on Gram-positives and DNA gyrase on Gram-negatives [61].

There are three main mechanisms of resistance to quinolones:

1. Reduced uptake by decreasing the expression of porins;
2. Increased efflux by expression of efflux pumps [22];
3. Alteration of target enzymes resulting in reduced binding affinities [61].

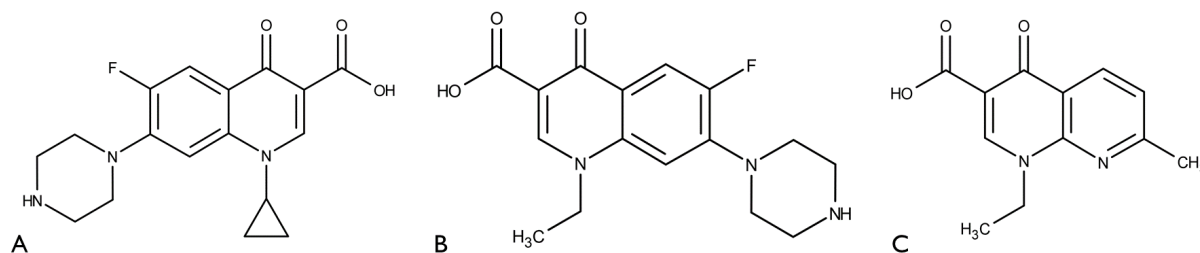


Figure 1.15. Structure of ciprofloxacin (A), norfloxacin (B) and nalidixic acid (C).

1.5 General considerations on the bacterial cell wall

Bacterial cell walls are layers of polysaccharides (dimers of N-acetylmuramic acid and N-acetylglucosamine) held together by crosslinked peptides, forming peptidoglycan. As depicted in Figure 1.1, the NAG-NAM-pentapeptides are synthesized in the cytosol and carried through the cell membrane by a lipid carrier and added to the peptidoglycan layer where their terminal D-Alanine residues are crosslinked with another molecule via removal of one D-Ala residue by DD-transpeptidases located in the cell membrane commonly known as PBPs (mechanism is represented in Figure 1.16).

Gram-positive and Gram-negative bacteria differ on the composition of their cell wall. While Gram-positives have a single thick peptidoglycan layer, the Gram-negatives have a thinner peptidoglycan layer that is surrounded by periplasmic space and an outer membrane (OM) (Figure 1.17). This OM confers more protection to antibiotics as the molecules need to cross an additional external barrier, reason why Gram-negative infections may be more challenging to treat. Indeed, glycopeptides are only active against Gram-positive bacteria and the first β -lactam antibiotics were also targeted only at Gram-positives, a limitation that was overcome with extended-spectrum drugs [62].

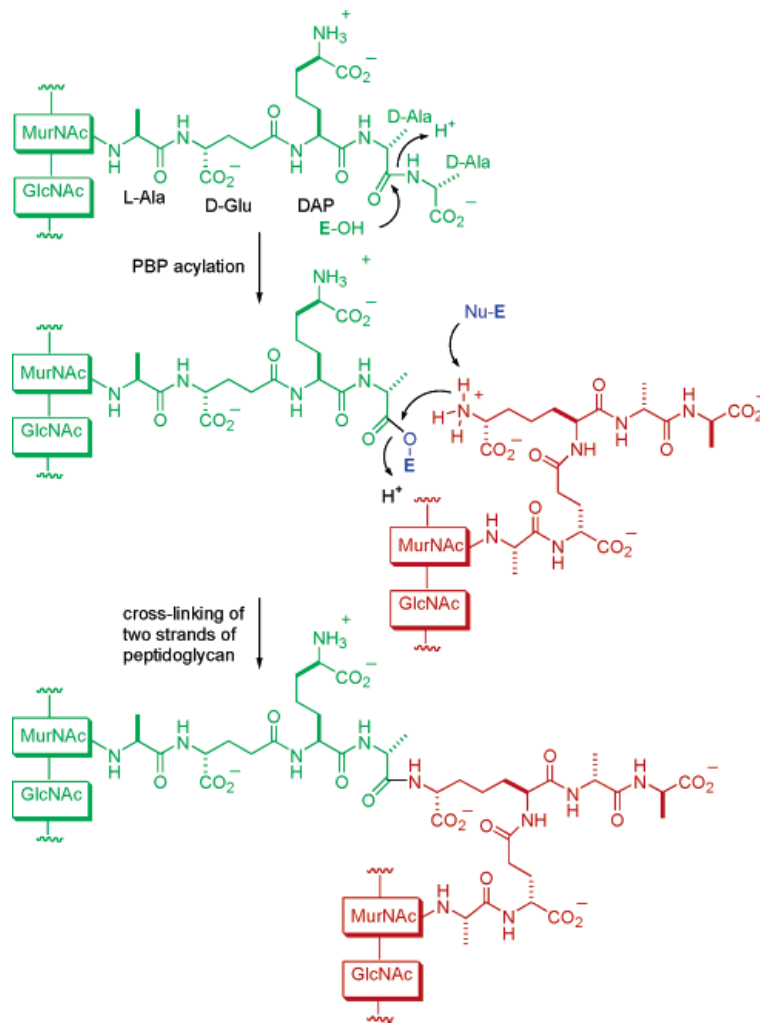


Figure I.16. Schematic representation of the mechanism of crosslinking of the peptides between the polysaccharide layers of the bacterial cell wall. Adapted from Fisher *et al.*, 2005 [62].

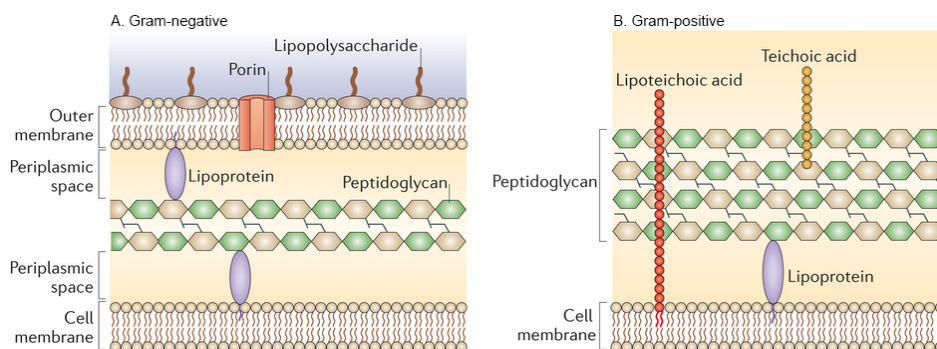


Figure I.17. Cell wall composition of Gram-positive and Gram-negative bacteria. Adapted from Brown *et al.*, 2015 [63]

1.6 β -Lactam antibiotics

Penicillins, cephalosporins, carbapenems, monobactams and some other antibiotics belong to the family of β -lactam antibiotics, which share the β -lactam ring moiety. In the penicillins the β -lactam ring is fused to a five-membered thiazolidine ring (Figure 1.18), whereas the cephalosporins display a six-membered dihydrothiazine ring structure (Figure 1.19). Being the central feature of this class, the β -lactam ring is also its weakness as many bacteria possess enzymes (β -lactamases, BL) that are capable of breaking open the ring by hydrolysing the amide bond, rendering the molecule antibacterially inactive.

Penicillins

Benzylpenicillin is the most common penicillin, and therefore the only just referred to as penicillin, as it was the easiest to synthesize by *Penicillium chrysogenum* and exhibited the most attractive properties. After the penicillin nucleus, 6-amino-penicillanic acid (6-APA), was isolated, several synthetic penicillins were developed to overcome high-dose resistance and address several shortcomings of benzylpenicillin:

1. restricted spectrum;
2. hypersensitivity reactions;
3. acid instability;
4. high renal clearance;
5. hydrolysis by β -lactamases.

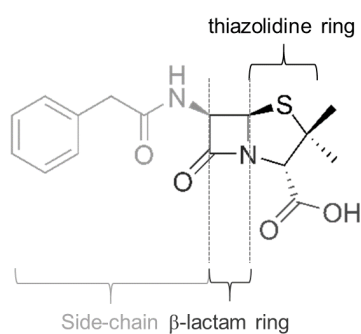
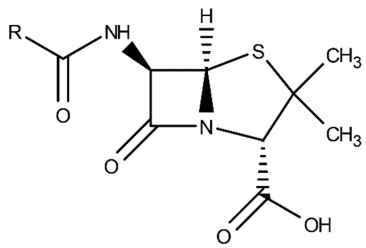
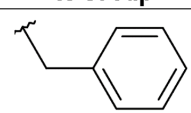
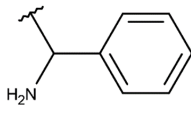
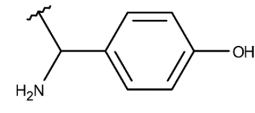
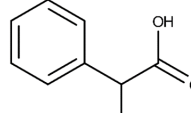
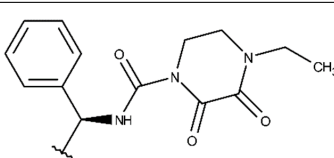
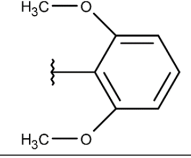
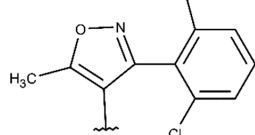


Figure 1.18. Structure of Benzylpenicillin (Penicillin G).

The addition of an aminogroup to the sidechain of benzylpenicillin yielded ampicillin that had its spectrum extended to Gram-negative bacilli. The addition of an hydroxyl group to the benzyl ring yielded amoxicillin with an improved availability (Table 1.3).

Despite even the enlarged spectrum of ampicillin, none of these drugs was effective against *Pseudomonas aeruginosa*, an important pathogen that was targeted with the discovery of carbenicillin and piperacillin, the first being administered as a prodrug and the latter parenterally.

Table 1.3. Structure of several penicillins.

Penicillin structure	R Group	Drug Name
		Benzylpenicillin
		Ampicillin
		Amoxicillin
		Carbenicillin
		Piperacillin
		Methicillin
		Flucloxacillin

The rise of β -lactamase mediated resistance in staphylococci stimulated the development of hydrolysis-resistant methicillin and isoxazolympenicillins, such as flucloxacillin. Despite resistance to methicillin first appearing by alteration of the target, often causing cross-resistance to other antibiotics as well, currently BLs have evolved to hydrolyze methicillin as well [3].

Cephalosporins

Cephalosporins have a broader spectrum than penicillins, although without activity against enterococci and are mostly stable to serine β -lactamases.

The addition of a carbon atom to the fused ring originating the dihydrothiazine opened the possibility for substitution at C-3 (R₂ in Table 1.4) that has a strong influence on pharmacokinetic properties. The modelling of the substituents of the cephalosporin nucleus aimed, just like in penicillins, to improve pharmacological properties such as oral absorption and stability to inactivating enzymes and/or better activity.

Generally of parenteral administration, cephalosporins started off being very unstable against ente-

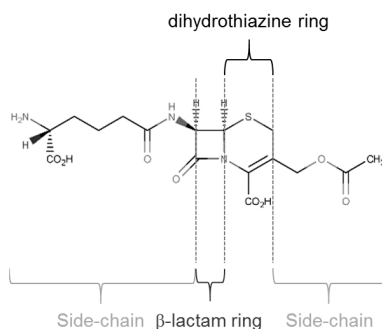


Figure I.19. Structure of Cephalosporin C.

rococci BLs with first generation compounds such as cefalotin, being followed by second generation molecules like cefoxitin (which is a cephamycin - note the added methoxy group on the β -lactam ring, depicted in gray on the cephalosporin nucleus in Table I.4) with improved stability against enterobacteria BLs. Finally, the development of third generation cephalosporins brought antibiotics that combine improved stability and activity such as cefotaxime, ceftriaxone and moxalactam (an oxa-cephem, replacing the sulfur of the the dihydrothiazine with an oxygen).

Pseudomonas aeruginosa is not usually susceptible to first and second generation cephalosporins. However, ceftazidime, ceftiprome and cefepime are useful in the management of *P. aeruginosa* infections in seriously ill patients, despite being less active against staphylococcal infections. These three molecules have very similar substituents on R1 and R2 (Table I.4).

Efforts to develop orally available cephalosporins were employed early in development, producing drugs such as cefalexin and cefaclor (Table I.4) with very similar properties and modest activity against Gram-negative bacilli [3].

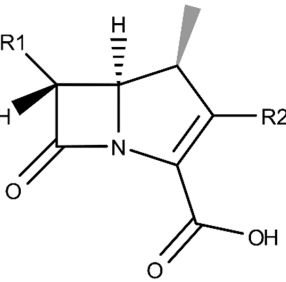
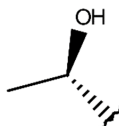
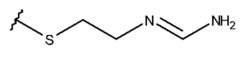
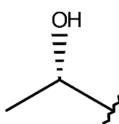
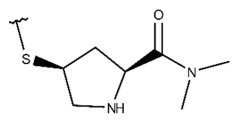
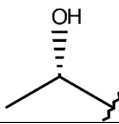
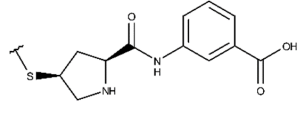
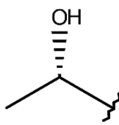
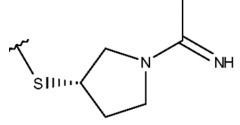
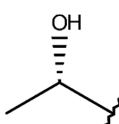
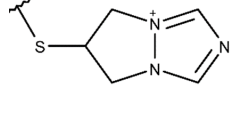
Table I.4. Structure of several cephalosporins.

Cephalosporin structure	R1 Group	R2 Group	Drug Name
			Cephalosporin C
			Cefalotin <i>1st gen.</i>
			Cefoxitin <i>2nd gen.</i> (cephamycin)
			Ceftriaxone <i>3rd gen.</i>
			Moxalactam <i>3rd gen.</i> (cephamycin; oxa-cephem)
			Cefprozil
			Cefepime
			Cefpirome
			Cefalexin
			Cefaclor

Carbapenems

In addition to penicillins and cephalosporins, carbapenems are the third big class of β -lactams (Table 1.5). These antibiotics are stable to most BLs, with the exception of metallo- β -lactamases, and a few serine β -lactamases (SBLs) (such as KPC and OXA-48) (Section 1.7.2) and present high-activity against nearly all Gram-positive and Gram-negative bacteria other than intracellular bacteria such as chlamydiae.

Table 1.5. Structure of several carbapenems.

Carbapenem structure	R1 Group	R2 Group	Drug Name
			Imipenem
			Meropenem
			Ertapenem
			Panipenem
			Biapenem

Structurally, carbapenems are very similar to penicillins, with a double bond on the thiazolidine ring and the sulfur replaced by a carbon. All carbapenems have a hydroxyethyl substituent on R1 and bulky heterocyclic substituents on R2, with the exception of imipenem (Table 1.5). Strictly, some of the compounds, meropenem, biapenem, and ertapenem, are methylcarbapenems with a methyl group added on C-10 (grey methyl on carbapenem nucleus in Table 1.5).

Penams

The penams, the group of which penicillins are part of, also includes structures with only residual antibacterial activity: clavulanate (strictly, an oxapenam), sulbactam and tazobactam which are serine-BL inhibitors (Section 1.7.1.2) as they have affinity for serine BLs, restoring activity to BL-labile agents.

Other β -Lactams

With a structurally different nucleus, aztreonam (Figure 1.20) is classified as a monobactam as the β -lactam ring is present but the fused ring structure is absent. The R1 substituent is the same as in ceftazidime and the β -lactam ring has a sulfonate group attached to the amide nitrogen.

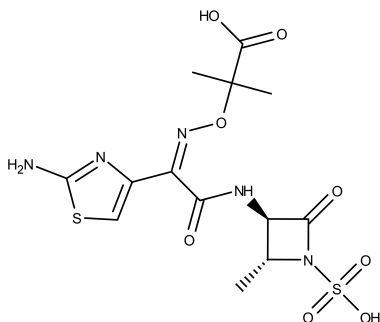


Figure 1.20. Structure of monobactam aztreonam.

The spectrum of aztreonam is restricted to Gram-negative bacteria but is susceptible to many extended-spectrum BLs. It is, however, at least partially resistant to most metallo β -lactamases (MBLs) [64] such as NDM [65] and VIM-1 [66], with some exceptions such as VIM-7 [64]. It is important to note that while most MBLs may be susceptible to inhibition by aztreonam, the bacteria harbouring them such as *P. aeruginosa* may produce other MBLs and often have many other resistance mechanisms in place such as reduced intake, increased efflux and target alterations that can make them resistant by other means [67].

1.7 β -lactamases

β -lactam antibiotics bind irreversibly to PBPs by mimicking the terminal D-Ala-D-Ala residues of the peptide subunits, preventing the crosslinking and disrupting the bacterial cell wall synthesis [62].

β -lactamases originated from PBPs by point mutations, acquiring a β -lactam hydrolyzing phenotype [62]. Thus, it is not strange that the β -lactams, that so resemble a tripeptide (Figure 1.18) with the β -lactam core (centre), a neighbouring carboxylate on the fused 5- or 6-membered ring (thiazolidine ring) and an acylamino substituent on the β -lactam ring (side-chain), are effective substrates of both enzyme families (PBPs and BLs), blocking the acylation/deacylation cycle of the PBP, but being hydrolysed by the β -lactamases [62].

β -lactamases are mainly found in the membrane (although also in the cytosol), where they evolved from the PBPs and can be classified structurally in four major classes A, B, C and D, based on their aminoacid sequence – the Ambler classification [68], and functionally in four groups, one through four, based on their affinity towards substrates and inhibitors [69–71]. Classes A, C and D of the Ambler classification are all SBLs, and all have great structural similarity and hydrolyse the β -lactam ring in a similar mechanism, directly involving a serine residue. Class B comprises MBLs that are Zn^{2+} -dependent and have distinct structure and hydrolytic mechanism [68].

1.7.1 Serine β -lactamases

Class A enzymes form the largest group of β -lactamases, hydrolysing penicillins, narrow- and extended-spectrum cephalosporins, carbapenems, and monobactams. Many members of this group are susceptible to commercially available β -lactamase inhibitors (clavulanate, tazobactam e sulbactam). Notable enzymes of this class are the CTX-M group (an extended-spectrum β -lactamase (ESBL)) that hydrolyses penicillin, first, second and third-generation cephalosporins, and KPCs that hydrolyse all β -lactams, including carbapenems, and are the most widely disseminated carbapenemases of class A [72].

Class C is not as numerous as class A, comprising enzymes that hydrolyse penicillins and cephalosporins (thus referred to as Serine cephalosporinases) that are usually resistant to clavulanate, tazobactam, and sulbactam but that are inhibited by cloxacillin, oxacillin and aztreonam (some antibiotics also present β -lactamase inhibitory activity). Horizontal transfer in this class is less pronounced as these enzymes are usually encoded in chromosomes, but can also be found in plasmids with potential for dissemination. Finally, despite being usually produced at a low-level in Gram-negatives, their production can be induced by cefoxitin, imipenem (strong inducers) and clavulanate. Notable enzymes of this class are AmpC and GC1; both are cephalosporinases but with different substrate preferences [72, 73].

Class D enzymes are serine β -lactamases with a special affinity for oxacillin (thus usually known as oxacillinases) and a spectrum that spans from penicillins to carbapenems, being usually resistant

to all inhibitors. Notable enzymes of this class are OXA-48, a carbapenemase and OXA-11, an extended-spectrum cephalosporinase [72, 73].

Table 1.6 summarizes the A, C and D classes of serine β -lactamases.

Table 1.6. Classification of β -lactamases

Bush-Jacoby group (2009)	Molecular class (subclass)	Substrate	Representative enzyme(s)
I	C	Cephalosporins	AmpC, P99, ACT-1, CMY-2, FOX-1, MIR-1
Ie	C	Cephalosporins	GCI, CMY-37
2a	A	Penicillins	PC I
2b	A	Penicillins, early cephalosporins	TEM-1, TEM-2, SHV-1
2be	A	Extended-spectrum cephalosporins, monobactams	TEM-3, SHV-2, CTX-M-15, PER-1, VEB-1
2br	A	Penicillins	TEM-30, SHV-10
2ber	A	Extended-spectrum cephalosporins, monobactams	TEM-50
2c	A	Carbenicillin	PSE-1, CARB-3
2ce	A	Carbenicillin, cefepime	RTG-4
2d	D	Cloxacillin	OXA-1, OXA-10
2de	D	Extended-spectrum cephalosporins	OXA-11, OXA-15
2df	D	Carbapenems	OXA-23, OXA-48
2e	A	Extended-spectrum cephalosporins	CepA
2f	A	Carbapenems	KPC-2, IMI-1, SME-1
3a	B (B1)	Carbapenems	IMP-1, VIM-1, CcrA, IND-1
	B (B3)	Carbapenems	LI, CAU-1, GOB-1, FEZ-1
3b	B (B2)	Carbapenems	CphA, Sfh-1

I.7.1.1 Catalytic mechanism of Serine β -lactamases

The general catalytic mechanism of classes A, C and D is based on a Serine residue strategically positioned at the active site. Activated by a water molecule, this Serine residue carries out a nucleophilic attack on the carbonyl of the β -lactam ring, forming an acyl-enzyme followed by protonation of the nitrogen on the amide (steps A to C of Figure I.21). The de-acylation step (steps C to E of Figure I.21) is put in motion by an activated water molecule that attacks the acyl-enzyme complex and ultimately leads to hydrolysis of the bond between serine and the β -lactam carbonyl [73].

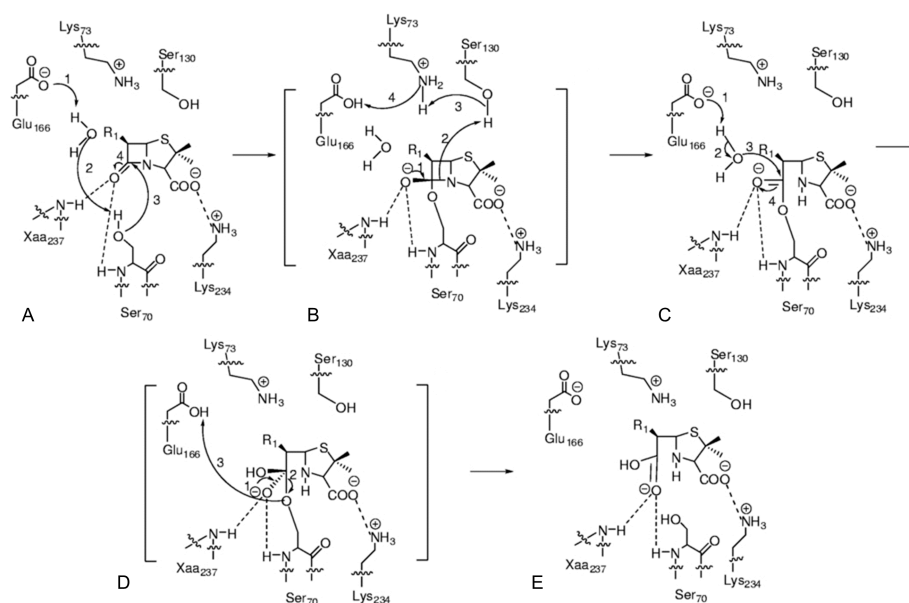


Figure I.21. Proposed reaction mechanism for a penicillin β -lactam substrate and a Class A Serine β -lactamase. Adapted from Drawz 2010 [73].

1.7.1.2 Inhibitors of Serine β -lactamases

Inhibitors of Classes A and C

Inhibitors of classes A and C are discussed together since many exhibit activity against enzymes from both classes.

Clavulanate, tazobactam and sulbactam

Clavulanate, tazobactam and sulbactam are irreversible β -lactamase inhibitors, mainly active against class A enzymes, being very less effective against class B, C and D enzymes [73–77]. All three are beta-lactams (Figure 1.22), with a strong resemblance to penicillin, being susceptible to resistance mechanisms such as up-regulation of β -lactamase expression and new β -lactamase acquisition. These limitations have motivated the search for new inhibitors.

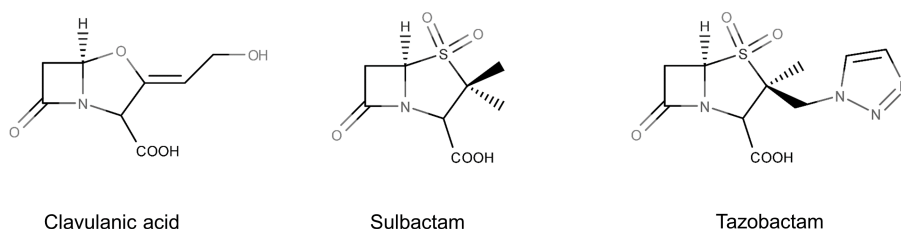


Figure 1.22. Structure of Clavulanate, Sulbactam and Tazobactam.

Avibactam

Currently, the β -lactamase inhibitor (BLI) most advanced in the development pipeline is avibactam, already approved by the Food and Drug Administration (FDA) in combination with ceftazidime for the treatment of complicated intra-abdominal infections and complicated urinary tract infections. This non- β -lactam β -lactamase inhibitor (Figure 1.23) is mainly active against Ambler classes A and C, and also against some class D enzymes [78]. Compared with the three inhibitors currently marketed: clavulanate, tazobactam and sulbactam, avibactam showed lower 50% inhibitory concentrations and decreased reactivation rates for the clinically relevant class A and C β -lactamases – TEM-1, KPC-2, P99 and AmpC [79]. Avibactam has produced remarkably low minimum inhibitory concentrations in combination with different β -lactams and, depending on its pairing, has potential to be highly effective against many multidrug-resistant pathogens [79]. Sadly, it has demonstrated activity against metallo- β -lactamases only when combined with aztreonam. Avibactam exhibits several properties that may contribute to its promising features:

1. rapid formation of a stable adduct with the enzyme;
2. stable acyl enzyme formed between the inhibitor and the serine residue of the β -lactamase that originates very slow deacylation rates;
3. possible regeneration of the inhibitor following deacylation, instead of hydrolysis, allowing acylation of a new enzyme [79].

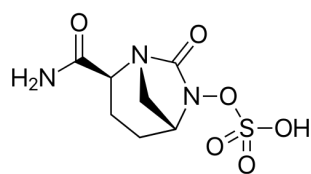


Figure 1.23. Structure of Avibactam.

MK-7655

MK-7655 (Figure 1.24) is a bridged bicyclic urea, a non- β -lactam compound, with a heterocyclic side-chain that is currently in phase III clinical trials [80]. This inhibitor has resulted from a drug discovery proGram extensively exploring heterocyclic side-chains in bridged bicyclic ureas carried out by Merck. It presents similar properties to avibactam and has demonstrated good activity against pathogens from classes A and C producing KPC and decreased-porin phenotypes, when combined with imipenem [79]. No activity has been found in OXA-48 class D enzyme and in MBLs IMP, NDM, and VIM [79].

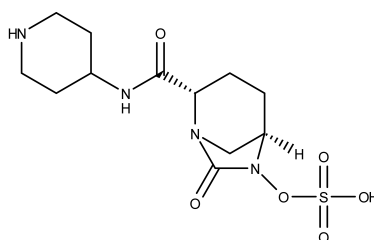


Figure 1.24. Structure of MK-7655.

Boronic acid derivatives

Boronic acid derivatives have been documented as effective SBL inhibitors since the 1970s [79]. This class of inhibitors blocks the β -lactamases by a different mechanism than β -lactams and is not hydrolysed by the enzyme. The known scaffold has been recently combined with fragments with good potential for interaction with active site residues in a fragment-based lead discovery strategy, resulting in potent *E.coli* AmpC inhibitors that provided low minimum inhibitory concentrations (MICs) when combined with ceftazidime and cefotaxime [79]. The development of boronates is still in an early stage. The only visible candidate is RPX7009 (Figure 1.25) combined with biapenem that has presented a good profile against class A carbapenemases, but no activity against isolates with impermeability, ESBL, OXA-48 or MBLs [81].

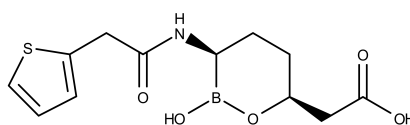


Figure 1.25. Structure of RPX7009.

Cyclobutanone-based

Cyclobutanone-based inhibitors mimic β -lactams and have demonstrated preferential activity against class C enzymes. These are reversible inhibitors that have affinity for broad-spectrum β -lactamases, having demonstrated activity against KPC-2, IMP-1, GCI and OXA-10. Although it has demonstrated some activity against MBLs, the authors consider that it probably has limited clinical application (Figure 1.26) [79].

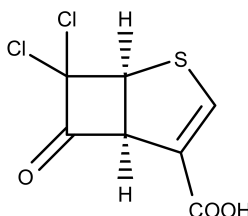


Figure 1.26. Structure of cyclobutanone inhibitor.

Hydroxamic acid derivatives

O-aryloxycarboxyl hydroxamates (Figure 1.27) are non- β -lactam inhibitors developed from the general structure of a depsipeptide [82] that have demonstrated activity against class A and C β -lactamases [82, 83]. Their mechanism of action is different from other inhibitors, cross-linking an oxygen from a Serine, a nitrogen from a Lysine, and the carbonyl from the inhibitor.

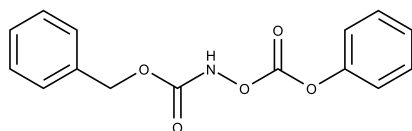


Figure 1.27. Structure of an O-aryloxycarboxyl hydroxamate.

Tilwala *et al.* [83] have explored the activity of several compounds by variations of leaving groups and found one suitable for further design that may lead to a new inhibitor class. Phosphyl analogues of these compounds are also potentially good inhibitors, being more stable in solution but they do not cross-link the active site like their counterparts. Leaving group optimization also seems to be the next step in their development [83].

Inhibitors of Class D

Class D enzymes are serine β -lactamases commonly known as oxacillinases for their ability to hydrolyse the β -lactam oxacillin faster than their counterparts of classes A and C [79]. They are a challenge in antibiotherapy because of their very large spectrum, hydrolysing penicillins, cephalosporins, extended-spectrum cephalosporins and carbapenems; and resistance to most BLIs.

Currently, there are no reports of class D enzymes with resistance to both carbapenems and extended-spectrum cephalosporins [84, 85] and they are, overall, thought to confer moderate

resistance levels to pathogenic bacteria, being commonly found in combination with other resistance mechanisms like porin deficiencies and efflux pump overexpression [72]. Additionally, these enzymes are sometimes difficult to detect, which does not favour recognition or suspicion and prevents appropriate treatment [85].

The literature does not provide insight into the development of any inhibitors especially targeted at this class, but some inhibitors have demonstrated activity towards some members: avibactam against OXA-2 and OXA-48 [78]; tazobactam against OXA-2 and OXA-32; and clavulanate against OXA-53 [79]. Sadly, the Merck inhibitor under clinical development (MK-7655) does not appear to have Class D potential [79].

Despite the existence of stronger carbapenemases than the ones in the OXA family (MBLs IMP and VIM, and Class A KPC), there is a lack of good inhibitors for this class and, should a cephalosporin-carbapenem resistant Class D strain emerge, and there is a good chance that it does, (OXA-48 has already emerged in *Enterobacteriaceae* [72]), an effective inhibitor would be a valuable tool.

1.7.2 Metallo β -lactamases

Class B comprehends a separate group of β -lactamases that require one or two Zn^{2+} ions in order to be catalytically active; they are thus denominated metallo- β -lactamases (MBL). These enzymes are structurally distinct from the other three Ambler classes and they hydrolyse penicillins, cephalosporins and carbapenems, being resistant to the usual inhibitors, but sensitive to zinc chelators (e.g.: EDTA) and also to the monobactam aztreonam [71,73].

The IMP-I MBL, discovered for the first time in Japan [86], may be produced by both *P. aeruginosa* and *K. pneumoniae* [87–90], can be encoded both in plasmids and integrons [91] and has been responsible for outbreaks of antibiotic-resistant bacterial infections in clinical settings throughout the globe. With a very broad substrate profile including carbapenems and broad-spectrum β -lactams [86,92–97], this enzyme is well-characterized and its crystal structure has been reported by several authors [98–101].

1.7.2.1 Structure of metallo β -lactamases

MBLs are divided in three subclasses: B1, B2 and B3 [102,103] by aminoacid sequence (particularly the amino acids in the active site that coordinate with the Zn^{2+} ions) [104,105] and substrate selectivity (Figure 1.28).

Table 1.7 summarizes the members of each subclass and the strains for which the enzymes were originally identified.

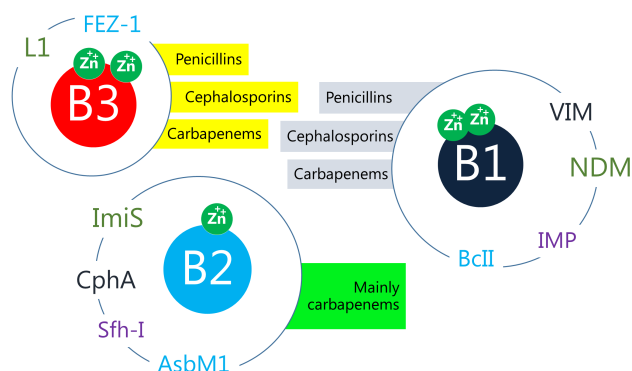


Figure I.28. Schematic representation of the three MBL subclasses with substrate selectivity, representative enzymes and catalytic properties.

The active site of most MBLs contains two Zn²⁺ ions, with the exception of subclass B2 enzymes and BcII (subclass B1), which are only catalytically active when coordinated with a single Zn²⁺ ion. The ions are located in two pockets (Zn1, or histidine site and Zn2, or cysteine site), each coordinated by three aminoacids, which vary among subclasses (Table I.9). In the mononuclear B2 enzymes or BcII, the Zn²⁺ ion usually occupies the histidine site [106].

In subclass B1, the zinc in histidine site is also coordinated with an additional water molecule, resulting in a tetrahedral coordination of the Zn²⁺ ion; similarly, the zinc in the cysteine site is additionally coordinated with two water molecules, assuming a trigonal bipyramidal geometry [107].

Despite the differences pointed out above and very low identity (25%) between some enzymes [103], the crystalized structures point to an overall structural similarity of the MBLs, sharing a $\alpha\beta/\beta\alpha$ quaternary fold, with the active site at the interface between the domains (Figure I.29.) [98, 108–119].

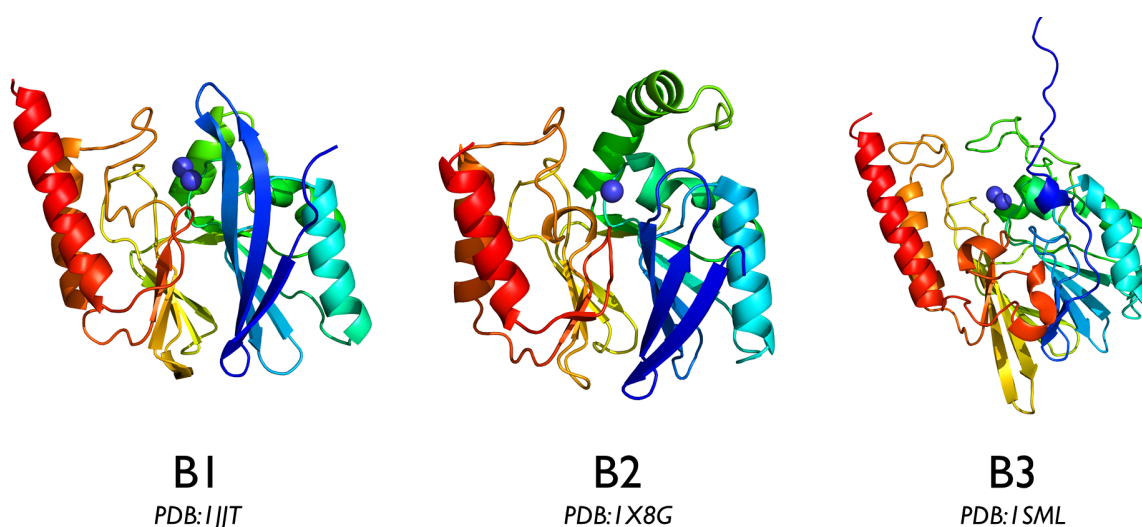


Figure I.29. Three dimensional representation of the structures of three MBLs. The B1 MBL is IMP-I, obtained from protein data bank (PDB) with code 1JJT. The B2 MBL is a CphA, obtained from PDB with code 1X8G. Finally, the B3 MBL is an L1, obtained from PDB with code 1SML. Zinc ions are represented as blue spheres. Images were obtained with Pymol.

Table 1.7. Metallo- β -lactamases from all subclasses. Adapted from Palzkill et al. [106].

Subclass	Enzyme ¹	Organism	
B1	BclI	<i>Bacillus cereus</i>	
	CcrA	<i>Bacteroides fragilis</i>	
	IMP-1	<i>Serratia marescens</i>	
	VIM-2		<i>Pseudomonas aeruginosa</i>
			<i>Acinetobacter baumannii</i>
	VIM-4		<i>Pseudomonas aeruginosa</i>
			<i>Acinetobacter baumannii</i>
	VIM-7		<i>Pseudomonas aeruginosa</i>
			<i>Acinetobacter baumannii</i>
	BlaB	<i>Chryseobacterium meningoseptica</i>	
	SPM-1	<i>Pseudomonas aeruginosa</i>	
	NDM-1		<i>Klebsiella pneumonia</i>
			<i>Escherichia coli</i>
	VIM-1		<i>Pseudomonas aeruginosa</i>
			<i>Acinetobacter baumannii</i>
GIM-1	<i>Pseudomonas aeruginosa</i>		
SIM-1	<i>Acinetobacter baumannii</i>		
DIM-1	<i>Pseudomonas stutzeri</i>		
TMB-1	<i>Achromobacter xyloabacter</i>		
Bla2	<i>Bacillus anthracis</i>		
KHM-1	<i>Citrobacter freundii</i>		
B2	CphA	<i>Aeromonas hydrophila</i>	
	Sfh-1	<i>Serratia fonticola</i>	
	ImiS	<i>Aeromonas veronii</i>	
B3	LI	<i>Stenotrophomonas maltophilia</i>	
	FEZ-1	<i>Legionella gormannii</i>	
	BJP-1	<i>Bradyrhizobium japonicum</i>	
	AIM-1	<i>Pseudomonas aeruginosa</i>	
	THIN-1	<i>Janthinobacterium lividum</i>	
GOB-1	<i>Chryseobacterium meningoseptica</i>		

¹ The strains listed represent the original strain(s) for which the enzymes were identified and do not include the bacteria to which the gene has spread.

Table 1.8. Metallo- β -lactamases from all subclasses. Adapted from Palzkill *et al.* [106].(cont.)

Subclass	Enzyme ¹	Organism
B3	SMB-I	<i>Serratia marcescens</i>
	CAU-I	<i>Caulobacter crescentus</i>
	CAR-I	<i>Erwinia caratovora</i>
	POM-I	<i>Pseudomonas otitidis</i>
	CRB I I	Uncultured bacterium

¹ The strains listed represent the original strain(s) for which the enzymes were identified and do not include the bacteria to which the gene has spread.

Table 1.9. Residues usually coordinating Zn^{2+} ions in each MBL subclass [105, 106].

Subclass	Aminoacids			Substrate profile
	Zn1		Zn2	
B1	His 116 His 118 His 196		Asp 120 Cys 221 His 263	Broad spectrum ¹
B2	Asn 116 His 118 His 196		Asp 120 Cys 221 His 263	Carbapenems
B3	His/Gln 116 His 118 His 196		Asp 120 His 121 His 263	Broad spectrum ¹

¹ penicillins, cephalosporins, carbapenems.

1.7.2.2 Catalytic mechanism of metallo β -lactamases

The hydrolytic mechanism of dizinc MBLs (B1 and B3) is thought to rely heavily on four important structures: The two zinc ions, a hydroxide ion bridged between the two Zn^{2+} ions, and an Asp120 residue (following the standard MBL numbering scheme [102, 103]) that coordinates with Zn2 and with the hydroxide ion, and without which the catalytic efficiency of MBLs is impaired [120–122], thus playing a crucial role in catalysis [123].

In short, hydrolysis seems to occur by a nucleophilic attack of the hydroxide ion on the carbonyl carbon of the β -lactam ring, cleaving the amide bond and releasing the hydrolysed product [124–126]. This reaction starts with the binding of the substrate in the active site, coordinating the carbonyl oxygen interacting with Zn1 and the carboxyl group of the fused ring and the nitrogen on the β -lactam ring coordinating with Zn2 [109, 113, 119, 124]. The coordination of the carbonyl with Zn1 increases the polarisation of the carbonyl bond, facilitating the nucleophilic attack of the hydroxide ion on the carbonyl carbon (Figure 1.30-A) [113]. The hydroxide ion is stabilized by both zinc atoms and Asp120, and, if the binding is as described above, in an optimal position to access the carbonyl carbon and carry out a nucleophilic attack (Figure 1.30-B). Upon breaking of the amide bond (Figure 1.30-C), Zn2 has an important role in stabilizing a reaction intermediate and in the protonation of the nitrogen by the hydroxide ion (Figure 1.30-D) [119], together with Asp120, releasing the final product (Figure 1.30-E) [106, 124, 127, 128].

This mechanism may not be exactly the same in all MBLs. In fact, several studies point out small differences between enzymes [129–132] or between different substrates on the same enzyme [133–136].

To stress the importance of the initial binding position of the substrate for the whole catalytic process, Yuan *et al.* explored different binding positions in docking experiments and found that mainly two binding modes existed. The first mode, coined S-mode for “substrate”, is as described above, coordinating a carbonyl group with ZnI and carboxyl / nitrogen groups with Zn2, positioning the nucleophilic hydroxide in place for attacking the carbonyl carbon. The second, the I-mode, for “Inhibitor”, places the carboxyl group in such a position between the zinc ions that the hydroxide ion is displaced and the amide bond is removed from the vicinity of the metal ions, avoiding hydrolysis. Interestingly, most active substrates were found mainly in S-mode, while the monobactam aztreonam and other inhibitors were mainly found in the I-mode.

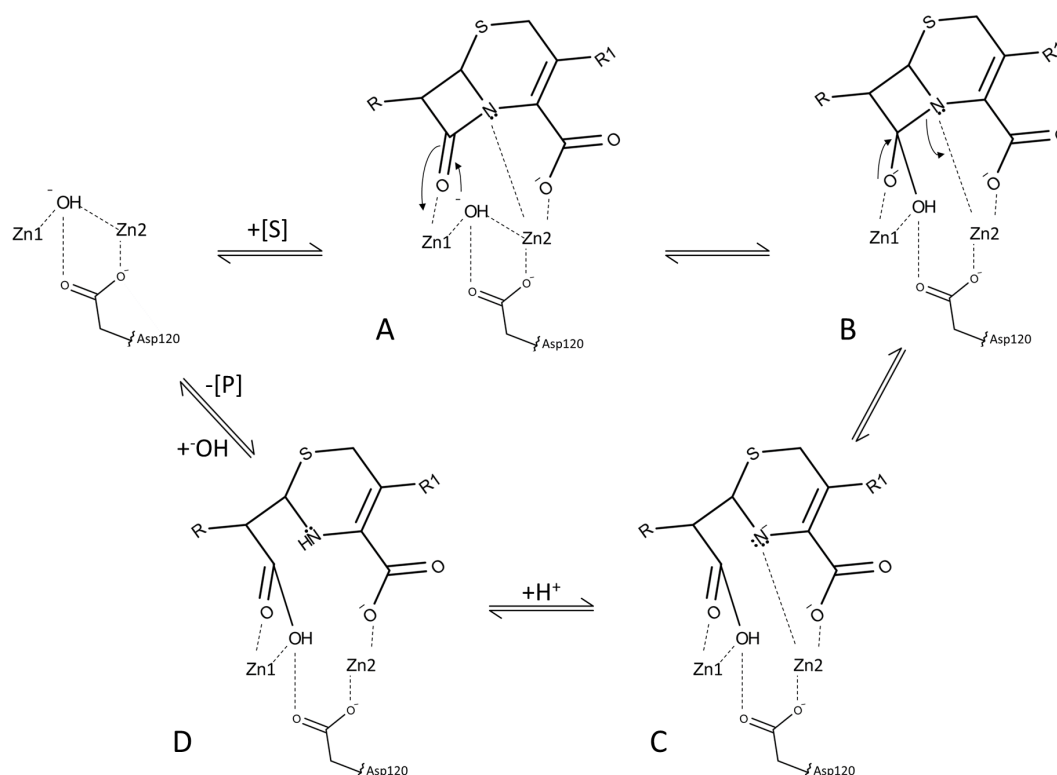


Figure 1.30. Proposed catalytic mechanism of di-zinc MBLs (adapted from Mojica *et al.* [137]).

The B2 subclass enzymes are only catalytically active when a single zinc ion is bound to the Zn I site. Similarly to the B1/B3 mechanism, here the zinc at Zn I coordinates with the carbonyl group and a water molecule is activated by interaction with the Zn^{2+} and an Asp residue [105, 138] (Figure 1.31-A), that will attack the electrophilic carbon, forming the tetrahedral intermediate (Figure 1.31-B). The Asp residue protonates the nitrogen, cleaving the β -lactam ring [105, 138] (Figures 1.31-C and 1.31-D) and releasing the hydrolysed molecule (Figure 1.31-E).

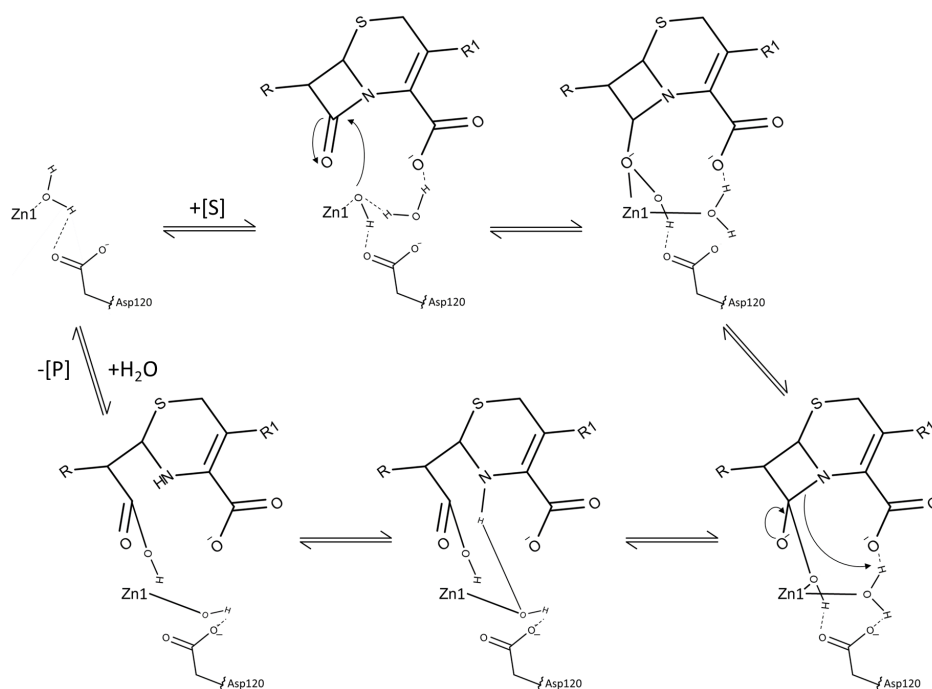


Figure 1.31. Proposed catalytic mechanism of monozinc MBLs (adapted from Crowder *et al.*) [127]

1.7.2.3 Metallo- β -lactamase inhibitors

There are currently no commercially available inhibitors for MBLs. These are particularly challenging targets for drug development for various reasons: (1) they are broad-spectrum enzymes, (2) new β -lactamases appear frequently and (3) the structural differences between subclasses are large enough to further difficult the task. Indeed, in order to be clinically useful, an inhibitor should be active against all three subclasses.

Since SBL inhibitors are ineffective against MBLs, there have been efforts to develop MBL inhibitors, and some have been reported, with a number of different zinc-binding moieties, mainly sulfur atoms and dicarboxylates. These categories are succinctly discussed below.

1.7.2.3.1 Sulfur containing inhibitors

Molecules with a zinc-binding sulfur have been the most commonly reported inhibitors of MBLs, with K_i values as low as 4 nM [104, 139–143].

Mercaptoacetic acid derivatives

In 1997, Payne *et al.* reported mercaptoacetic acid (Figure 1.32) as an irreversible inhibitor of *Bacillus cereus* II MBL when delivered by one of its thiol esters, presumably by establishing a covalent disulfide bond with an active site cysteine at Zn2, in monozinc BcII under aerobic conditions [139]. On the same year, Goto *et al.* showed that free mercaptoacetic acid (Figure 1.32) behaved as a

reversible competitive inhibitor, suggesting a different binding mechanism, driven by the coordination of the thiol group to the Zn^{2+} [141]. The IC_{50} of thioesters for LI MBL were consistently lower than for BclI, despite the covalent bond being impossible in LI which is a B3 subclass enzyme, having a histidine in place of the cysteine residue usually coordinating Zn^{2+} in $Zn2$ binding site in the other subclasses [141].

Mercaptophenylacetic acid analogues of mercaptoacetic acids produced lower IC_{50} values despite only demonstrating competitive inhibitor behaviour, suggesting that the compounds establish hydrophobic interactions with the residues on the $\beta3$ - $\beta4$ loop, that have been shown to be of paramount importance for substrate binding [98, 99]. Mercaptoacetic acid, 2-mercaptoacetic acid and 3-mercaptoacetic acid were also reported as reversible IMP-I inhibitors by Goto *et al.* (Table 1.10) [141].

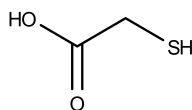


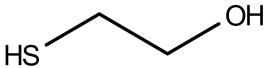
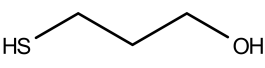
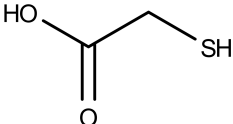
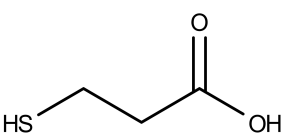
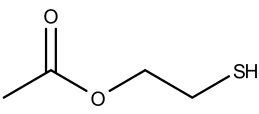
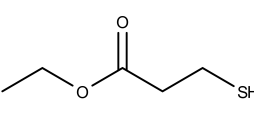
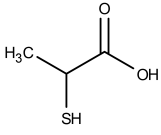
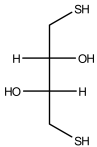
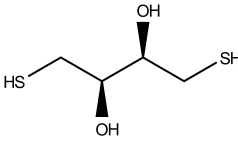
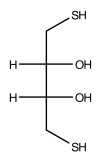
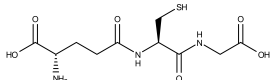
Figure 1.32. Mercaptoacetic acid.

Hammond *et al.* [142] demonstrated for the first time that IMP-I inhibitors could reverse the effect of MBL-mediated carbapenem resistance in bacteria, however with reserves regarding effectiveness on Gram-negatives and on species producing several BLs [142]. Thioester derivatives were found to be competitive inhibitors and substrates of IMP-I, with their thiol hydrolysis products showing good IMP-I inhibitory properties. The authors postulated that the thiols might be the actual inhibitors, and not the esters (Figure 1.33) [142], in line with Payne *et al.* who suggested that the esters may be important for placing the thiol molecule in the active site for inhibition in monozinc MBLs, by enabling a disulfide bond with the $Zn2$ cysteine residue, in its hydrolysed form [139].

Bulky substituents on the alpha carbon seem determinant to increase potency against IMP-I. In the case of compounds with methylindole (10, 13 (Figure 1.33) and 16 (Figure 1.34) perhaps by establishing hydrogen bonds with Ser80 either in its ester or thiol form, and in the case of compounds with apolar substituents by establishing hydrophobic interactions, apparently not in the $\beta3$ - $\beta4$ loop as might be expected. Finally, the thioester analogues have lower IC_{50} than N-acetyl-D-ala-thioester analogues [142], perhaps due to the higher ester hydrolysis rates in the first group and reinforcing the notion that the thiols and not the esters are responsible for the inhibitory activity.

Motivated by the activities of mercaptoacetic acid and related compounds, Mollard *et al.* explored the BclI inhibiting properties of thiomandelic acid and 35 synthetic analogues (Figure 1.35) [143]. When evaluating the remaining enzymatic activity of BclI (4.8 nM) after incubation with 20 μ M of nitrocefin and 1 mM of each compound, it was evident that the thiol group of thiomandelic acid (Figure 1.35, 4a (in gray) and Figure 1.36) is essential for inhibition as its substitution for several other groups (-H, -Br, -OH, -NOH) practically voids the molecule of its inhibitory activity. In

Table 1.10. Activity (K_i in μM) of inhibitors against IMP-I [141].

Inhibitor	IMP-I (BI)	Inhibitor	IMP-I (BI)
	12		2.5
2-mercaptoethanol		3-mercapto-1-propanol	
	0.23		1.20
Mercaptoacetic acid		3-mercaptopropionic acid	
	1.4		0.25
Ethyl mercaptoacetate		Ethyl 3-mercaptopropionate	
	0.19		0.55
2-mercaptopropionic acid		(\pm)-Dithiotreitol	
	2.1		2.2
(-)-Dithiotreitol		Dithioerythritol	
	4.6		
Glutathione			

fact, the compounds with a thiol group or a thioester (**3aa**, **3ab**, **4a-d**, **5a-b**, **8** and **11** in Figures 1.35 and 1.36) present more potent inhibitory profiles. The good inhibitory performance of the thioesters is likely due to the inhibition by their hydrolysis products, in line with the findings of Payne *et al.* [139] and Hammond *et al.* [142].

A close spatial proximity of a carboxyl and a thiol seems to be a favourable combination for a good MBL inhibition profile, with greater potency for molecules with thiol groups on the alpha carbon to the carboxylate, and still presenting a potent effect when the thiol group is on the beta carbon (compounds **4a** and **8** on Figure 1.36) - this was also observed in Goto *et al.*, where mercaptoacetic acid and 2-mercaptopropionic acid were the best inhibitors (thiol group in alpha carbon), followed by 3-mercaptopropionic acid (thiol group in beta carbon) [141]. Compound

Compound		IMP-1 IC ₅₀ (μ M)	CcrA IC ₅₀ (μ M)	Rate of hydrolysis by IMP-1 ($\text{nM}^{-1} \text{min}^{-1} \mu\text{M}^{-1}$)	Effective conc for 4-fold reduction of MIC in <i>E. coli</i> ^a (μ M)
	R ₁ R ₂				
1		240	>1000	225	125
2		20	>1000	650	25
3		3.6	1000	335	6.3
4 ^b		1.4	680	250	3.1
5		63	>1000	1124	–
6		18	1000	4850	6.3
7		2	>1000	250	3.1

		IMP-1 IC ₅₀ (μ M)	CcrA IC ₅₀ (μ M)	Rate of hydrolysis by IMP-1 ($\text{nM}^{-1} \text{min}^{-1} \mu\text{M}^{-1}$)	Effective conc for 4-fold reduction of MIC in <i>E. coli</i> ^a (μ M)
	R ₁ R ₂				
8		0.064	>1000	16000	50
9		0.0004	180	24000	3.1
10		0.0013	>500	1400	0.2
11		12	>1000	10500	12.5
12		0.08	750	19000	25
13		0.045	>500	900	≤ 0.1

Figure 1.33. Inhibitors synthesized by Hammond *et al.* [142]

9, para-mercaptobenzoic acid, is significantly less active than compound **8**, showing that potency further decreases with a greater distance between carboxylate and thiols. Removal of the acid group from thiomandelic acid, however, only has a modest effect on potency (compounds **4a** and **11**), suggesting that thiol is essential for BclI affinity in this scaffold, while the carboxylate leads to a significant increase in potency but alone is not enough for a good inhibitory profile (compounds **1a-d** in Figures 1.35 and 1.36) [143].

Although Mollard postulated that the carboxyl group of thiomandelic acid could coordinate with Arg91 [143], Karsisiotis elucidated the structure of the thiomandelate - BclI complex and showed

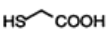
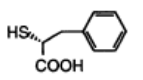
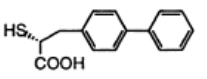
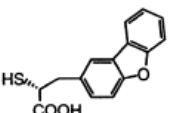
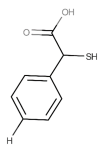
Compound		IMP-1 IC ₅₀ (μ M)
Mercaptoacetic acid		0.32
14		0.086
15		0.057
16		0.023

Figure 1.34. Inhibitors synthesized by Hammond *et al.* [142] (cont.)

that the carboxylate is too far from Arg91 for this to be possible (~ 6 Å), being even too far away for interaction with Lys171 or Asn180 [144], residues usually coordinated with other MBL inhibitors [98, 145–147], and the addition of one or more methylene groups would be necessary for this interaction to be possible [144].

Thiomandelic acid was still tested on several B1 and B3 enzymes, and demonstrated to be a potent inhibitor of B1 and B3 MBLs (Table 1.11) [143], an unprecedented finding at the time.

Table 1.11. Activity of racemic thiomandelic acid inhibitor against subclasses B1, B2 and B3 [143]

Inhibitor	B1		B2	B3	
	IMP-I	BcII	CphA	LI	FEZ-I
	0.029	0.34	144	0.081	0.27

Despite the several sources showing that the spatial proximity of the thiol and carboxylate groups is important, it does not seem to be a crucial factor. In the work developed by Liénard *et al.* [104] compounds **3** and **4** (Table 1.12) were found to be more potent inhibitors than thiomandelic acid (**1**), with **3** displaying a sub-micromolar potency against MBLs from all three subclasses (IMP-I and BcII, CphA, LI and FEZ-I) [104] (Figure 1.37). Curiously, compound **3** does not present the α or β relation between thiol and carboxylate groups, and compound **4** is devoid of a carboxylate moiety. In this work, the authors verified by electrospray ionisation mass spectrometry (ESI-MS) that the distance between carboxylate and thiol groups influenced not only the potency but also the binding mechanism, as thiomandelic acid binds as a CphA-Zn₂ complex, by increasing the affinity of the enzyme to the binding of a second zinc ion and compounds **3** and **4** seem to bind as a CphA-Zn complex [104, 148].

The binding mode of mercaptocarboxylates to monozinc MBLs such as CphA appears to be dif-

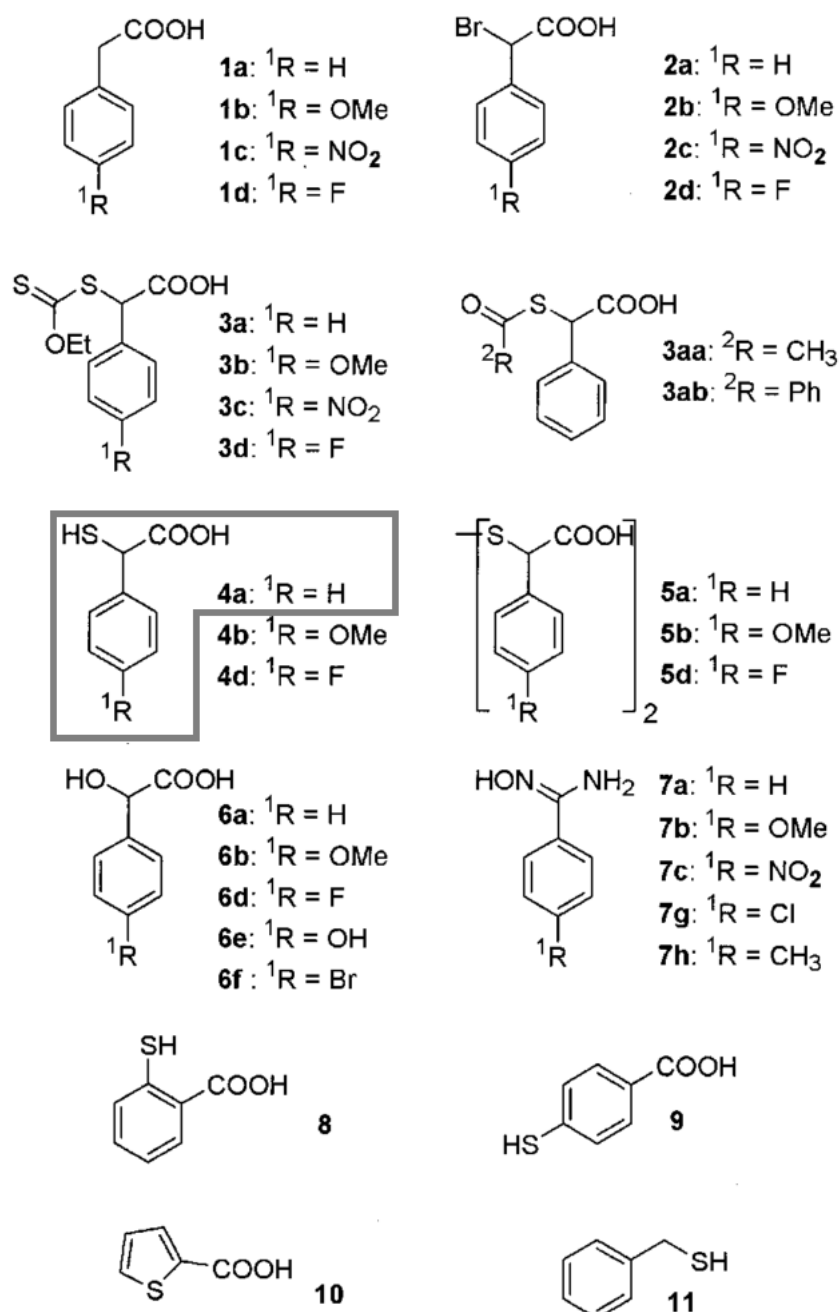


Figure 1.35. Structure of thiomandelic acid and analogues. Source: Mollard *et al.* [143]

ferent than to dizinc enzymes. Liénard *et al.* [104] crystalized monozinc CphA in complex with D-captopril, which revealed a coordination of the carboxylate with the zinc ion on x-ray diffraction (1.66 Å resolution, PDB accession code: 2QDS), while the thiol group was oriented towards the hydrophobic region of the active site, in close spatial proximity with Phe156, Arg233, Trp87, Leu161 and Val67. A D-captopril derivative, with the thiol replaced by hydroxyl (compound **9**), showed some inhibitory potency against CphA ($K_i = 189 \pm 12 \mu M$) but none against IMP-I, suggesting that the thiol is not essential for inhibition of B2 enzymes, but determinant for B1 enzyme inhibition [104]¹. In line with these findings were the several binding modes predicted in mod-

¹Inhibition assays methods for compound **9** in CphA and IMP-I are not detailed in the paper by Liénard *et al.*, but the methodology reported for assays with other inhibitors is: inhibitor at 100 μM ; enzyme at 0.03 to 0.7 nM; and substrate (imipenem and nitrocefin) at 20 to 200 μM , at a minimum of two inhibitor concentration and in its

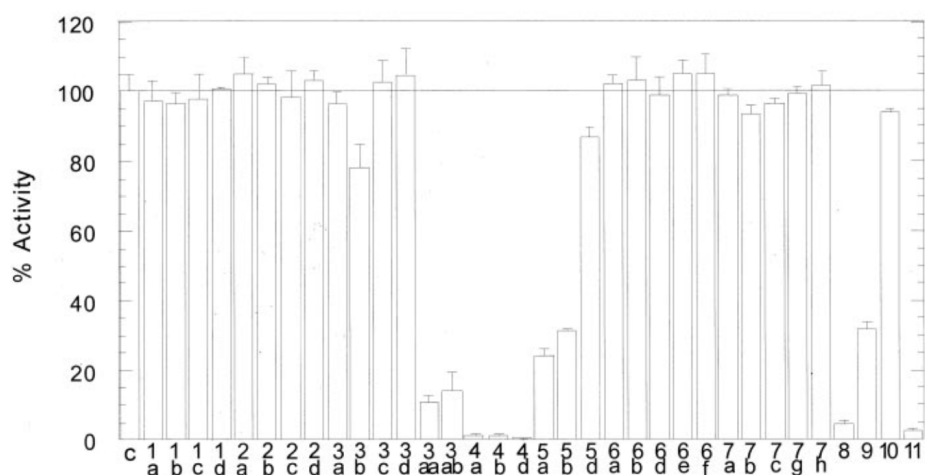


Figure I.36. Thiomandelic acid and analogues inhibition of BclI. Source: Mollard *et al.* [143]

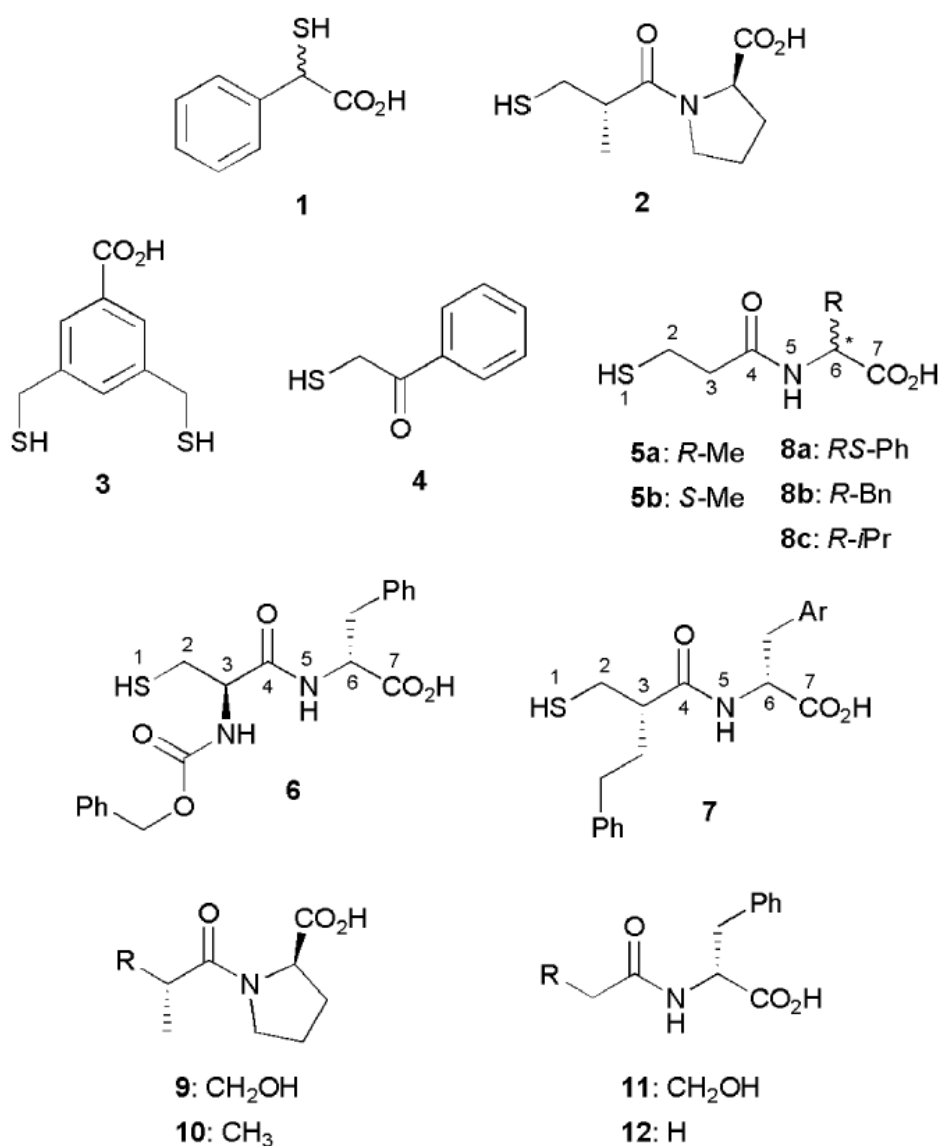


Figure I.37. Mercaptocarboxylates, and their non-sulfur counterparts (9-12), explored by Liénard *et al.* [104]

elling studies for compound **4** against CphA, coordinating either the thiol or the carbonyl group
 absence [104].

with the single Zn^{2+} in CphA, while the literature favours thiol-metal coordination on binding to dizinc MBLs [98, 116, 149, 150]. This suggests that the same inhibitor might coordinate differently with different MBLs [104], particularly where different metal stoichiometries are considered.

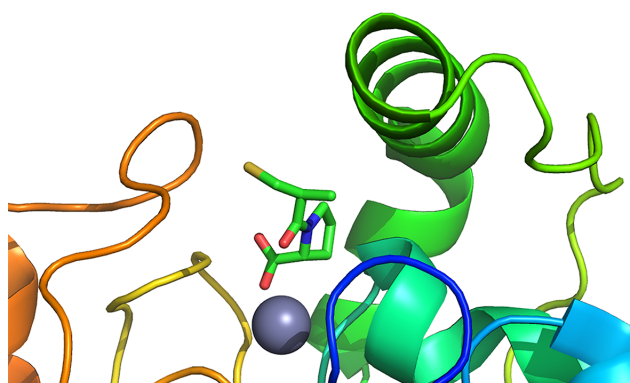
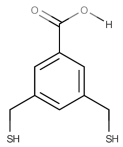
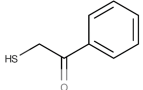


Figure 1.38. Captopril (in green) co-crystallized with CphA MBL (PDB: 2QDS, [104]). The sulfur group (yellow) is oriented upwards, towards the flap.

Compounds **5a** and **5b** were found to inhibit subclasses B1 and B3 enzymes, but not CphA. The modelling studies on CphA predicted the coordination of the carboxylate (on C-7) and the nitrogen on its imidic acid with the zinc ion, and the interaction of the thiol group with the hydroxyl sidechains of Thr119 and Thr157 [104]. Upon exploration of **5a** derivatives (**5b** was found to be less active, perhaps due to lack of β 3- β 4 loop interactions), substitutions on C-2 or C-3 positions yielded compounds prone to structural clashes in CphA active site, and substitutions on C-6 with bulkier hydrophobic groups (**8a**:RS-Ph; **8b**:R-Bn; **8c**:R-*i*Pr) and no substitutions on C-2 or C-3 carbons, produced compounds with K_{is} down to 19 nM for B1 and B3 MBLs and micromolar potencies for CphA, showing monozinc complexes on ESI-MS, coordinating C-7 carboxylate with the zinc ion and the thiolate group with the hydroxyl sidechains of Thr157 [104].

Table 1.12. Activity of mercaptocarboxylates explored by Liénard *et al.* [104]

Inhibitor	B1		B2	B3		
	IMP-I	BcII	CphA	LI	FEZ-I	
	3	0.36 ± 0.01	0.97 ± 0.2	0.09 ± 0.004	0.21 ± 0.01	0.3
	4	0.67 ± 0.09	2.7 ± 0.2	0.05 ± 0.02	0.24 ± 0.01	1

Captopril, developed in the 1970s to inhibit the angiotensin-converting enzyme, a metallo-enzyme with a zinc ion in its catalytic centre, and a therapeutic target for blood pressure diseases, was found to be an MBL inhibitor [150]. The structural basis for D- and L-captopril inhibition activity were studied in detail [101, 104, 150]. Both isomers (L-(S,S)- and D-(S,R)-captopril) are active

against MBLs, but D-captopril has been reported to be more potent against BclI, CphA [101, 150], NDM-1 [101, 151], IMP-1, VIM-2 and SPM-1 [101]. Brem *et al.* explored the binding of D-captopril in LI MBL in crystallization studies (PDB accession code: 2FU8), concluding that it coordinates with the metal ions through its thiol group [101] (Figure 1.39). Simplified captopril analogues were also studied as NDM-1 inhibitors, where a molecule of similar complexity was found with an IC_{50} of $\sim 1.5 \mu\text{M}$, along with a simpler molecule with a comparable inhibitory potency to captopril, with $\sim 10 \mu\text{M}$ were disclosed (Table 1.13) [152].

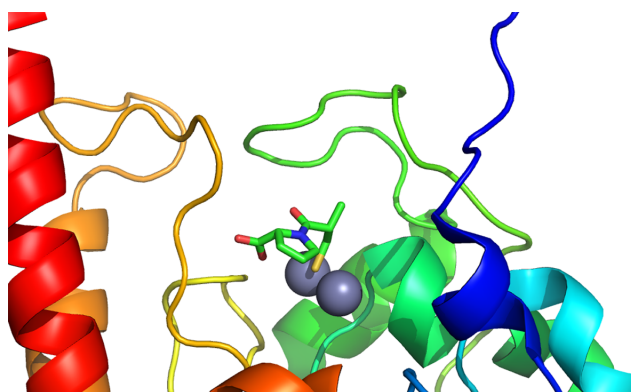
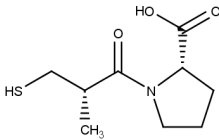
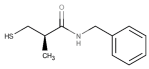
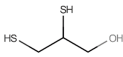


Figure 1.39. Captopril (in green) co-crystallized with LI MBL (PDB: 2FU8, [153]). The sulfur (yellow) can be seen coordinated with the zinc ions.

Table 1.13. Activity of D-captopril and captopril analogues against MBLs [152]

Inhibitor	IMP-1	NDM-1	Ref.
	7.2 ± 1.2	20.1 ± 1.5	[101]
	—	7.9 ± 0.1	[152]
	1.5 ± 0.2		[152]
	10.4 ± 1.0		[152]

On the wake of the works by Liénard and Mollard, Lassaux *et al.* studied the MBL inhibitory behaviour of the replacing the carboxylate by a phosphonate group on the already effective combination of thiols and carboxylates, by synthesizing and testing a series of mercaptophosphonate acids and their esters (Figure 1.40 and Figure 1.41) [154].

Compounds **1**, **10**, **11**, and **12** were the starting point for the structure activity relationship analysis. The ester form of compound **1**, (**1a**) did not present any inhibitory activity, while the acid form (**1b**) presented K_i up to $12 \mu\text{M}$, independently of zinc concentration. The C-5 fluorinated

derivative of **1b**, compound **13**, maintained similar inhibition profile for VIM-4 and FEZ-I, but a reduced activity towards CphA. Compound **10** showed very different behaviour between its ester (**10a**) and acid (**10b**) forms, with the acid form displaying activity strongly dependent on zinc concentration, perhaps due to chelation of zinc ions [154] and **10a** presenting low K_i against all three MBLs, independently of zinc concentration. Compound **11**, the only aliphatic of the four initial compounds, exhibited some activity against CphA in both forms and against VIM-4 in its acid form.

Compound **12** exhibited a good transversal inhibitory profile in both forms. The acid form was used as scaffold for deriving compounds **18** to **22** with several substitutions on the aromatic ring, all with a fair degree of activity and worthy of further exploration. An inspection of these results shows that there is a wide heterogeneity of behaviours of related molecules. Compounds **12a**, **22** and **10b** all display potent activity against CphA with fairly different structures and substitutions.

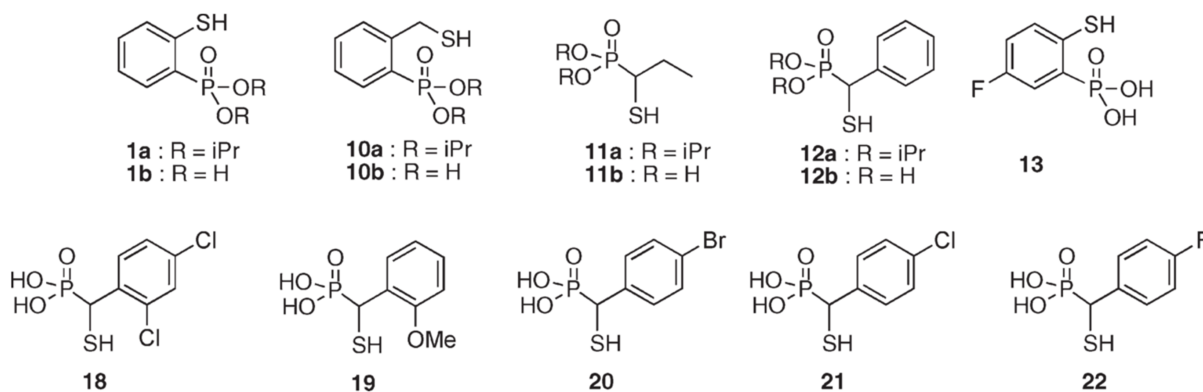


Figure I.40. Mercaptoposphonates library of potential MBL inhibitors [154].

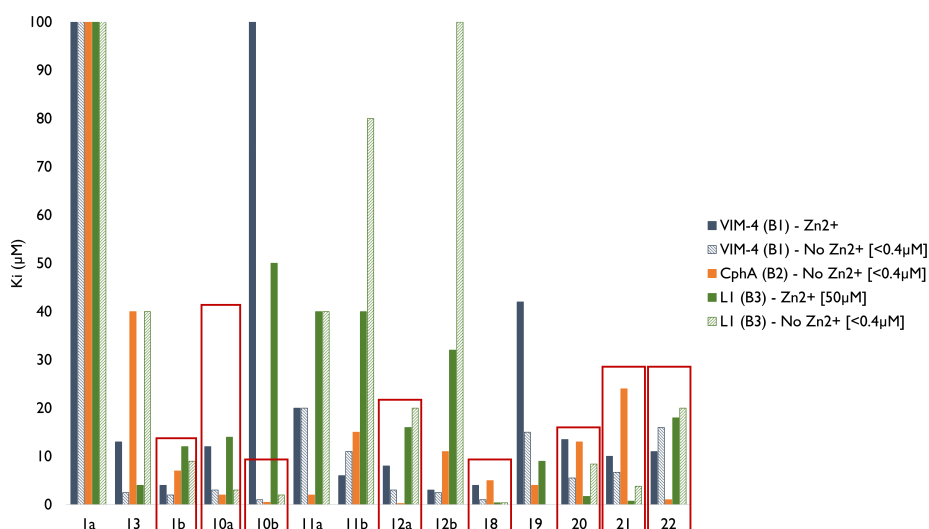


Figure I.41. Activity of mercaptoposphonates as MBL inhibitors [154].

Thiomaltol (Figure I.42) has shown promising results as a zinc-binding group in the development of matrix metalloproteinase inhibitors. Matrix metalloproteinases are involved in physiological functions like growth and wound repair, and also in pathological processes such as cancer and

arthritis. These enzymes contain a Zn^{2+} bound to a tri-Histidine site in hydrolysis of the connective tissue [155], and therefore, may have some common features with MBLs since both enzymes share Zn^{2+} moieties.

Thiomaltol was found to be a slow-binding inhibitor of Bla2 with a K_i of $85 \pm 30 \mu M$, coordinating its hydroxyl group with Zn^{2+} and its thione with an active site Lysine residue (Lys200) [156].

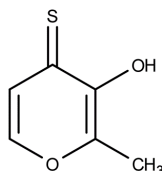


Figure 1.42. Thiomaltol structure [156].

Fragment-based screening of a 500 compound Maybridge™ library allowed the identification of 4-methyl-5-(tri-fluoromethyl)-4H-1,2,4-triazole-3-thiol (Table 1.14 - compound **10**) as a promising compound lead for development of an IMP-I inhibitor ($K_i=0.97 \pm 0.60$ mM) [87]. On the optimization of this lead compound, a family of molecules was synthesized (Figure 1.14 and Figure 1.15), with the thiol group found to be a requirement for IMP-I inhibitory activity (notice the absence of activity of compound **8**) while other substitutions had only modest effects on the inhibitory profile (from 1 mM (**1**) to $\sim 70 \mu M$ (**4i**)) [157].

Several compound **4** synthesis intermediaries, acylated thiosemicarbazides, showed high potency against IMP-I and were further explored specifically as leads by acylation of the hydrazine with bulky groups. The addition of pivalic acid led to lack of activity, the addition of anionic alkyl side-chains led to a modest increase in potency, and the addition of bulky aromatic groups led to the best results and were explored in kinetic analyses, with compound **31** reaching the lowest competitive K_i of $11 \pm 4 \mu M$ (Table 1.16), which is comparable with D-captopril ($\sim 12.5 \pm 2.4 \mu M$).

Regarding the binding mode, the nitro group was found to coordinate with the zinc ions, forming oxygen-zinc interactions, the aryl groups establishing hydrophobic interactions with the $\beta 3$ - $\beta 4$ loop and the N-H bonds on the terminal thiourea establishing hydrogen bonds with Tyr227. The sulfur seems to have, at best, a modest role in this interaction [157].

Table 1.14. Inhibitory activities of 1,2,4-triazole-3-thiols against IMP-I [157].

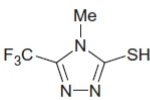
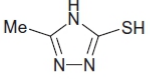
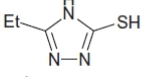
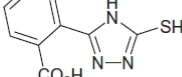
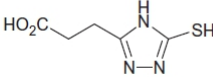
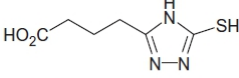
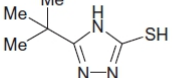
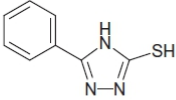
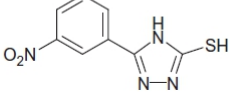
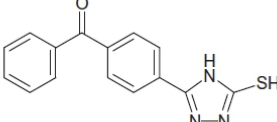
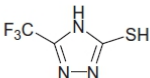
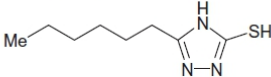
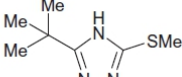
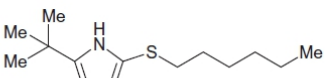
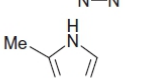
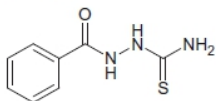
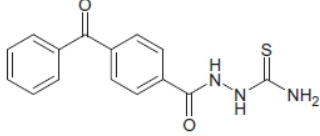
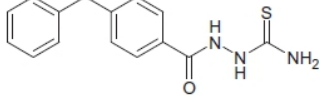
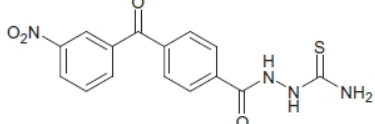
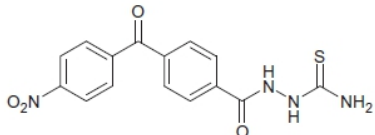
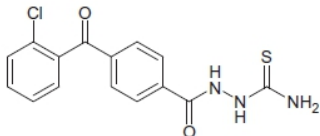
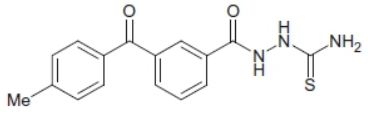
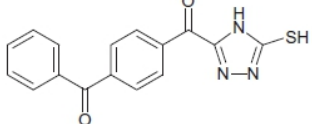
Compound	Structure	Inhibition % (1000 μ M)	Inhibition % (100 μ M)	Inhibition % (10 μ M)
1		51	—	—
4a		33	—	—
4b		32	—	—
4c		—	7	0
4d		—	10	10
4e		—	5	0
4f		32	—	—
4g		0	—	—
4h		—	—	Insoluble

Table 1.15. Inhibitory activities of 1,2,4-triazole-3-thiols against IMP-I (cont.).

Compound	Structure	Inhibition % (1000 μ M)	Inhibition % (100 μ M)	Inhibition % (10 μ M)
4i		—	44	10
4o		45	—	—
4p		—	—	Insoluble
7a		10	—	—
7b		—	—	Insoluble
8		0	—	—

— Not determined.

Table I.16. Inhibitory activities of selected compounds against IMP-I.

Compound	Structure	K_{ic} (μ M)	K_{iuc} (μ M)
3g		19 \pm 8	30 \pm 8
3i		13 \pm 4	26 \pm 7
3j		18 \pm 10	37 \pm 15
3k		16 \pm 7	15 \pm 5
3l		11 \pm 4	20 \pm 5
3m		14 \pm 4	13 \pm 2
3n		41 \pm 24	20 \pm 4
4i		75 \pm 30	56 \pm 10

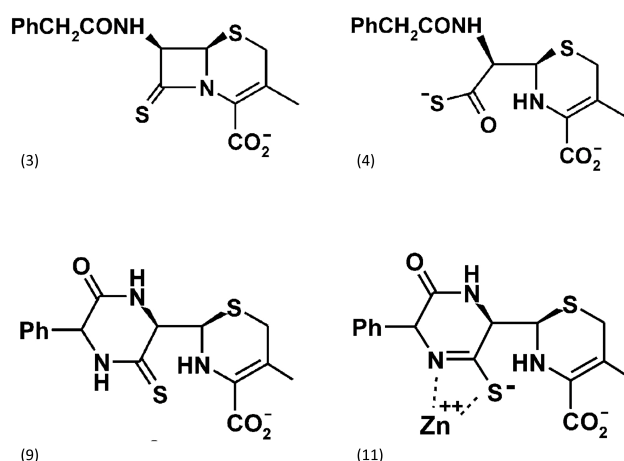
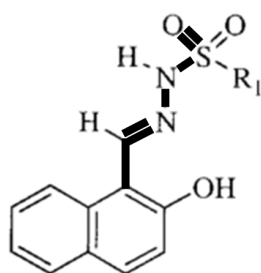


Figure I.44. Thioxocephalosporins [161].

Sulfonylhydrazones

Sulfonyl hydrazones resemble the lactam core of the cephalosporins (section lined in bold on Figure I.45) and have the ability to bind to divalent metal ions. These two properties spurred Siemann *et al.* to explore their potential as IMP-I inhibitors [162].

The substitution of both the radical on the sulfonyl group and the radical on the hydrazine by bulky aromatic groups seems to be the major drive of good interactions as can be seen by the big difference in IC_{50} of compound **6e** in comparison with compounds **6a-d** (Figure I.46) and the consistently lower IC_{50} of column (c) compounds with anthracyl group in Figure I.47. The substitution on the sulfonyl group brought some subtle improvements to the affinity of the compounds. Molecules **6 - 10** have halogen atoms with increased affinity for the heavier, bigger and less electronegative atoms. The replacement with a naphthyl moiety (compounds **12** and **13**) produced the best results, reinforcing the idea that large substituents with weak electron-withdrawing properties on the sulfonyl group improve the IMP-I affinity of sulfonylhydrazones [162].



Compound	R_1	IC_{50} (μ M)
1	Ph (4- CH_3)	40 ± 3.5
2a	Ph [4- $C(CH_3)_3$]	16 ± 1.3
3	Ph (4- NO_2)	48 ± 4.6
4	Ph (4- OCH_3)	40 ± 3.8
5	Ph (4- OCF_3)	25 ± 2.4

Figure I.45. Sulfonyl hydrazone derivatives (part I) [162].

Compound	R ₂	IC ₅₀ (μM)
6a		17.5 ± 1.6
6b		6.3 ± 0.6
6d		10.5 ± 1.0
6e		>250

Figure I.46. Sulfonyl hydrazone derivatives (part 2) [162].

Tiophenes

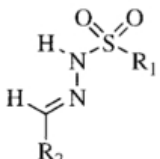
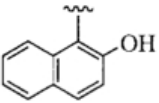
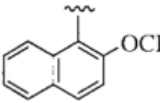
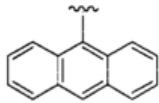
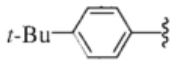
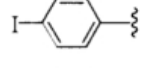
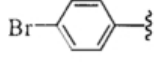
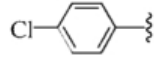
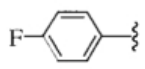
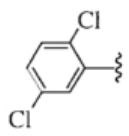
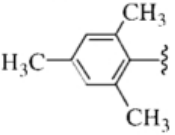
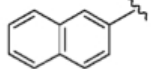
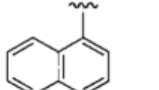
Shen *et al.* set out to explore the inhibitory activity of substituted thiophenes against NDM-1 hydrolysing meropenem (Figure I.48) [65].

The molecule with lowest IC₅₀ on steady-state kinetics was compound **2**. However, on studying the activities at various inhibitor concentrations and determining MICs, compound **4** was the most promising candidate. It is worth noting that the two benzyl rings on compound **2** appear to increase potency dramatically when compared with compound **1**.

1.7.2.3.2 Dicarboxylates

Dicarboxylates have been found to inhibit MBLs with potencies reaching IC₅₀ of 3 nM [99]. Several scaffolds have been used to bridge the carboxylates: alkanes (succinic acids) [99, 163], alkenes, furan, pyridine rings, and thiazolidine rings.

Toney *et al.* explored substitutions of succinic acids with hydrophobic groups and their inhibitory activity against IMP-1 [99] (Figure I.49). Succinic acid alone did not show any inhibitory activity (IC₅₀=6300 μM), nor did monosubstituted succinic acid (IC₅₀=490 μM), methyl and methyl/ethyl substituted compounds (IC₅₀>10000 μM). In contrast, disubstituted compounds with aromatic substituents revealed good inhibitory activities [99] (compounds **1**, **2**, **3**, **9**, **10** and **11** in Figure I.49), and even higher when the substitutions are in *S,S* configuration (compounds **1**, **2**, **9**, **10**

Compound		IC_{50} (μM) ^a			
		(a)	(b)	(c)	
	R_1	$R_2 =$			
2		16	3.8	2.2	
6		17.5	6.3	3.0	
7		25	13	4.6	
8		55	19	7.0	
9		150	55	13.5	
10		40	10	4.5	
11		10	4.8	1.6	
12		10	4.0	1.6	
13		20	6.2	2.4	

^a The precision of the IC_{50} determinations was within the range of $\pm 10\%$.

Figure I.47. Sulfonyl hydrazone derivatives (part 3) [162].

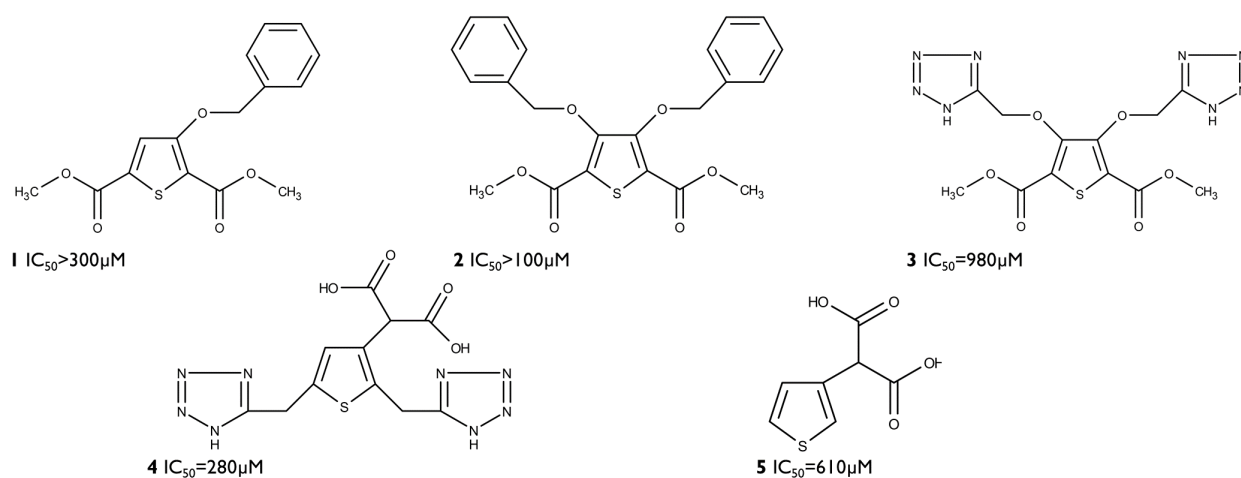
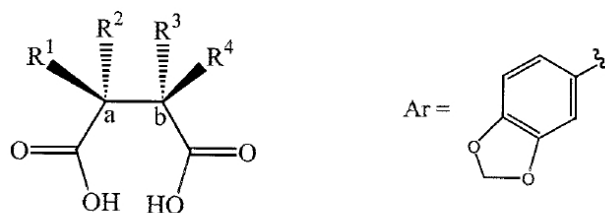


Figure I.48. Thiophene inhibitors [65]).

and II). The high resolution crystal structures obtained and molecular modelling studies indicate that the inhibitor binds to IMP-I overlaying one of its carboxylates with a carboxylate of imipenem,

establishing a salt bridge with Lys161 and Asn167, while the other carboxylate group seems to replace the water molecule that is coordinated with the two zinc atoms and probably works as the nucleophile (hydroxyl) in the hydrolysis reaction.



Compound	R^1	R^2	R^3	R^4	a,b-Configuration	IMP-1 IC ₅₀ μM
1	ArCH ₂	H	ArCH ₂	H	<i>S,S</i>	0.009
2 ^a	PhCH ₂	H	PhCH ₂	H	<i>S,S</i>	0.0027
3 ^a	H	PhCH ₂	H	PhCH ₂	<i>R,R</i>	≥ 0.21
4 ^b	H	PhCH ₂	PhCH ₂	H	<i>R,S</i>	200
5	H	H	H	H		6300
6	H	H	PhCH ₂	H	<i>S</i>	490
7	H	H	CH ₃	CH ₃		>10000
8	H	H	CH ₃	CH ₂ CH ₃	<i>Racemate</i>	>10000
9	PhCH ₂	H	(<i>R</i>)-PhCH(CH ₃)	H	<i>S,S</i>	0.013
10	PhCH ₂	H	(<i>S</i>)-PhCH(CH ₃)	H	<i>S,S</i>	≥ 2.7
11	ArCH ₂	H	PhCH ₂	H	<i>S,S</i>	0.0037

^a D, L pair.

^b Meso compound.

Figure 1.49. Substitutions on succinic acid and their inhibition of IMP-I [99]

In 2005, Moloughney *et al.* screened⁴ the National Cancer Institute (NCI) chemical diversity set, selecting compounds that inhibited >80% of IMP-I activity at 40 μM as leads [163].

The five resulting compounds (Figure 1.50) are succinic acid derivatives (except for **114609**) and exhibited affinities down to $K_i=3.3\pm 1.7 \mu\text{M}$. These activities appear to be less potent than the succinic acid derivatives reported by Toney *et al.* [99] and the authors attribute this difference in potencies to monosubstitution of the succinic acid (compounds **20707** and **140905**) or disubstitution with a fused ring system (compounds **6138** and **9746**) [163].

Alkenes

Meiji Seika Kaisha Ltd. (Tokyo, Japan) discovered an MBL inhibitor derived from maleic acid, named ME1071 (Figure 1.51) [164].

This inhibitor potentiates the activity of ceftazidime and carbapenems (it is particularly active in combination with biapenem that is, together with meropenem, one of the weakest substrates for IMP-I and VIM-2 [66, 92, 164, 165] against MBL-producing *P.aeruginosa* [164] and Enterobacteriaceae isolates, being weaker in species producing NDM MBLs than in those with VIM or, particularly, IMP [165]). Kinetic studies indicate that ME1071 has a higher affinity ($K_i=0.41\pm 0.1 \mu\text{M}$) for IMP-I in comparison with other studied MBL inhibitors such as mercaptoacetic acid, mercaptopropionic acid or SB238569, but lower than J-110,441 and J-111,225 (both with lower

⁴Using nitrocefin as substrate up to 60 μM in 50mM MOPS buffer (pH 7.0) at final volume of 100 μL and inhibitor concentration up to 40 μM .

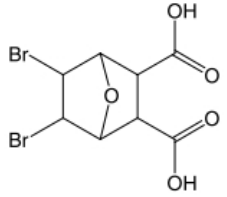
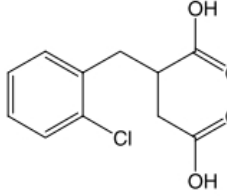
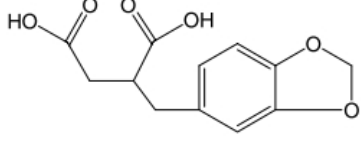
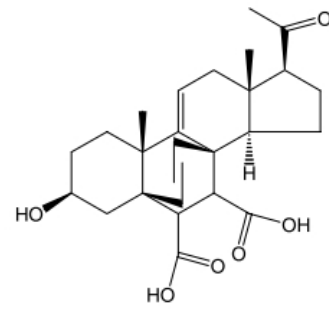
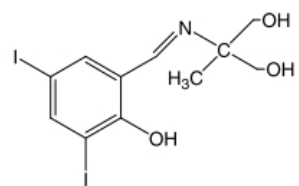
Compound (NSC#)	Structure	IC ₅₀ (μ M)	K _i (μ M)
6138		17	17.3 \pm 2.8
20707		5.0	3.3 \pm 1.7
140905		6.0	5.3 \pm 2.9
9746		8.9	6.7 \pm 1.5
114609		1.2	4.7 \pm 2.4

Figure I.50. Lead compounds selected after NCI chemical diversity set screening by Moloughney *et al.* [163].

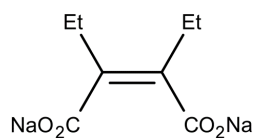


Figure I.51. ME1071, an MBL inhibitor derived from maleic acid [164].

K_i (Section 1.7.2.3.1) and the 2,3-(S,S)-disubstituted succinic acids reported by Toney *et al.* [99].

Phthalic acid derivatives

A compound library screening on the IMP-I subclass enzyme using nitrocefin as substrate, followed by another screening for combination effect with meropenem or ceftazidime against IMP-I producing *E. coli* yielded a phthalic acid derivative as lead compound (Figure 1.52) with an IC_{50} of $16.0 \mu\text{M}$ [166].

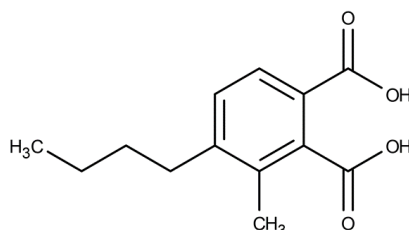
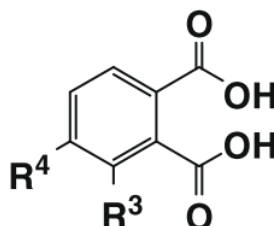


Figure 1.52. Phthalic acid derivative [166].

While phthalic acid itself is not active against IMP-I, some of its derivatives are. Substitutions at C-3 appear to be particularly important for IMP-I activity (Figure 1.53) and Hiraiwa *et al.* synthesized several 3-substituted phthalic acid derivatives, most of which presented good inhibitory activity against IMP-I, especially when substituted with a bulky phenyl group, a phenol or a benzoic acid (Figure 1.54) [166].



Compd	R ³	R ⁴	IMP-1 inhibitory activity IC_{50} (μM)
1	Me	<i>n</i> -Bu	16.0
5a	H	<i>n</i> -Bu	243
5b	H	<i>t</i> -Bu	>300
5c	H	Ph	>300
5d^a	H	H	>100
5e^a	H	Me	>300

Figure 1.53. Phthalic acid derivatives [166].

Most compounds with good IC_{50} showed a good combination effect with Biapenem against *P. aeruginosa*, with compound **12f** being the most potent (Table 1.17) [166].

From compound **12f** the same group synthesized more molecules, 3-alkyloxy and 3-aminophthalic acid derivatives [167].

The 3-alkyloxy compounds (Figure 1.55) were active against IMP-I, showing stronger inhibition (IC_{50}) for longer alkyl chains with bulky groups (**5e** and **5f**) but that were not always correlated

Compd	R ³	IMP-1 inhibitory activity IC ₅₀ (μM)
12a	-Me	160
12b		13.2
12c		0.968
12d ^a		2.44
12e		1.75
12f		1.55
12g		207
12h		17.9
12i		2.25

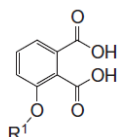
Figure 1.54. 3-substituted phthalic acid derivatives [166].

with good combination effects with Biapenem, particularly in *P. aeruginosa* strains with efflux pump (PAOI). In contrast, compounds with higher IC₅₀ demonstrated stronger combination effects (**5g-i**) in *P. aeruginosa* strains, with and without efflux pump (KG5002) [167].

Some 3-amino phthalic acid derivatives showed good inhibitory potency, with piperidine **16b** showing particularly good IC₅₀ and combination effects (Figure 1.56) [167]. Similarly to alkyloxy derivatives, compounds with longer alkyl chains (compound **10**) had worse combination effects in species

Table 1.17. Combination effect of 3-substituted phthalic acid derivatives with biapenem against *P. aeruginosa* [166].

Inhibitor	MIC of Biapenem ($\mu\text{g/mL}$)	
	<i>P. aeruginosa</i> w/ efflux system	<i>P. aeruginosa</i> w/o efflux system
I2a	4	16
I2b	1	4
I2c	≤ 0.5	2
I2d	2	8
I2e	0.5	4
I2f	≤ 0.25	1
I2g	64	64
I2h	32	64
I2i	0.5	2
Biapenem only	64-128	64-128



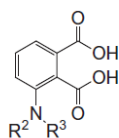
Compd	R ¹	IMP-1 inhibitory activity IC ₅₀ (μM)	Combination effect (50 $\mu\text{g/mL}$) with BIPM MIC of BIPM ($\mu\text{g/mL}$)	
			<i>P. aeruginosa</i> KG5002 /pMS363 (ΔmexAB)	<i>P. aeruginosa</i> PAO1/pMS363
5a	-H	>300	NT	NT
5b	-CH ₃	142	NT	NT
5c		7.40	NT	NT
5d		5.10	NT	NT
5e		2.00	4	64
5f		1.70	0.5	64
5g		18.8	2	8
5h		47.8	16	16
5i		21.4	16	16
		(BIPM alone)	64-128	64-128

Figure 1.55. 3-alkoxy phthalic acid derivatives [167].

with efflux pump.

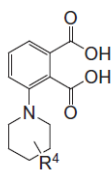
The piperidine derivatives showed worse results (lower IC₅₀ and increased affinity for the efflux system) for compounds with longer alkyl chains (**I6g**), but an apparent correlation between hydroxyl substitutions on the third or fourth position and good inhibitory properties and good combination effects (compounds **I6c-f**), with piperidine **I6e** demonstrating the most potent combination effect [167].

This last compound **I6e** showed not only a dose-dependent combination effects with biapenem but also with ceftazidime and meropenem, although some *P. aeruginosa* strains were not sensitive to ceftazidime or meropenem, suggesting that additional resistance mechanisms may be in place [167].



Compd	R ²	R ³	IMP-1 inhibitory activity IC ₅₀ (μM)	Combination effect (50 μg/mL) with BIPM	
				MIC of BIPM (μg/mL)	
				<i>P.aeruginosa</i> KG5002 /pMS363 (Δ mexAB)	<i>P.aeruginosa</i> PAO1/pMS363
	-H	-H	300	NT	NT
10	-H		13.1	1	64
14	-CH ₃	-CH ₃	94.5	4	4
16a			2.80	0.5	4
16b			10.8	≤0.5	4
(BIPM alone)				64–128	64–128

Figure I.56. 3-amino phthalic acid derivatives [167].

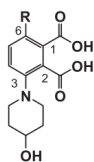


Compd		IMP-1 inhibitory activity IC ₅₀ (μM)	Combination effect (50 μg/mL) with BIPM	
			MIC of BIPM (μg/mL)	
			<i>P.aeruginosa</i> KG5002/pMS363 (Δ mexAB)	<i>P.aeruginosa</i> PAO1/pMS363
16b		10.8	≤0.5	4
16c		2.70	≤0.5	1
16d		2.10	0.5	2
16e		2.70	≤0.25	1
16f		2.60	1	2
16g		25.6	8	32
16h		2.30	≤0.5	16
16i		3.70	≤0.25	2
(BIPM alone)			64–128	64–128

Figure I.57. Piperidine derivatives [167].

Crystallographic studies of compound **16e** showed that the carboxylates establish interactions with the Zn²⁺ atoms and hydrogen bonds with Asn233 and Lys224; the piperidine moiety with a hydrophobic pocket that comprises Val61, Phe87, His118 and Asp120; the hydroxyl group establishes a hydrogen bond with Ser119, suggesting an explanation for the lower IC₅₀ of compound **16e** versus **16b** (Figure I.56) that lacked the hydroxyl group; and finally the phthalic acid scaffold establishes hydrophobic interactions with the Trp64 residue on the β 3- β 4 loop and His263 that forms Zn2 [100].

The observation of a pocket suitable for interactions next to the 6-position of the phthalic acid led the authors to synthesize 3,6-disubstituted phthalic acids derivatives (Figure I.58).



Compound	R	IMP-1 inhibitory activity IC ₅₀ (μ M)	Effect of combination (50 μ g/mL) with BIPM MIC of BIPM (μ g/mL)	
			<i>P. aeruginosa</i> KG5002/pMS363 (Δ mexAB)	<i>P. aeruginosa</i> PAO1/pMS363
1	-H	2.70	≤ 0.25	1
7	-CH ₃	0.700	≤ 0.25	1
12	-F	17.5	1	2
13		0.270	≤ 0.25	0.5
15		4.10	≤ 0.25	1
		(BIPM only)	64–128	64–128

Figure 1.58. 3,6-disubstituted phthalic acid derivatives [100].

Compound **7** is about four times more potent than **16e** (compound **1** on Figure 1.58) and probably establishes more hydrophobic interactions with Trp64 and His263 with the phthalic acid scaffold and the additional methyl. Compound **12** has a poor interaction with IMP-I likely due to repulsion between the fluoro moiety and the hydrophobic residues Trp64 and His263. Compound **15** has a worse IC₅₀ than **16e** but the combination effect seems to be similar. The observation of the pocket structure, suggests that it establishes favourable interactions with Trp64 and His263. Finally, compound **13** presents the best inhibitory profile and is 10 times more potent than **16e**, with a promising combination effect with biapenem in *P. aeruginosa* with and without efflux system [100].

1.7.2.3.3 Heterocyclics

Pyrrole derivatives

Supported by the literature on the antibacterial effect of the pyrrole nucleus and pyrrolo[2,3-d]pyrimidines the IMP-I inhibitory activity of pyrrole derivatives was explored and six compounds with considerable inhibitory activity were disclosed [168]. The pyrrole nucleus alone (compounds **1c** and **1d**, Figure 1.59) did not produce an inhibitory effect, while the pyrrolo[2,3-d]pyrimidine nucleus produced various degrees of inhibitory activity (compounds **3a-10**), with compound **3b** affording the lowest K_i ($12 \pm 4 \mu$ M) (Figure 1.59) [168]. This compound was submitted to docking simulations, coordinating the oxygen of the methoxy group with the Zn²⁺ ions on the IMP-I active site, establishing hydrophobic interactions with the tryptophan on the β 3- β 4 loop and hydrogen bonds between the N3 on the pyrimidine ring and an oxygen of an active site glutamate [168].

Biphenyltetrazoles

By screening of a Merck library, Toney *et al.* found that biphenyl tetrazoles (BPTs) linked to various heterocyclic aromatic rings had inhibitory activity against an imipenem-resistant *Bacteroides fragilis*

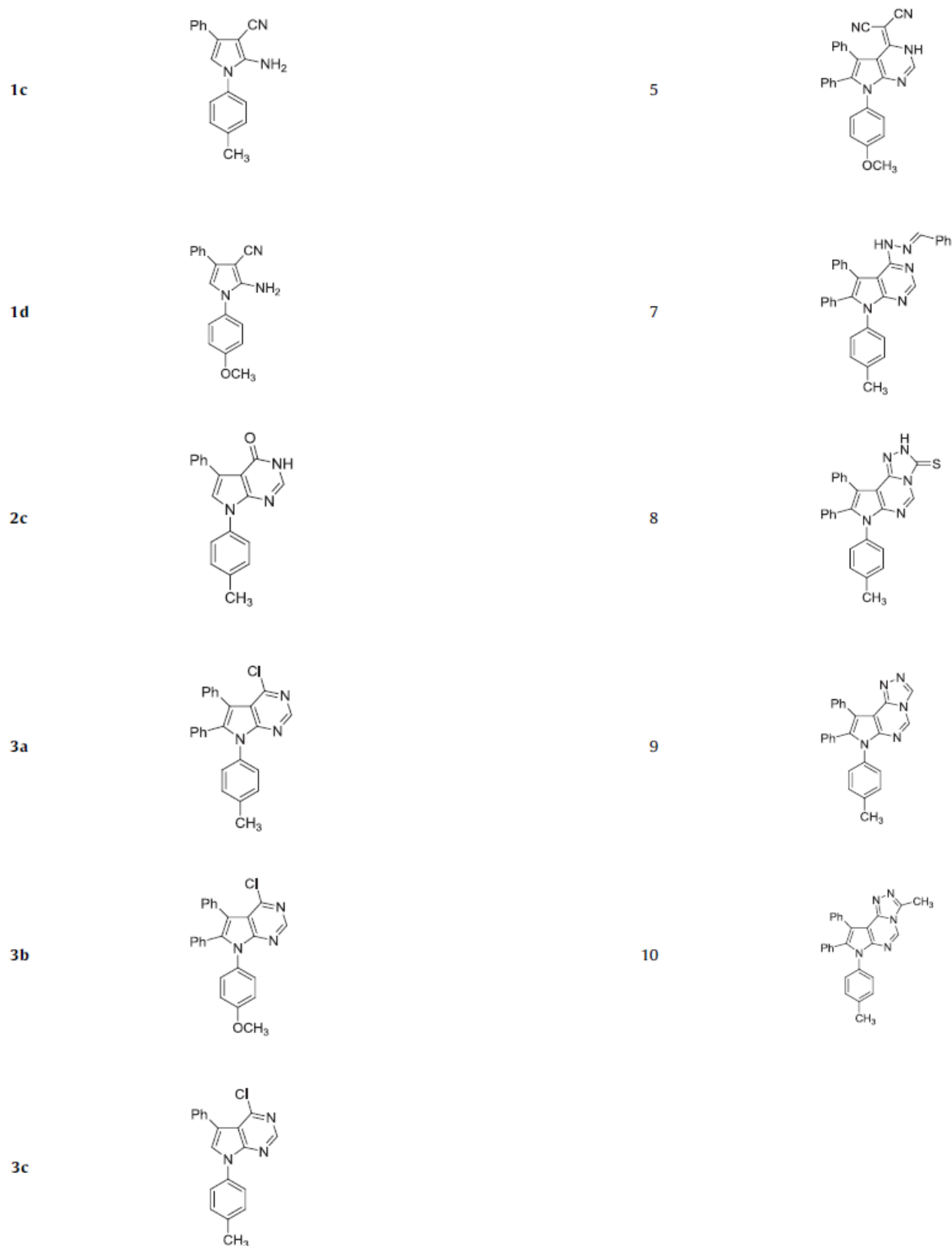


Figure 1.59. Pyrrole derivatives with IMP-I inhibitory activity [168].

MBL [169]. These bulky compounds were shown to have biological activity in combination with imipenem on a *B. fragilis* culture [169].

The tetrazole ring coordinates with Zn^{2+} , while the two phenyl rings establish hydrophobic interactions with the hydrophobic residues on the $\beta 3$ - $\beta 4$ loop [169]. The biphenyl ring system with

ortho tetrazole group was found to be important for enzyme inhibition as meta or para positions of the tetrazole group resulted in IC_{50} of 10-20 mM and replacing the tetrazole for a carboxamide resulted in $IC_{50} > 20$ mM [169].

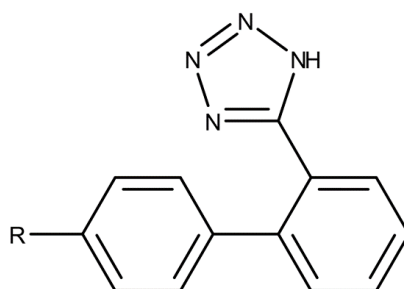


Figure 1.60. Biphenyl tetrazole structure [169]).

Still, the raw biphenyl tetrazole structure (Figure 1.60) displayed only a 860 ± 60 μ M IC_{50} . The *para* substitution of the biphenyl system with a methyl was enough to bring IC_{50} down to 160 ± 20 μ M and the substitution with various heterocyclic aromatic groups led to compounds with increased potencies (Figure 1.61). Biological activity testing against a culture of *B. fragilis* by measuring zones of inhibition revealed a combination effect with imipenem and penicillin G but not with rifampicin [169].

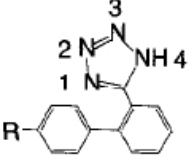
The same group explored the biological activity of another series of BPTs against *B. fragilis* and *P. aeruginosa* using nitrocefin as substrate [170]. The unsubstituted parent compound (Figure 1.62) presented a IC_{50} of 200 ± 8 μ M for *B. fragilis*. The addition of a chlorine at position two of the phenyl ring (compound **2**, Figure 1.63) has an almost 7-fold improvement in IC_{50} (30 ± 10 μ M). The exploration of other substitutions reveal that the chlorine at position two is likely involved in an important interaction with the protein as most compounds with that substitution (compounds **2**, **5**, **7**, and **9**) and compounds with $-CF_3$ in place of chlorine at position two (compounds **11** and **23**) present a good inhibitory profile, whereas compounds with other substitutions seem to be weaker inhibitors [170].

Diverse heterocyclics

Feng *et al.* explored the broad-spectrum activity of N-heterocyclics against CcrA, ImiS and LI as representatives of subclasses B1, B2 and B3, respectively (Figure 1.64) [171].

The steady-state inhibition results are summarized in Figure 1.65. The lack of inhibition of ImiS by **1a**, **1c**, **3a** and **3b** suggests that the sulfur in the azole ring is determinant for the inhibition of this enzyme. The lack of inhibition of LI by **2a**, **2b**, **3a** and **3b** is not clear. The only broad spectrum diacid was **1b**, with low micromolar potency against all subclasses [171].

The determination of the MICs were consistent with the steady-state studies, enhancing the potential of compound **1b** that reduced the MIC of cefazolin against CcrA and LI by half and the MIC of imipenem against ImiS by one eighth [171].



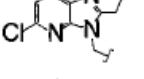
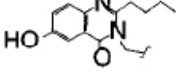
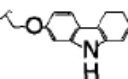
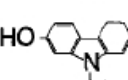
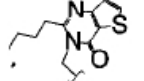
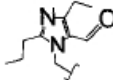
Compound	R	IC ₅₀ (μ M)	
		Metallo- β -lactamase	DHP-I
L-809,022	H	860 \pm 60	>1000
L-158,507	CH ₃	160 \pm 20	>1000
L-808,509		110 \pm 9	>500
L-809,559		4 \pm 1	>250
L-809,558		42 \pm 10	>250
L-158,678		3.5 \pm 0.4	240 \pm 12
L-158,817		1.8 \pm 0.4	>100
L-159,061		1.9 \pm 0.2	>100
L-809,339		42 \pm 7	>100
L-809,370		6 \pm 1	>100
L-161,189		0.30 \pm 0.02	120 \pm 10
L-159,906		0.4 \pm 0.1	>100
L-707,581		7 \pm 3	190 \pm 8

Figure 1.61. Biphenyl tetrazole derivatives - 1998 series [169].

Following the exploitation of pyrrole and pyrrolo-pyrimidines, the same group investigated the inhibitory potential of novel tetrahydropyrimidines and pyrrole derivatives for IMP-I [172]. An initial screening of enzyme activity in the presence of fixed substrate (70 μ M) and inhibitor (10 μ M) concentrations was performed, selecting six thiopyrimidine derivatives and six pyrrole derivatives for further kinetic analysis - determination of inhibition mode and inhibition constants.

Compound **5c**, a thiopyrimidine, (Figure 1.66) was shown to be the overall best inhibitor, with a

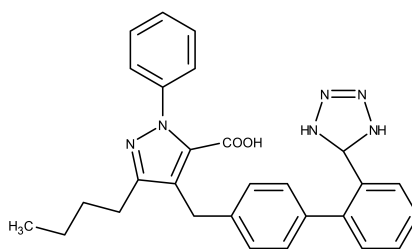
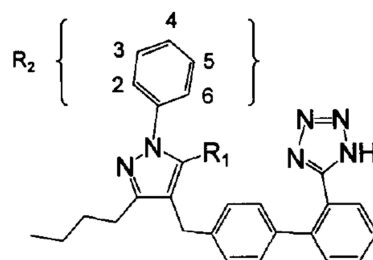


Figure 1.62. Biphenyl tetrazole - unsubstituted parent compound [170].



Compound	R ₁	R ₂	IC ₅₀ (μM)		K _i ^{app} (μM)
			<i>B. fragilis</i> MBL	IMP-1 MBL	DHP-I
1	CO ₂ H	Ph	200 ± 8	>200	590 ± 100
2	CO ₂ H	Ph (2-Cl)	30 ± 10	>200	350 ± 100
3	CO ₂ H	Ph (3-Cl)	190 ± 20	>200	425 ± 60
4	CO ₂ H	Ph (4-Cl)	230 ± 4	>200	430 ± 70
5	CO ₂ H	Ph (2,3-Cl ₂)	37 ± 3	>200	310 ± 20
6	CO ₂ H	Ph (2,4-Cl ₂)	80 ± 40	>200	400 ± 100
7	CO ₂ H	Ph (2,5-Cl ₂)	50 ± 20	>200	380 ± 130
8	CO ₂ H	Ph (2,6-Cl ₂)	100 ± 40	>200	500 ± 50
9	CO ₂ H	Ph (2,4,6-Cl ₃)	33 ± 2	>200	800 ± 300
10	CO ₂ H	Ph (2-CH ₃)	80 ± 20	>200	470 ± 80
11	CO ₂ H	Ph (2-CF ₃)	40 ± 20	>200	380 ± 130
12	CO ₂ H	Ph (2-NO ₂)	120 ± 30	>200	640 ± 140
13	CO ₂ H	Ph (2-Ph)	180 ± 20	65 ± 10	420 ± 70
14	CO ₂ Et	Ph	100 ± 20	>200	250 ± 50
15	CO ₂ Et	Ph (2-Cl)	170 ± 20	200 ± 20	250 ± 50
16	CO ₂ Et	Ph (3-Cl)	170 ± 60	76 ± 10	450 ± 50
17	CO ₂ Et	Ph (4-Cl)	290 ± 60	70 ± 25	380 ± 120
18	CO ₂ Et	Ph (2,3-Cl ₂)	100 ± 20	175 ± 20	170 ± 10
19	CO ₂ Et	Ph (2,4-Cl ₂)	100 ± 40	66 ± 10	480 ± 20
20	CO ₂ Et	Ph (2,5-Cl ₂)	100 ± 10	60 ± 30	80 ± 25
21	CO ₂ Et	Ph (2,4,6-Cl ₃)	80 ± 30	>200	450 ± 80
22	CO ₂ Et	Ph (2-CH ₃)	70 ± 30	>200	--
23	CO ₂ Et	Ph (2-CF ₃)	22 ± 10	>200	--
24	CO ₂ Et	Ph (2-NO ₂)	18 ± 2	>200	--
25	CO ₂ Et	Ph (2-Ph)	>200	150 ± 10	--

Figure 1.63. Biphenyltetrazole derivatives - 1999 series [170].

K_i of 19 ± 9 μM. Docking experiments of (R)-5c shown that the sulfur on the thiolate moiety coordinated with the zinc ions, while the nitrogen on the pyrimidine ring formed hydrogen bond with

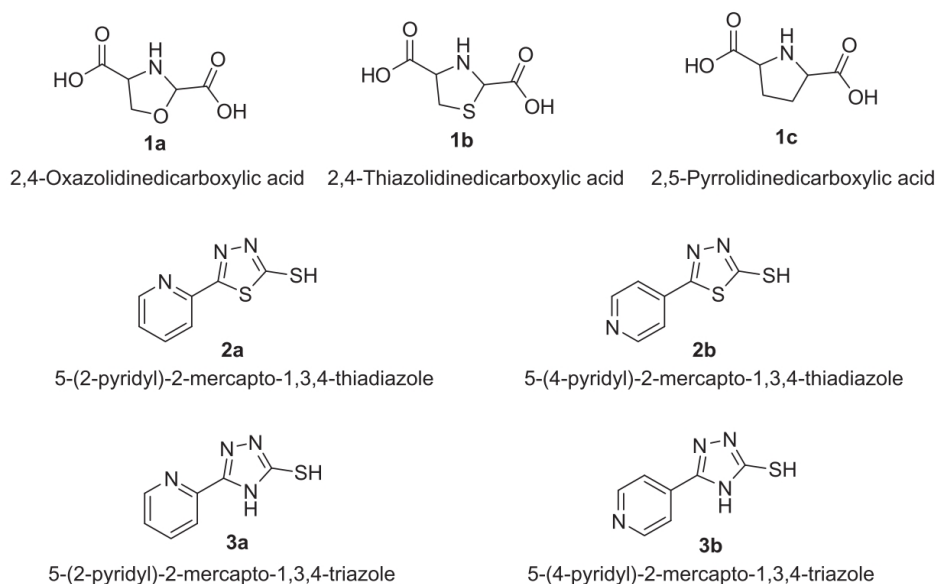


Figure 1.64. N-heterocyclics synthesized and explored by Feng *et al.* [171].

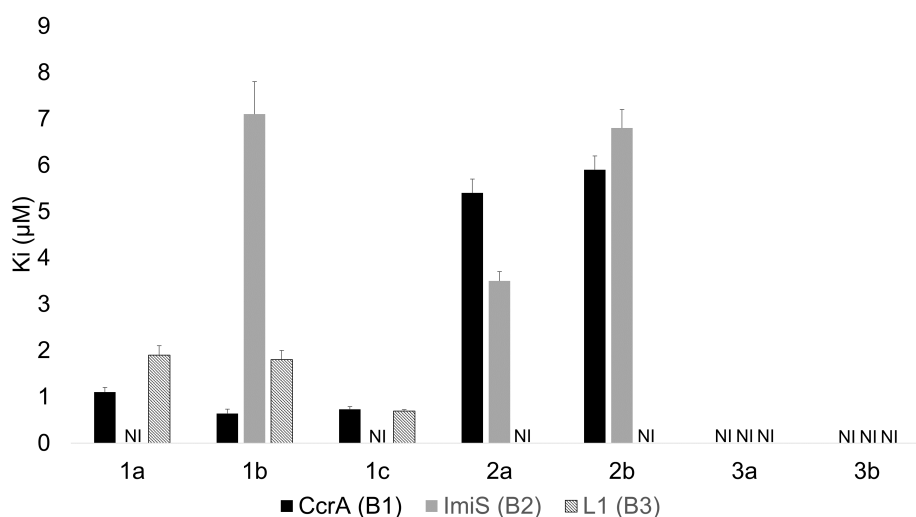


Figure 1.65. Steady-state inhibition studies of N-heterocyclics by Feng *et al.* [171]. NI: No inhibition at 50 μM .

active site Lys224, and the methoxybenzene moiety and the benzene ring of the styryl group established hydrophobic interactions with Val67, Phe87 and Val61. The lowest energy conformation of (S)-**5c** does not coordinate any group with the zinc ions but establishes hydrogen bonds between (1) the oxygen of the methoxy group and the backbone N-H of Asn233 and (2) between one of the nitrogens of the pyrimidine ring and the nitrogen atom of Lys224. Hydrophobic interactions are also established between the aromatic rings and the hydrophobic residues on the β 3- β 4 loop (Phe87, Val61 and Val67) [172].

The most potent inhibitor of the pyrrole series was compound **7a** (Figure 1.66), with a K_i of $21 \pm 10 \mu\text{M}$. The docking experiment revealed coordination between the nitrogen of the amino group of the inhibitor and the zinc ions. The proton on the N-H group of the inhibitor establishes a hydrogen bond with a nitrogen atom on His197. Similarly to **5c**, hydrophobic interactions are established between aromatic rings and the hydrophobic residues of the β 3- β 4 loop (Phe87 and

Val67).

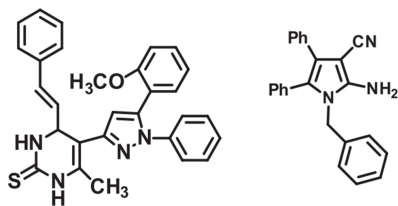


Figure I.66. Compounds **5c** and **7a** from Hussein *et al.* [172]).

1.8 Structure-based drug design

1.8.1 Docking

Docking is an *in silico* technique that simulates the binding of a ligand to a protein and estimates the affinity of that bond. The first docking methods considered both ligand and protein as rigid molecules, with movements limited to rotation and translation of the ligand in the active site. More recent approaches, still feasible in acceptable timespans with regular computers, consider increased ligand flexibility by also rotating bonds while others, more computer intensive, consider flexible protein structures as well. The latter are not practical for screening as they require increased computation time.

The docking software used in this thesis was GOLD v5.2.2 from Cambridge Crystallographic Data Centre [173] that uses a genetic algorithm to explore the range of ligand and protein conformations. Genetic algorithms are based on genetics principles such as chromosomes, mutations and crossing-over, and parent and children populations. In the application of the genetic algorithm to docking, GOLD performs the following steps:

1. Assignment of several sets of poses of both protein and ligand with angles of rotating bonds and mapping between features (hydrogen-bond, donor protons, acceptor lone pairs and ring centres) of both molecules → the “chromosomes”;
2. Least-squares fitting procedure to maximise the overlap between the features of both molecules;
3. Calculation of fitness of the resulting pose by the scoring function;
4. Biased probabilistic selection of the poses with higher fitness scores;
5. Application of genetic operators on the poses selected in step four (“parent chromosomes”) that produced “children chromosomes”:
 - (a) “Crossover” exchanged parts of the configuration data between two parent chromosomes creating two new children chromosomes → combines information from two chromosomes, generating two children chromosomes;
 - (b) “Mutation” replaced a value in the configuration by a new random value → introduces random perturbations, generating one new chromosome.
6. Replacement of the least fit members of the original population (see step 4) of chromosomes by the children chromosomes.
7. Repetition from step three until a predefined limit is reached and choosing of the best solution (highest fitness).

For each ligand pose GOLD applies a scoring function that estimates the binding affinity between the ligand and the protein. Scoring functions can be roughly classified in three major categories:

1. **Force-field** functions, such as GoldScore, estimate affinity by applying the non-bonded terms of molecular mechanics force fields;
2. **Empirical** functions, such as ChemScore, PLP and CHEMPLP, estimate affinity by summing the partial contributions of several interaction terms like van der Waals, hydrogen bond, intramolecular, and solvation energies;
3. **Knowledge-based** functions, such as PMF and DrugScore, use statistics of the observations of geometry distributions collected from high-quality X-ray protein-ligand complexes to estimate affinity [174].

In this thesis, CHEMPLP was used as it is the standard function in GOLD and has been observed to produce the best results in GOLD software on the DUD test set [175]. Additionally, it performs much faster than GoldScore, the previous standard scoring function in GOLD, which is important for screening purposes.

1.8.2 Pharmacophore modelling

A pharmacophore is the ensemble of steric and electronic features that is necessary to ensure the optimal supramolecular interactions with a specific biological target structure and to trigger (or to block) its biological response. While not a real molecule itself, the pharmacophore is an abstract concept that accounts for the common molecular interaction capacities of a group of compounds towards their target structure [176]. In addition to the electronic features such as hydrogen bond acceptors and donors, positive and negative ionizable groups, pi-stacking groups, and hydrophobic regions [177] it is of utmost importance that the relative orientation of these groups towards each other is taken into account to consider the 3D structure of the active site and the ligands in the pharmacophore model.

Pharmacophore models can be structure- or ligand-based. In a structure-based model the active site of the protein is the scaffold for the determination of pharmacophoric features like hydrogen bond acceptors and donors, positive and negative ionizable groups, and hydrophobic regions. In a ligand-based model, known ligands of the protein are superimposed on a 3D space and their pharmacophoric features are identified.

In both cases, a 3D model is built with the ensemble of features determined, and will be used for mapping functional groups of the candidate molecules in a screening process, considering, in addition to the functional groups themselves, distance constraints between features, and angle and torsion constraints between oriented features (e.g. hydrogen bonds) [177]. When building the models, it is possible to include volume exclusion spheres that will help the screening process to filter out molecules with evident steric clashes with the receptor, by considering either the structure of the receptor or common shape of the known ligands.

In order to screen a library of compounds against a pharmacophore model, multiple poses of the

compounds will be generated and then tested on the pharmacophore 3D model. Typically, a least squares method is employed to reduce the deviation between ligand and pharmacophore features. Additional 2D substructure filters usually reduce computation time and improve efficiency.

Pharmacophore modelling is thus an effective and quick method to screen large compound libraries.

Chapter 2

Aims

The work described in this thesis aimed primarily to identify candidate molecules to be developed as IMP-I MBL inhibitors.

Therefore, to achieve this main goal, the following aims were pursued:

1. To generate a structure-based pharmacophore model from the IMP-I X-ray crystallographic structure;
2. To screen compound libraries from the NCI, ZINC and DrugBank databases against the pharmacophore model;
3. To perform molecular docking of the most promising hits obtained by pharmacophore screening;
4. To select the best fitting docking compounds for *in vitro* testing.

Chapter 3

Methods

3.1 Preparation of the compound library

Three compound libraries were used in this work: the NCI database; the ZINC database [178]; and the Drugbank database [179].

From NCI and ZINC databases, compounds were selected and filtered with the parameters described in Table 3.1. The DrugBank database was not filtered with these parameters given that the molecules in that database are either marketed drugs or drugs in-development, and thus assumed to be drug-like.

Table 3.1. Selection parameters for the NCI, ZINC and DrugBank databases.

Parameter	NCI <small>(accessed on 05-May-2015)</small>	ZINC <small>(accessed on 07-May-2015)</small>	DrugBank <small>(accessed on 01-Apr-2015)</small>
Molecular weight (g/mol)	0-500	32-500	N.A.
Number of rotatable bonds	0-10	0-10	N.A.
logP	-7-5	-4-6	N.A.
Number of hydrogen donors	N.A.	0-10	N.A.
Number of hydrogen acceptors	N.A.	0-20	N.A.
Functional group restriction	No aldehydes and 0-2 acid groups	N.A.	N.A.
Total number of compounds	6,963	5,075	7,034

The NCI and ZINC databases subsets were downloaded in SMILES format and converted to structure data format (SDF) with Molecule File Converter, version 15.6.29.0, 2015, ChemAxon (<http://www.chemaxon.com>). The DrugBank database was readily downloaded in SDF format.

The compound library was then processed with Calculator, version 15.6.29.0, 1998-2015 ChemAxon Ltd. for determining the 3D structure under Merck Molecular Force Field (MMFF94) [180], generating up to five tautomers and five stereoisomers and calculating the protonation state at pH 7.5.

Considering the extensive literature on thiol MBL inhibitors, thiol molecules were selected with the support of the structural query capability of Instant JChem 15.5.11.0, 2015, ChemAxon and had their protonation state recalculated at pH 14 in order to deprotonate the thiol and the carboxylic acid groups. Finally, in order to comply with technical specificities of CCDC GOLD for the docking experiments, the order of the atoms on the SDF file of the thiol molecules was rearranged so that the sulfur atoms were the first atoms in the file with a custom python script developed in house by a former PhD student.

After all preparation steps were carried out, a total of 57,779 compounds were obtained, considering all the tautomers and stereoisomers.

3.2 Selection and preparation of the target protein

At least five IMP-I structures have been crystalized and are available on the PDB co-crystalized with different candidate inhibitors, with codes IDD6 (Res.: 2.0 Å) [98], IJJT (Res.: 1.8 Å) [99], IJJE (Res.: 1.8 Å) [99], 3WXC (Res.:2.1 Å) [100], and 4CIG (Res.:1.71 Å) [101].

All five structures were downloaded in PDB format and co-crystalized ligands were removed from the protein structures and re-docked on the same structure and on all others (cross-validation). The root mean square deviation (RMSD) found on the pose with the best fitness score and the lowest RMSD of all poses, both in relation to the original ligand pose can be seen in Figure 3.1.

Protein IDD6 presents the seemingly better results, with RMSDs no higher than eight and finding the best fitness in the poses most similar to the ligand binding mode exhibited in the crystalized structure, meaning that GOLD is seemingly predicting a correct binding mode. Structure IDD6 presented, however, a rotation of the C α -C β bond of Phe51 [98] in order to accommodate the phenyl group of the inhibitor that was not present in any of the other four structures. As this seemed the exception rather than the rule, IJJT was the most balanced option, with almost perfect correlation between the RMSD of the pose with the best fit and the lowest RMSD (Figure 3.1) and consistent results between IJJT and IJJE ligands that are very similar in structure [99]. In all structures, except IDD6, the binding pose of the mercaptocarboxylate sourced from IDD6 is not achieved, due to the position of Phe51 sidechain clashing with the phenyl group of the mercaptocarboxylate.

In practical terms, the protein structure of the A chain of IJJT was prepared for docking using the Prepare Protein protocol of Discovery Studio, using standard configurations, deleting waters and ligands, deleting protein-metal bonds, and setting pH for protonation at 7.5.

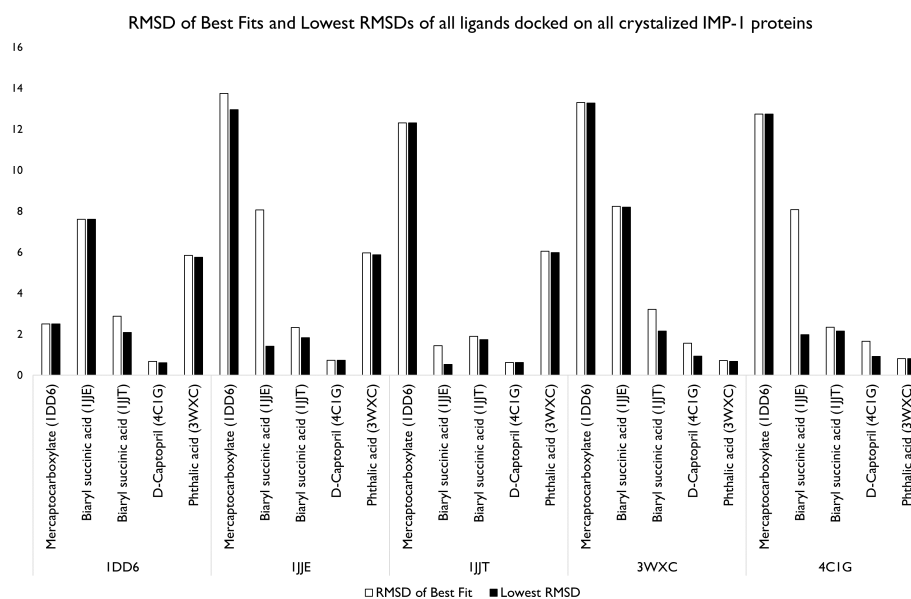


Figure 3.1. RMSD of the poses with the best fitness score and the lowest RMSD of all poses, both in relation to the original ligand pose.

3.3 Validation of reported IMP-I inhibitors

After a literature search on MBL inhibitors on March 8, 2015¹, 681 compounds were drawn from 47 papers [87, 98, 99, 104, 112, 139, 143, 150, 153, 154, 156–166, 168–172, 181–201] in MarvinSketch from ChemAxon 15.6.29.0 from 29-06-2015 and were prepared in the same way as the library compounds, as described in Section 3.1. Additionally, K_i , IC_{50} and/or inhibition % data was collected for each compound, as well as the MBL tested on each inhibition assay.

3.3.1 Molecular Docking

The 681 compounds with MBL inhibitory activity were docked in the IJJT protein with the GOLD configurations described in Table 3.2 and exported through GoldMine for statistical analysis.

Inhibition assay data of each compound was plotted against the GOLD PLP Fitness score and the strength and direction of the monotonic relationship between the two parameters was measured with Spearman's ρ . In order to disregard compounds with no activity in which the correlation is predictably weaker, molecules in the 4th quartile of each enzyme inhibition parameter were filtered out of the analysis.

Results of the correlation analysis are shown in Tables 3.4 to 3.5.

Each table summarizes the correlations between each parameter (IC_{50} , K_i , or Inhibition %) and three sets of molecules: (1) all molecules; (2) BI MBLs; and (3) IMP-I. These sets are not mutually exclusive and represent the available data for each compound in each literature reference collected

¹A literature search was performed on ISI Web of Knowledge with the search terms “metallo-beta-lactamase” AND “inhibitors”

Table 3.2. Docking configurations for validation runs.

Parameter	Setting
Genetic algorithm settings	
Search efficiency	100%
Protein	
Cavity	11 Å radius centered on Zn2
Metal atoms coordination geometry	
Zn1	Tetrahedral
Zn2	Bipyramidal trigonal
Ligand	
Number of GA runs per ligand	10
Intramolecular H-bonds	No
Flip ring corners	No
Flip amide bonds	No
Flip planar nitrogens	Yes
Flip pyramidal nitrogens	Yes
Flip protonated carboxylic acids	Yes
Use of Torsion Angle Distributions	Yes
Ligand search options Run	
Early termination	No
Generate Diverse solutions	No
Fitness function	
Fitness Function	ChemPLP
Constraints	
	(used only for molecules with thiol groups)
Scaffold constraint	Yes
Constraint weight	5

as many studies focused on only one MBL or on one specific subclass while others performed assays on representatives of all MBL subclasses. Given the focus of this work, only IMP-1 was validated in separate.

These results show a particularly good association between lower K_i values and higher GOLD fitness scores, reflecting this technique's ability to distinguish between stronger and weaker inhibitors (Table 3.3). Correlation between lower IC_{50} and higher fitness scores is less pronounced, but still present (Table 3.4). Percentage of inhibition was used as an initial measurement for screening libraries at steady state concentrations and was present in very few sources, thus the small number of molecules that did not provide enough numbers for a solid correlation and did not reach

Table 3.3. Literature validation results - Docking Ki.

Enzyme	N ^l	Spearman's ρ	p-value	Scatterplot
Any MBL	446	-0.4617	<0.001	
BI MBLs	342	-0.5171	<0.001	
IMP-1	115	-0.4123	<0.001	

^l This is the number of positions obtained with the 681 molecules.

Table 3.4. Literature validation results - Docking IC₅₀.

Enzyme	N ^l	Spearman's ρ	p-value	Scatterplot
Any MBL	997	-0.2708	<0.001	
B1 MBLs	768	-0.3665	<0.001	
IMP-1	458	-0.1327	0.004	

^l This is the number of positions obtained with the 681 molecules.

Table 3.5. Literature validation results - Docking % Inhibition.

Enzyme	N ¹	Spearman's ρ	p-value	Scatterplot
Any MBL	90	-0.0523	0.624	
BI MBLs	75	-0.0434	0.712	
IMP-1	75	-0.0434	0.712	

¹ This is the number of positions obtained with the 681 molecules.

statistical significance (Table 3.5).

3.3.2 Pharmacophore modelling

The same set of literature molecules was used to validate the pharmacophore model after the same procedure used for docking and described in the section above. The results are summarized in Tables 3.7 to 3.8.

Table 3.6. Literature validation results - Pharmacophore modelling (K_i).

Enzyme	N^l	Spearman's ρ	p-value	Scatterplot
Any MBL	1326	-0.2872	<0.001	
B1 MBLs	1120	-0.2837	<0.001	
IMP-1	375	-0.1689	0.001	

^l This is the number of positions obtained with the 681 molecules.

The correlations are weaker for pharmacophore modelling as compared to previous docking results. Still, moderate correlations can be seen between higher Pharmacophore modelling Fit Value and lower K_i values, indicating that the technique is sensitive to stronger and weaker inhibitors (Figure 3.6). The larger number of positions tested in this technique is probably detrimental to the correlation as a great number of Fit Values will exist for the same K_i , IC_{50} or Inhibition % largely increasing variance, influencing even a non-parametric parameter such as Spearman's ρ .

Table 3.7. Literature validation results - Pharmacophore modelling (IC₅₀).

Enzyme	N	Spearman's ρ	p-value	Scatterplot
Any MBL	3333	-0.1583	<0.001	
BI MBLs	2590	-0.0408	0.038	
IMP-1	1565	-0.0440	0.082	

¹ This is the number of positions obtained with the 681 molecules.

Table 3.8. Literature validation results - Pharmacophore modelling (% Inhibition).

Enzyme	N ^l	Spearman's ρ	p-value	Scatterplot
Any MBL	259	-0.0808	0.195	
B1 MBLs	208	-0.0912	0.190	
IMP-1	208	-0.0912	0.190	

^l This is the number of positions obtained with the 681 molecules.

3.4 Pharmacophore modelling runs

In this thesis, Discovery Studio 2.5 from Accelrys Software Inc. was used to perform the pharmacophore analysis.

Using the protein structure prepared with the Prepare Protein protocol (see section 3.2), the Interaction Generation protocol of Discovery Studio was used to build the pharmacophore model from the active site of IMP-I. This protocol generates an interaction map of the active site considering the following as pharmacophore features:

1. Hydrogen-bond acceptors

- 1.1. sp or sp^2 nitrogens that have a lone pair and charge less than or equal to zero;
- 1.2. sp^3 oxygens or sulfurs that have a lone pair and charge less than or equal to zero;
- 1.3. Non-basic amines that have a lone pair;
- 1.4. Nitrogens, oxygens, or sulfurs (except hypervalent) that have a lone pair and charge less than or equal to zero;

2. Hydrogen-bond donors

- 2.1. Non-acidic hydroxyls;
- 2.2. Thiols;
- 2.3. Acetylenic hydrogens;
- 2.4. NHs (except tetrazoles and trifluoromethyl sulfonamide hydrogens);

3. Hydrophobic

- 3.1. A contiguous set of atoms that are not adjacent to any concentrations of charge (charged atoms or electronegative atoms), in a conformation such that the atoms have surface accessibility, including phenyl, cycloalkyl, isopropyl, and methyl;

4. Negatively charged

- 4.1. Negative charges not adjacent to a positive charge;

5. Negatively ionizable

- 5.1. Atoms or groups of atoms that are likely to be deprotonated at physiological pH, such as:
 - i. Trifluoromethyl sulfonamide hydrogens;
 - ii. Sulfonic acids (centroid of the three oxygens);
 - iii. Phosphonic acids (centroid of the three oxygens);
 - iv. Sulfinic, carboxylic, or phosphinic acids (centroid of the two oxygens);
 - v. Tetrazoles;

- vi. Negative charges not adjacent to a positive charge;

6. Positively charged

- 6.1. Positive charges not adjacent to a negative charge;

7. Positively ionizable

- 7.1. Atoms or groups of atoms that are likely to be protonated at physiological pH, such as:

- i. Basic amines;
- ii. Basic secondary amidines (iminyll nitrogen);
- iii. Basic primary amidines, except guanidines (centroid of the two nitrogens);
- iv. Basic guanidines (centroid of the three nitrogens);
- v. Positive charges not adjacent to a negative charge;

8. Ring aromatic

- 8.1. Aromatic rings with five or six member atoms.

Once the pharmacophore features were mapped, volume exclusion spheres were added manually on the atoms of the binding site residues. Since the interaction generation protocol produces a large number of features, they were clustered by Discovery Studio using a hierarchical clustering method [202], the Unweighted Pair Group Method with Arithmetic mean (UPGMA) algorithm, computing the distances between features to calculate the clusters. The clusters were then reviewed and averaged manually to reduce the number of features.

The pharmacophore generated had eight features, two being hydrogen-bond donors; four being hydrogen-bond acceptors, and two being hydrophobic. Nine volume exclusion spheres were added manually.

The ligand-pharmacophore mapping was computed with the Screen Library protocol of Discovery Studio. This protocol enumerates several possible pharmacophores from the input pharmacophore model by generating combinations of the existing pharmacophore features, and maps an input library of ligands, i.e. a pharmacophore model that has eight features with the *minimum features* parameter set to four, the *maximum features* parameter set to six, and the *maximum subset of pharmacophores* parameter set to 100 will generate 100 pharmacophore with subsets of four, five and six features and will run the ligands against those 100 pharmacophores.

The Screen Library protocol was run with the standard configuration and the setup summarized in Table 3.9.

Table 3.9. Screen Library configurations.

Parameter	Setting
Minimum features	2
Maximum features	8
Maximum subset of pharmacophores	100

3.5 Docking calculations

Docking runs were performed with GOLD. Four separate protocols (Table 3.10) were prepared for four different purposes:

1. Initial docking screening of pharmacophore hits (A);
2. Initial docking screening of thiol pharmacophore hits (A-T);
3. Re-docking of first screening hits (B);
4. Re-docking of first screening thiol hits (B-T).

The reason for separate protocols for molecules containing thiol moieties is rooted in the literature where thiol inhibitors have repeatedly been found to coordinate with the deprotonated sulfur to the zinc ions in BI enzymes, displacing the bridging water molecule. GOLD preferably coordinates the deprotonated oxygen of the carboxylates, failing to reproduce the binding mode of captopril found in PDB entry 4CIG [101] if a scaffold constraint is not put in place.

For this purpose, a file with a single sulfur atom on the place of the bridging water molecule was created and input as a scaffold constraint with the standard constraint weight of 5. This parameter determines how strictly the ligand will be placed onto the scaffold location.

Table 3.10. Docking protocols.

Parameter	A	A-T	B	B-T
Genetic algorithm settings				
Search efficiency (%)	30	30	100	100
Protein				
Cavity	11 Å radius centered on Zn2			
Metal atoms coordination geometry				
Zn1	Tetrahedral			
Zn2	Bipyramidal trigonal			
Ligand				
Number of GA runs per ligand	5	5	10	10
Intramolecular H-bonds	No			
Flip ring corners	Yes			
Flip amide bonds	No			
Flip planar nitrogens	Yes			
Flip pyramidal nitrogens	No			
Flip protonated carboxylic acids	Yes			
Use of Torsion Angle Distributions	Yes			
Ligand search options Run				
Early termination	No			
Generate Diverse solutions	No			
Fitness function				
Fitness Function	CHEMPLP			
Constraints				
Scaffold constraint	No	Yes	No	Yes
Constraint weight	n.a.	5	n.a.	5

n.a. Not applicable.

Chapter 4

Results

In order to identify candidate molecules to be developed as IMP-I MBL inhibitors, the methods laid out in Chapter 3 were employed by generating a pharmacophore (Section 4.1) and screening the compound libraries, first with the structure-based pharmacophore (Section 4.2) and then with the molecular docking protocols (Section 4.3).

4.1 Generation of a structure-based pharmacophore model

The pharmacophore generated in Discovery Studio according to the methodology described in Section is depicted in Figure 4.1.

The blue sphere represents hydrophobic interactions and it is located near the β 3- β 4 flap that closes over the active site upon ligand binding, mainly near Trp28 and Val25 (Figure 4.2).

The green spheres represent hydrogen-bond acceptors and are located between the zinc ions, next to the sidechain NH_3^+ of Lys161, the backbone NH of Asn167, and the backbone NH of Ser80 (Figure 4.3).

The purple spheres represent hydrogen-bond donors and are located near the hydroxyl of the sidechain hydroxyde of Ser80 and the carbonyl oxygen on the sidechain amide of Asn167 (Figure 4.4).

Nine volume exclusion spheres were placed in locations that would help delimiting the active site without hindering the execution of the Screen Library protocol, specifically on Trp28, Val25, Val31, Phe51, Asp81, His197, His79, Cys158, and Gly166 (Figure 4.5).

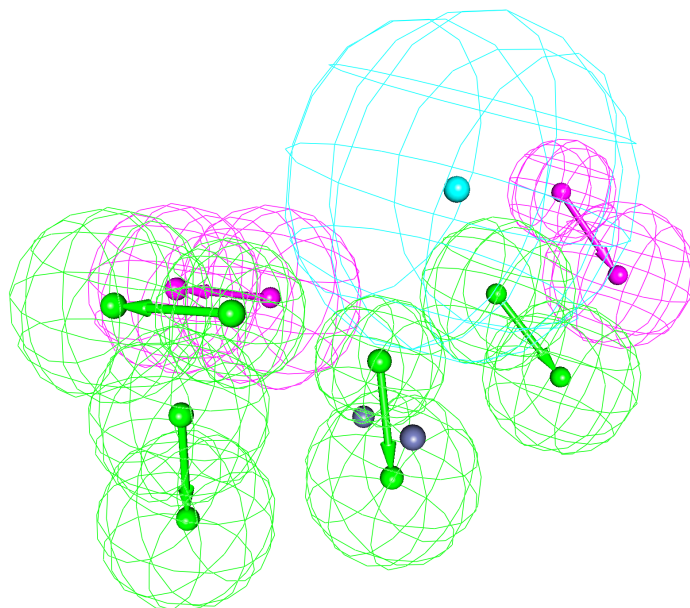


Figure 4.1. Structure-based Pharmacophore generated from IMP-I MBL. This figure was created using Discovery Studio.

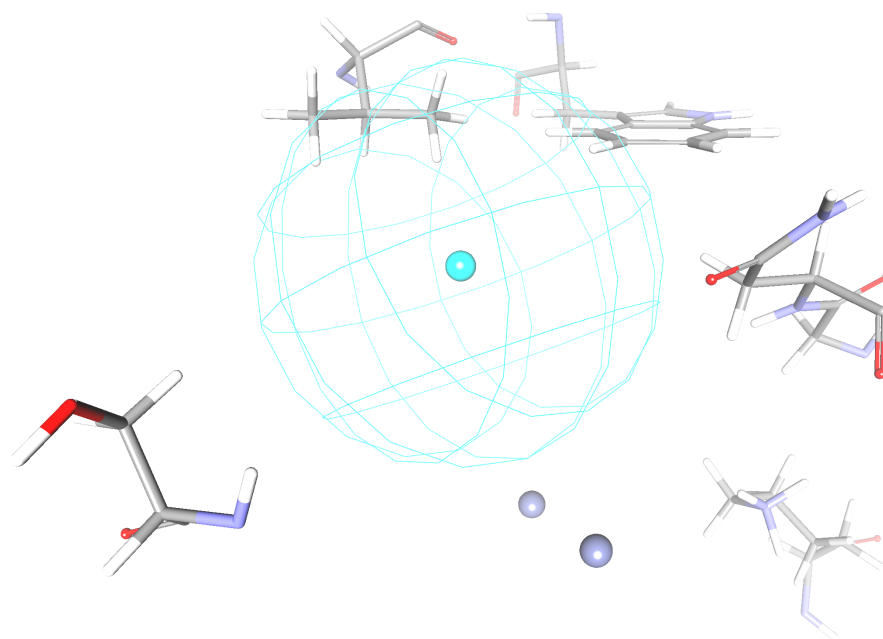


Figure 4.2. Pharmacophore feature: Hydrophobic. This figure was created using Discovery Studio.

4.2 IMP-I pharmacophore screening results

The compound library obtained from pooling query results from the NCI, ZINC and DrugBank databases was first screened with the pharmacophore model presented in the previous section.

From this initial screening, 257,002 positions of the 57,779 compounds were selected that fitted

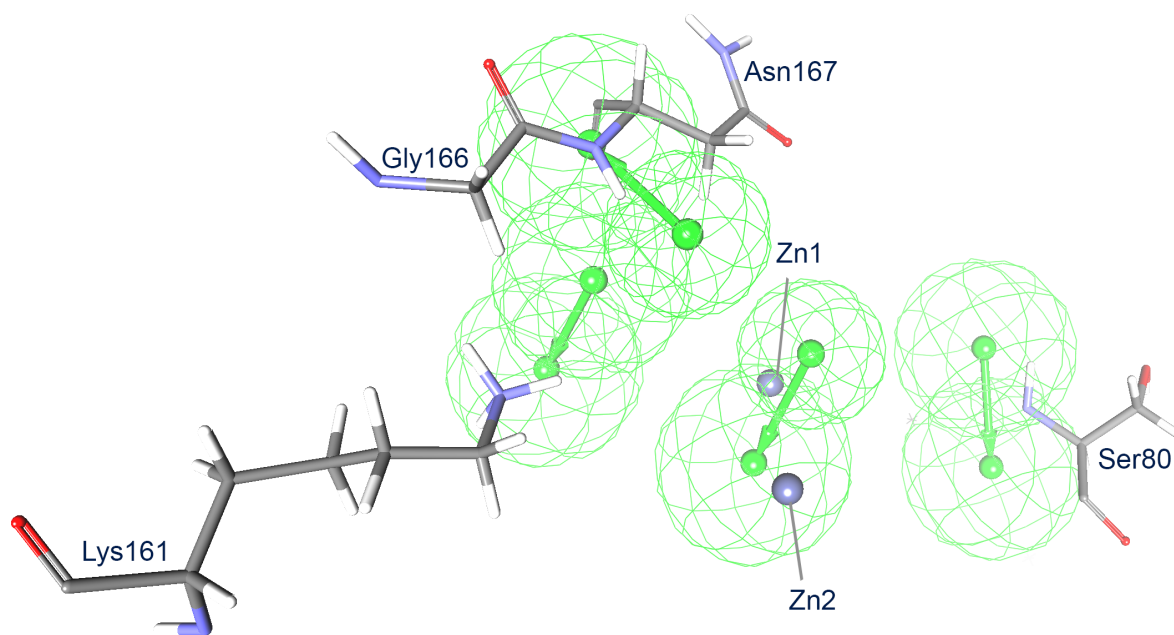


Figure 4.3. Pharmacophore feature: Hydrogen-bond acceptors. This figure was created using Discovery Studio.

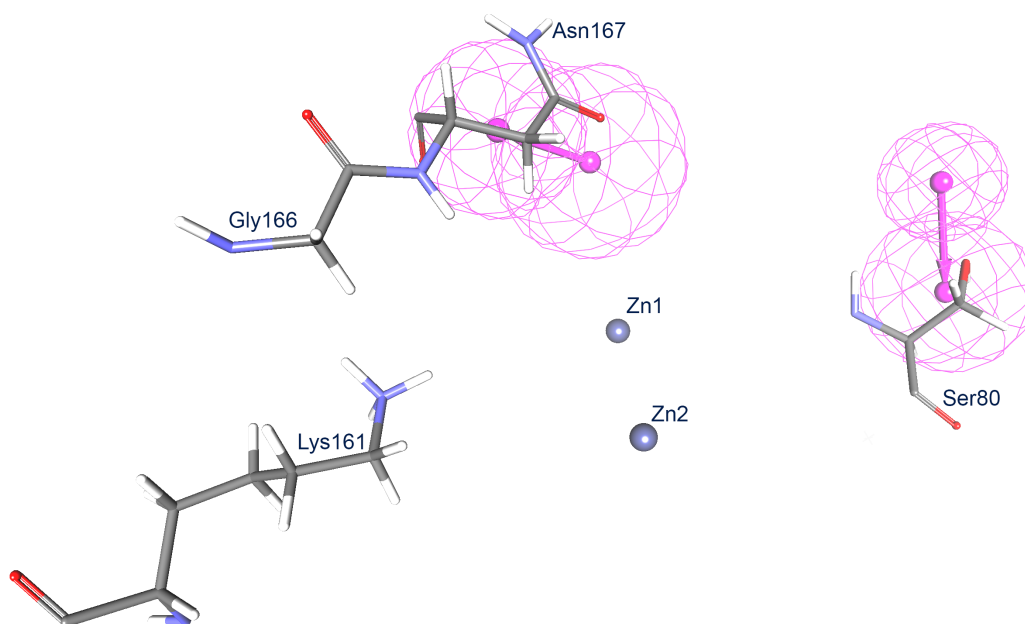


Figure 4.4. Pharmacophore feature: Hydrogen-bond donors. This figure was created using Discovery Studio.

the three hydrogen-bond acceptor pharmacophore features on Lys 161, Asn 167 and between the Zn^{2+} ions. This corresponded to 10,168 unique molecules, about 18% of the compound library. The pharmacophore screening took about 37 hours to be completed on an Intel Core i7 2.5GHz processor.

The summary of this pharmacophore screening is presented on Table 4.1.

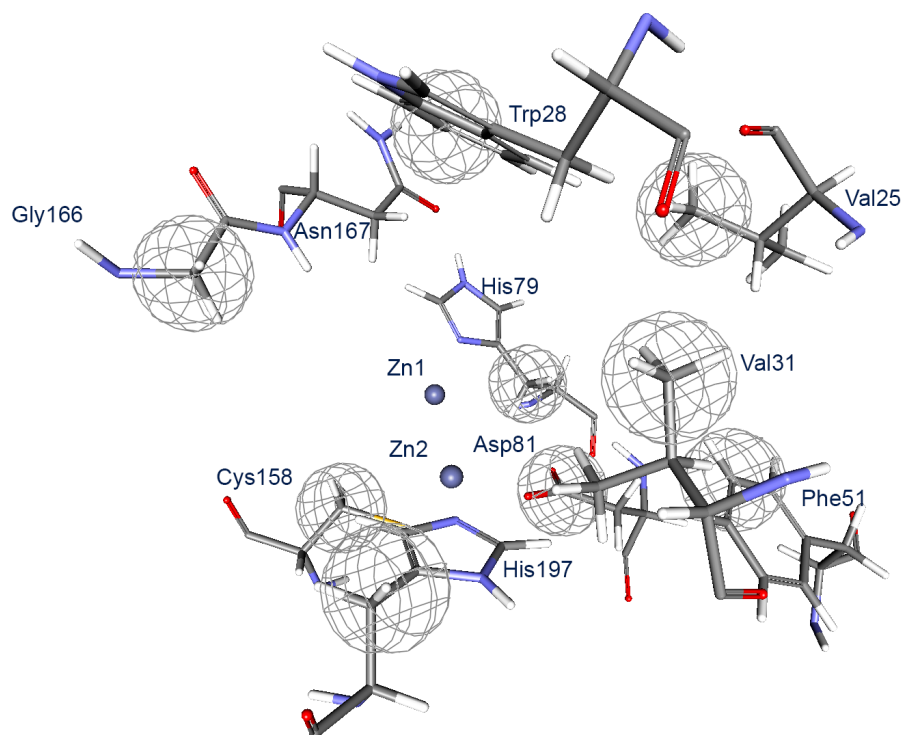


Figure 4.5. Pharmacophore feature: Volume exclusion. This figure was created using Discovery Studio.

Table 4.1. Pharmacophore screening summary. Number and percentage of positions that were fit into each feature.

Pharmacophore feature	Residue(s)	n (%)
H-Bond acceptor	Asn 167	105,960 (41)
	Lys 161	116,151 (45)
	Ser 80	121,292 (47)
	Zinc	134,991 (53)
	Asn 167 & Lys 161 & Zinc	19,603 (8)
H-bond donor	Ser 80	23,444 (9)
	Asn 167	68,791 (27)
Hydrophobe	Trp 28 / Val 25	123,467 (48)

The pharmacophore screening run showed that about half the compounds in the library fitted the H-bond acceptor features independently. Only 8%, however, fitted the H-bond acceptor features of Asn167, Lys161 and the Zinc ions simultaneously. The H-bond donor features were fit less by far less compounds, while the hydrophobe features were also fit by approximately half the compounds.

4.3 Molecular docking

The compounds selected from the pharmacophore run were included in Docking screening models following the steps described in Section 3.5.

Figure 4.6 summarizes the results of the screening process, including the docking steps.

The results of the first docking screening (performed with the configurations described in Section 3.5, Table 3.10, column A) were filtered by keeping only the molecules with a Fitness score greater than the lowest Fitness score with a realistic conformation of the reference ligands (the molecules co-crystallized with the IMP-1 structures referred in Section 3.2). Each subset had a different Fitness threshold as they were screened in separate GOLD runs; the thresholds are summarized in Table 4.2. This allowed to keep the half to two thirds of the conformations in the datasets (depending on the dataset) that translated into 4,532 distinct molecules (Figure 4.6).

Table 4.2. First Docking screening results.

Dataset	Fitness threshold
NCI	54.11
ZINC	52.15
DrugBank	
Approved subset	55.20
Experimental subset	55.16
Investigational subset	54.38
Thiols	77.95

In the specific case of thiols, the only co-crystallized ligands used as reference were D-captopril (4C1G) and the mercaptocarboxylate from IDD6 as the only ones with the thiol moiety. The docking simulation was performed with the configurations described on Section 3.5, Table 3.10, column A-T and the criterion used for choosing a Fitness score threshold was different as the minimum Fitness score of the reference ligands only reduced 8% of the dataset. Thus, the 3rd quartile Fitness score of the reference ligands was chosen as it reduced the dataset to about one third, keeping the best tercile of conformations, which resulted in 118 distinct molecules (Table 4.6).

The first screening run on GOLD took almost 63 hours on an Intel Core 2 Quad 2.4 GHz cpu.

The second screening performed on GOLD with the configurations described in Section 3.5, Table 3.10, column B used as input the results from the first screening. The second screening on GOLD took about 39 hours on an Intel Core 2 Quad 2.4 GHz cpu.

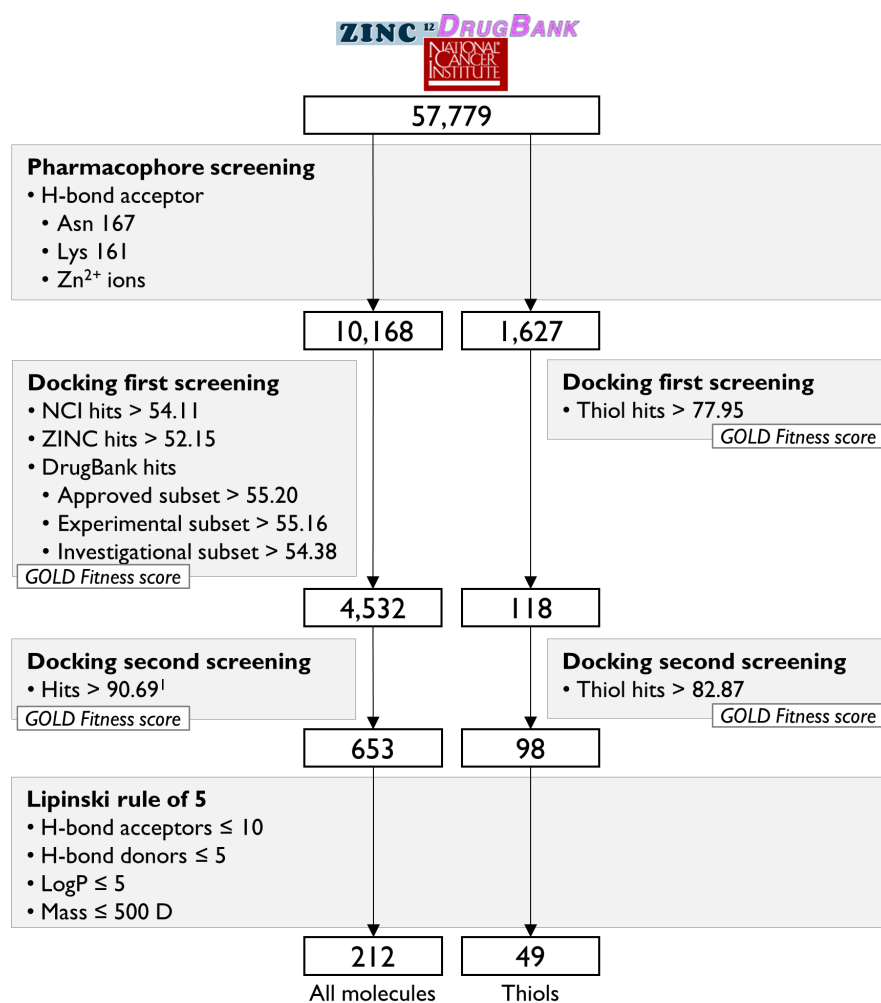
The subsets were filtered by the arithmetic mean of the average reference ligands Fitness score from the three subsets, 90.69 (Figure 4.6).

The second GOLD screening of thiol molecules with the configurations described in Section 3.5, Table 3.10, column B-T used as input the results from the first thiol GOLD screening. The results were filtered using the 3rd quartile Fitness score of the reference ligands, similarly to the first screening. This resulted in 98 distinct molecules (Figure 4.6) and took about one hour on an Intel Core 2 Quad 2.4 GHz cpu.

All molecules were finally filtered with Lipinski's rule of five. Molecules that violated any of the parameters below were filtered out:

1. ≤ 10 H-bond acceptors;
2. ≤ 5 H-bond donors;
3. $\text{LogP} \leq 5$;
4. $\text{Mass} < 500$ D

This last filter produced 212 distinct molecules and 49 molecules with a thiol moiety (Figure 4.6).



[†] Arithmetic mean of the average GOLD fitness score of the reference ligands from the 3 subsets.

Figure 4.6. Screening summary.

The visual inspection of the molecules obtained reveals quite diverse chemotypes. Nonetheless, in order to organise information and to lately obtain structure-activity relationships, the compounds were divided into chemical families.

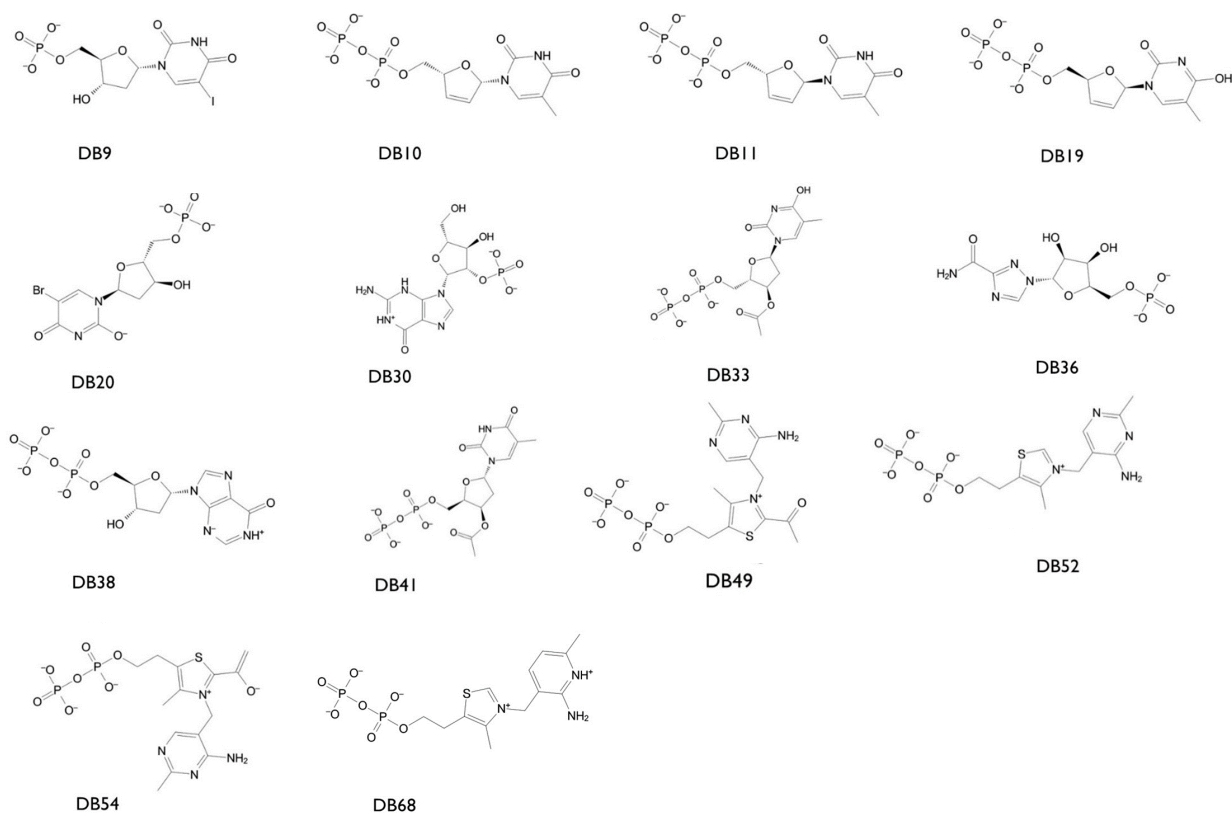


Figure 4.7. Docking screening results: Nucleotides from the DrugBank subset.

Several molecules in the DrugBank subset are nucleotides: DB9, DB10, DB11, DB19, DB20, DB30, DB33, DB36, DB38, DB41, DB49, DB52, DB54, and DB68 (Figure 4.7), and one is a nucleoside: DB2 (Figure 4.8).

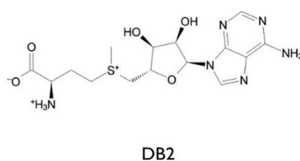


Figure 4.8. Docking screening results: Nucleoside from the DrugBank subset.

Four are phenylalanine derivatives, two with a hydrazine and a pyridine ring, DB67, and DB72 (gray square in Figure 4.9), one with a cyclopropane and a phenyl, DB69 (blue square), and one with a naphthol moiety, DB25 (yellow square).

Three molecules are β -lactams: DB5, DB6, and DB7 (grey square in Figure 4.10), and one is a methicillin derivatives: DB44 (black square).

One compound is a gamma-glutamyl peptide, more specifically, glutathionyl-hydroxy-dihydrophenanthrenes, DB40 (Figure 4.11).

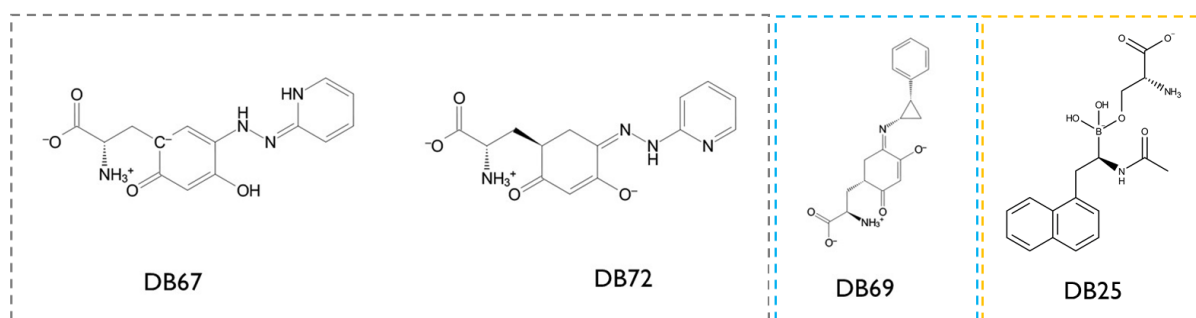


Figure 4.9. Docking screening results: phenylalanine derivatives from the DrugBank subset.

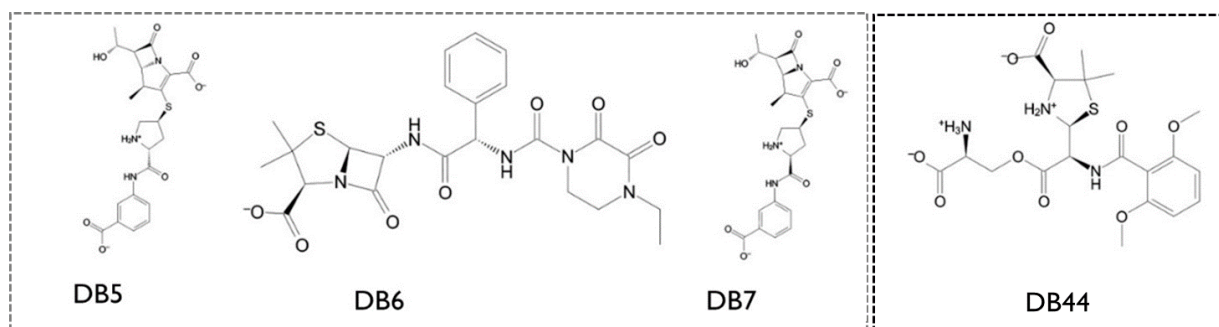


Figure 4.10. Docking screening results: β -Lactams from the DrugBank subset.

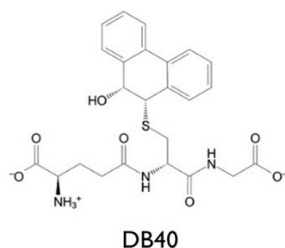


Figure 4.11. Docking screening results: Gamma-glutamyl peptides from the DrugBank subset.

Three molecules are aliphatic compounds such as phosphatidylserine, DB3, DB51, and DB73 (Figure 4.12).

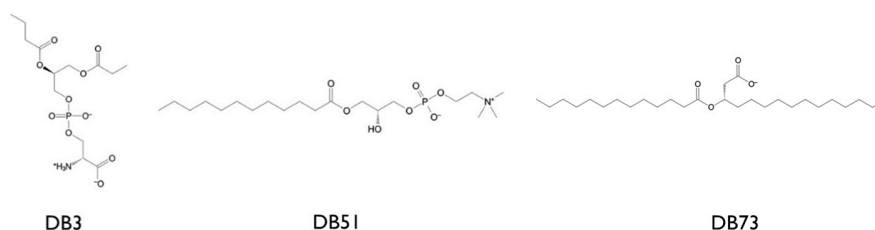
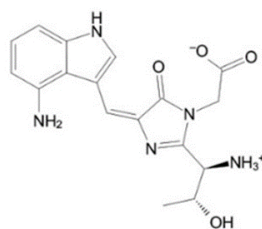


Figure 4.12. Docking screening results: Aliphatic molecules from the DrugBank subset.

One molecule has a moiety very similar to tryptophan with a indole and imidazole moieties, DB58 (Figure 4.13)

Two molecules are vitamin B6 derivatives. One is a phosphono-pyridoxyl isoleucine, DB28 (grey square) and one is a pyridoxyl-glutamic acid-monophosphate, DB56 (black square in Figure 4.14).

A diverse set of molecules was grouped as miscellaneous and is shown in Figure 4.15. One molecule is agatroban, DB1, an anticoagulant thrombin inhibitor, another is an aminoacid polyamine deriva-



DB58

Figure 4.13. Docking screening results: Molecules with indole and imidazole moieties from the DrugBank subset.

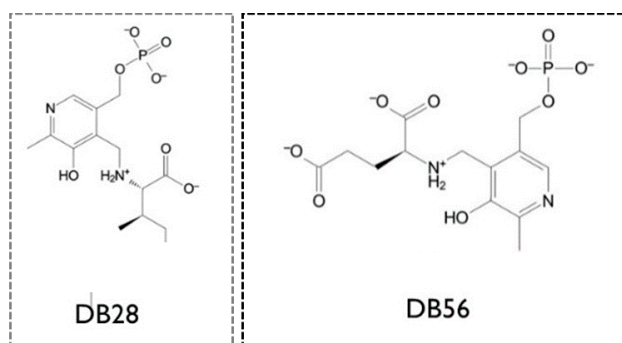


Figure 4.14. Docking screening results: Vitamin B6 derivatives from the DrugBank subset.

tive, part of the MRI contrast agent gadodiamide, DB4, and one is an indirubin derivative, DB48 (Figure 4.15).

Moreover, a dipeptide of phenylalanine and asparagine with gamma-phenyl-butyric acid, DB23, an argininosuccinate, DB26; an alpha-amino adipoyl-cysteinyl-valine, DB46; a peptide, Glycyl-L-Alpha-Amino-Epsilon-Pimelyl-D-Alanyl-D-Alanine, DB53; an alpha amino acid amide, DB59; an organic pyrophosphate, DB61; a pyrazinecarboxamides, DB63; and benzoylecgonine, the major metabolite of cocaine, DB64 (Figure 4.15) were pointed as promising by the docking screening studies.

In the NCI subset there is a much greater variety than in the DrugBank subset.

Twenty molecules have one or two aminoacids in their structures: NCI13, NCI14, NCI15, NCI18, NCI20, NCI21, NCI22, NCI27, NCI29, NCI32, NCI33, NCI38, NCI40, NCI47, NCI55, NCI56, NCI58, NCI63, NCI68, and NCI77 (Figure 4.16).

Three molecules are similar to catechins: NCI3, NCI6, and NCI53 (Figure 4.17) and three are thymidine derivatives: NCI42, NCI49, and NCI52 (Figure 4.18).

Lacking homogeneity among the remaining molecules, there are a lot of heterocyclic, polycyclic aromatic compounds (Figure 4.19), some sulphates NCI1, NCI9, and NCI69 (Figure 4.20) and a group of unrelated compounds (Figure 4.21).

The ZINC subset is the most heterogeneous, with a wide diversity of compounds. The norburene group is featured in four compounds (Figure 4.22) and the remaining molecules are presented in Figure 4.23. Similarly to the NCI subset, the molecules are mainly heterocyclic, polycyclic aromatic compounds.

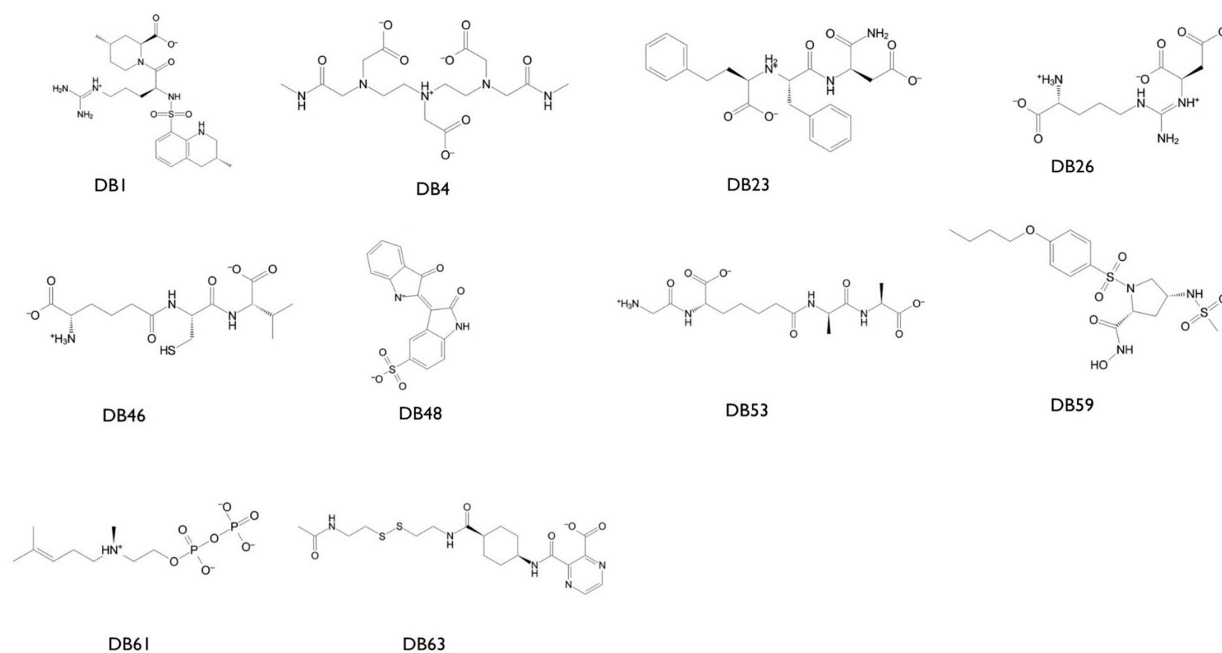


Figure 4.15. Docking screening results: Miscellaneous molecules from the DrugBank subset.

Most compounds of the final thiol subset have a central thiourea group, in combination with several substituents such as methoxyacetophenones, phenylbenzotriazoles, phenylloxazolopyridines, and anthraquinone with several positional and geometrical isomers and tautomers figuring in the final subset (Figure 4.24).

Other compounds are represented in Figure 4.25 and are structurally diverse, all containing carboxylates and hydrolysed thiols.

Many compounds of all the subsets had reactive groups such as nitro, terminal alkenes and aldehydes, and some had terminal esters that would be hydrolysed *in vivo*, likely changing the behaviour of the molecules. These molecules are gathered in Appendix A, Figures A.1-A.9.

A complete list of the 212 molecules, their docking fitness score and their database identifiers can be found in Appendix B.

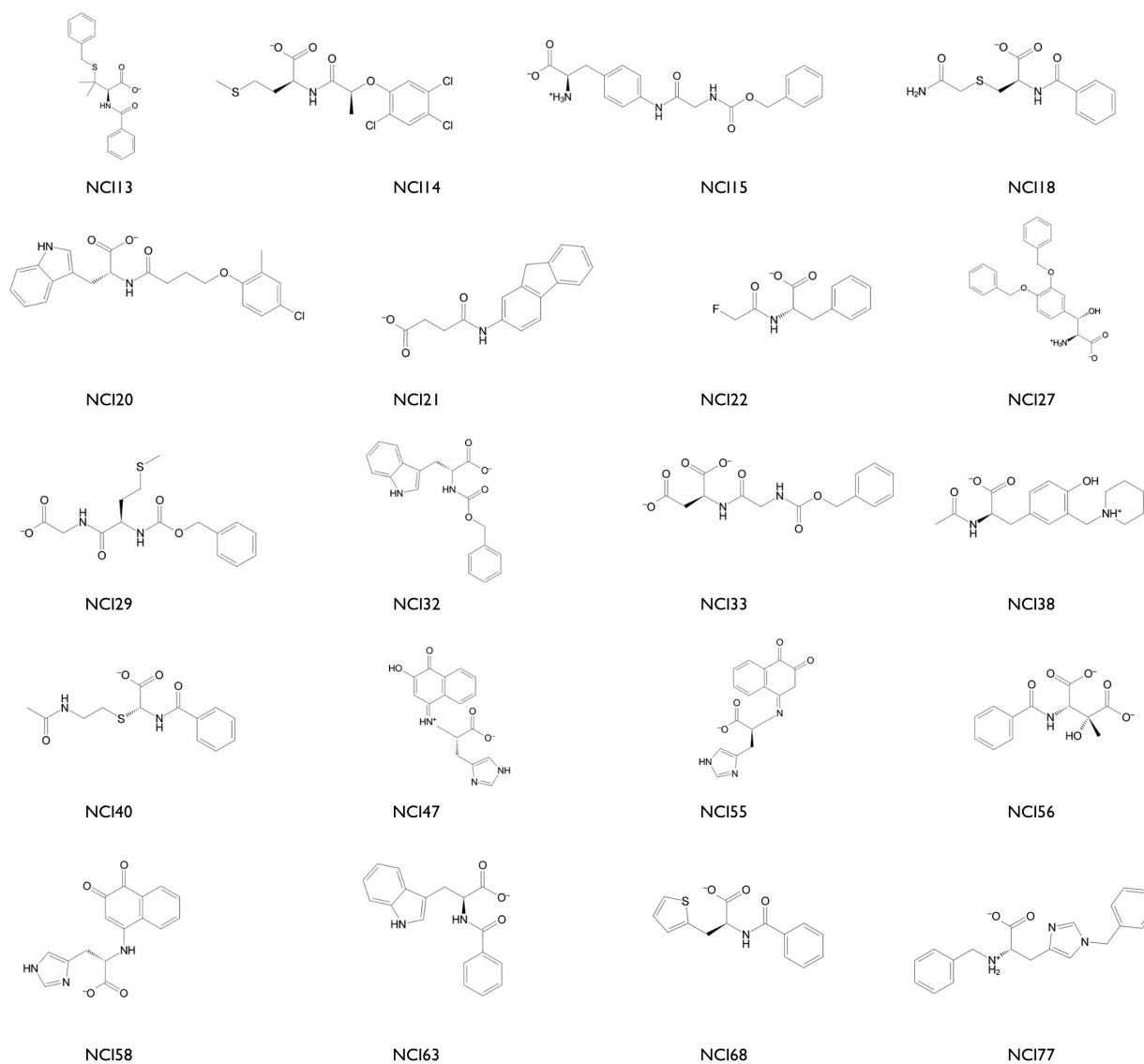


Figure 4.16. Docking screening results: Amino acid derivatives with a free carboxylic group from the NCI subset.

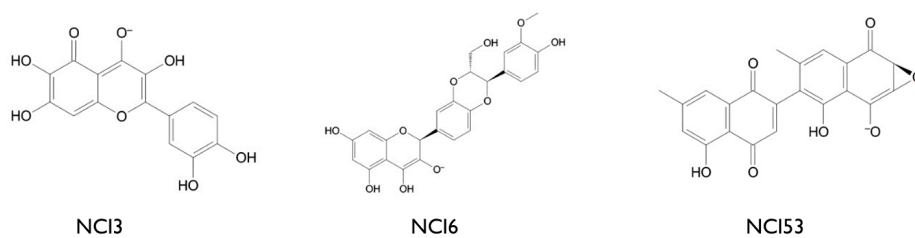


Figure 4.17. Docking screening results: Catechin-like molecules from the NCI subset.

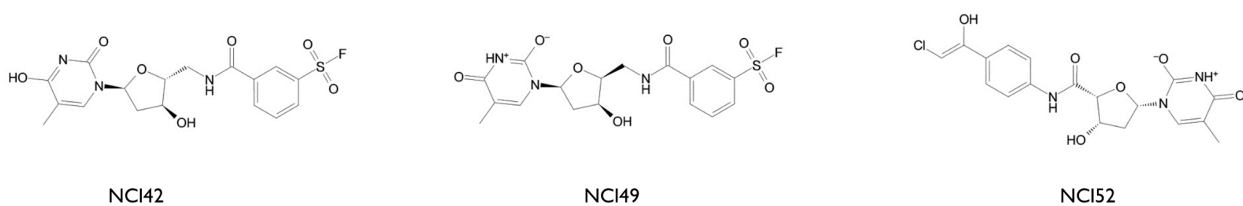


Figure 4.18. Docking screening results: Thymidine derivatives from the NCI subset.

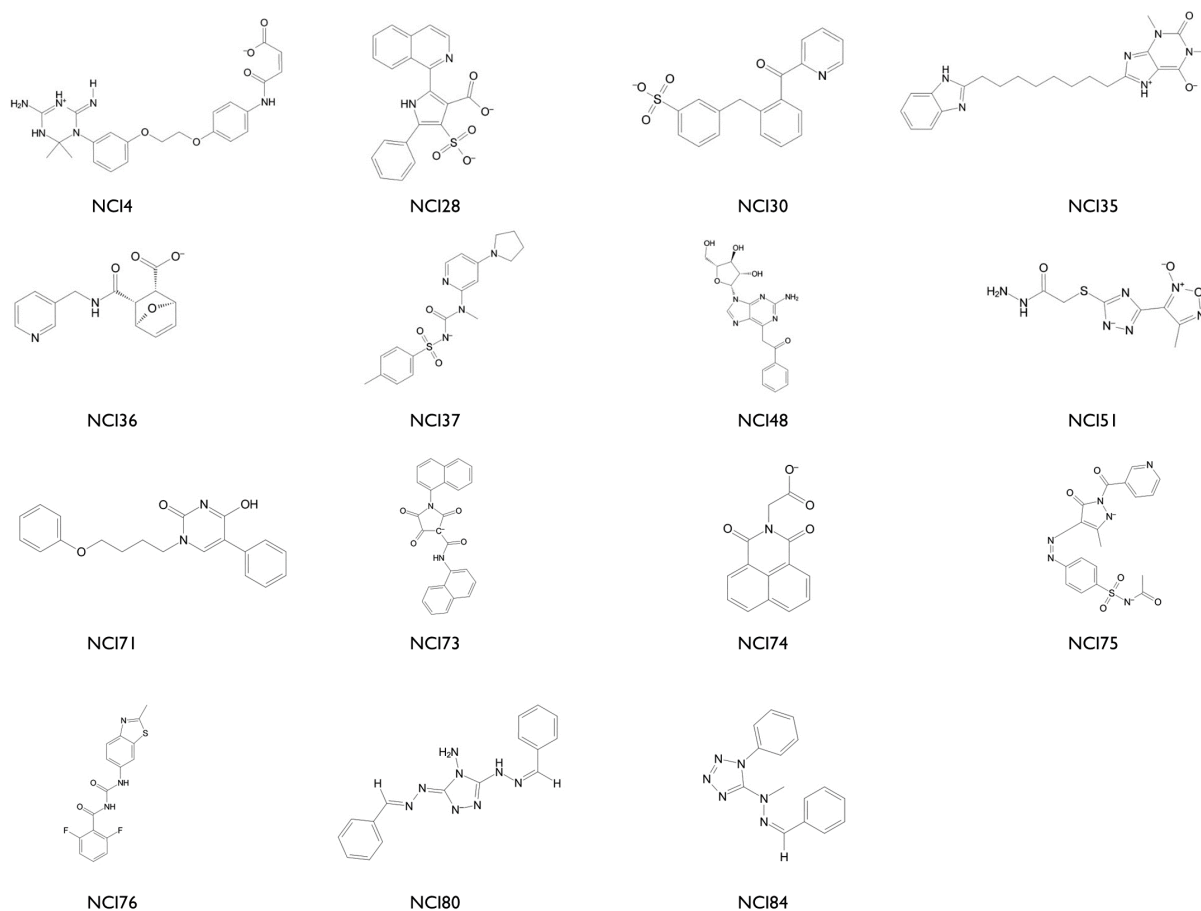


Figure 4.19. Docking screening results: Diverse heterocyclic, polycyclic aromatic compounds from the NCI subset.

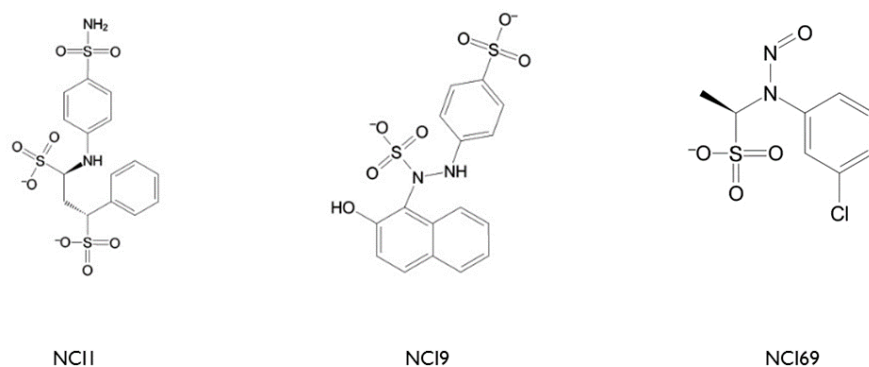


Figure 4.20. Docking screening results: Sulphate compounds from the NCI subset.

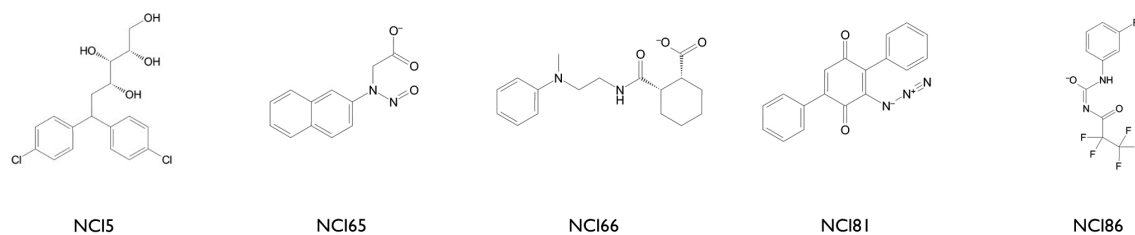


Figure 4.21. Docking screening results: Miscellaneous molecules from the NCI subset.

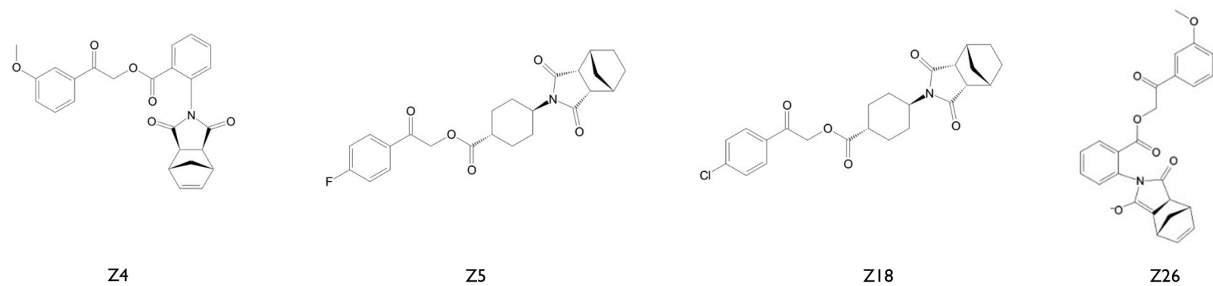


Figure 4.22. Docking screening results: Compounds with norburene moiety from the ZINC subset.

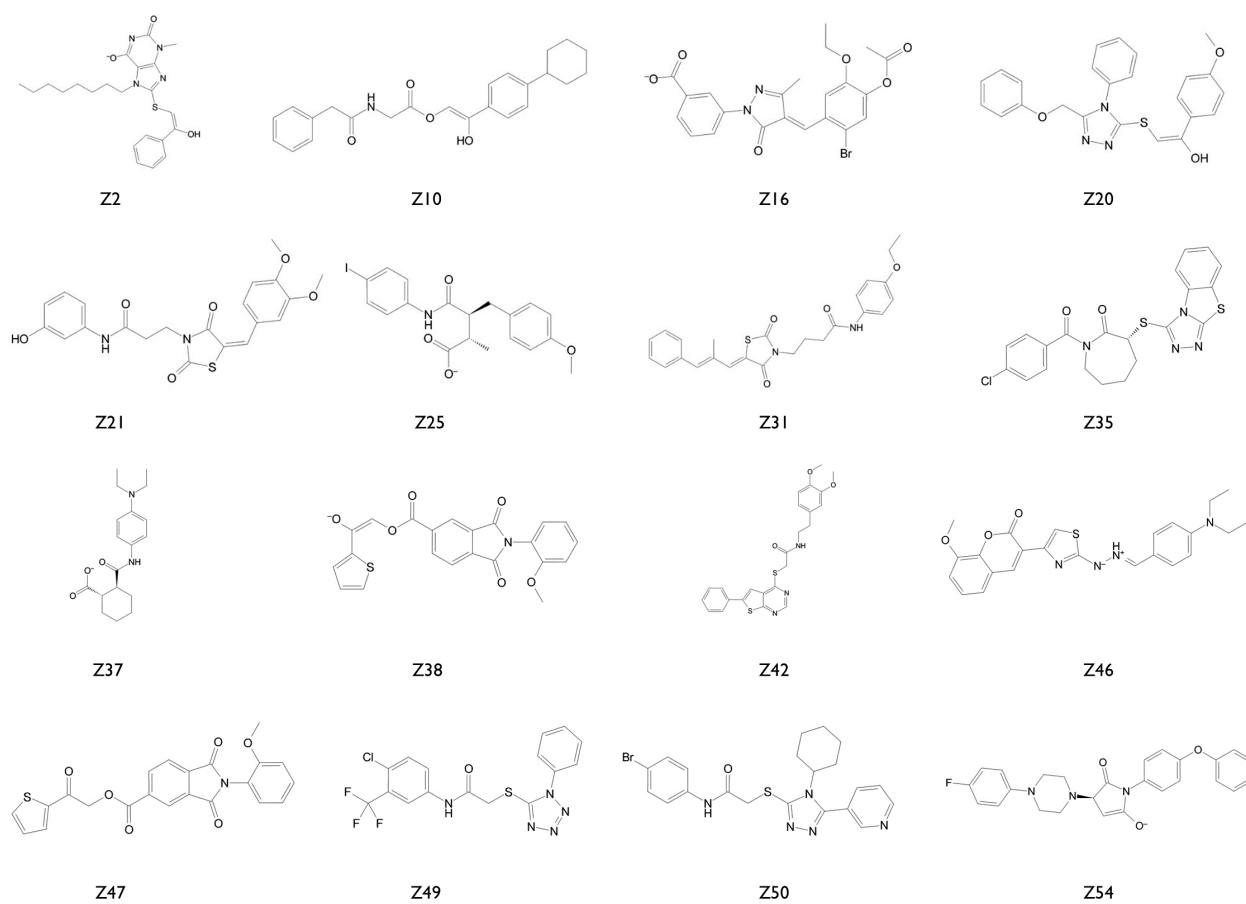


Figure 4.23. Docking screening results: Diverse compounds from the ZINC subset.

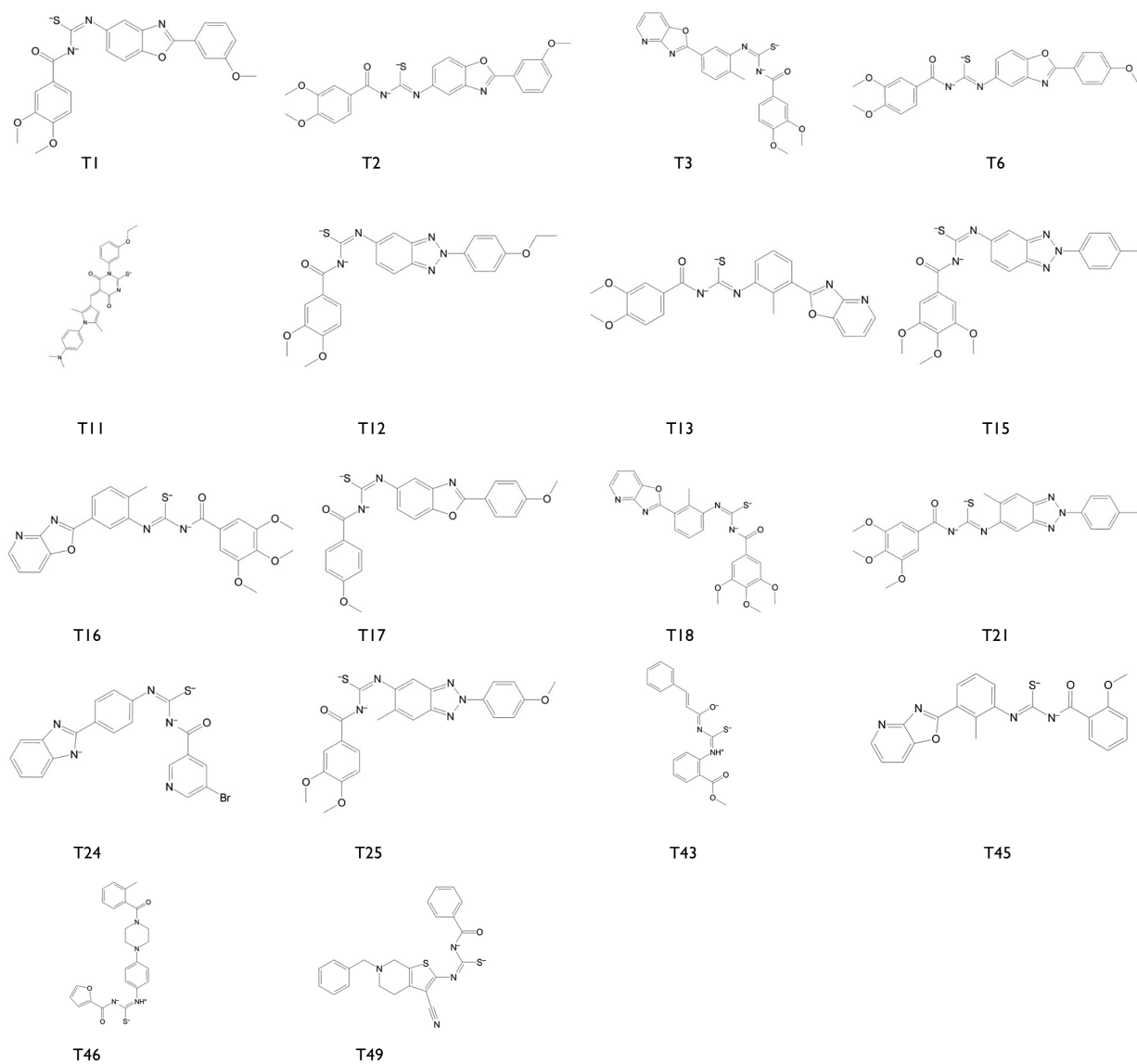


Figure 4.24. Docking screening results: Thioureas from the Thiol subset.

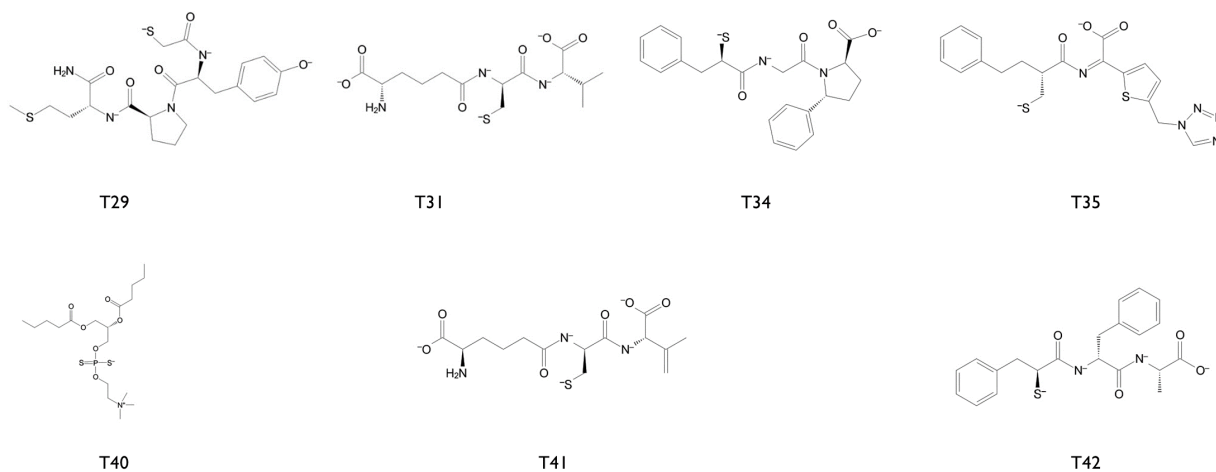


Figure 4.25. Docking screening results: Diverse compounds from the Thiol subset.

Chapter 5

Discussion

Antimicrobial resistance is on its way to become the biggest global health threat of the twenty-first century. The World Health Organisation has recently published a report [203] that, despite its limited coverage, showed alarmingly high rates of resistance in bacteria that cause common health-care associated and community-acquired infections such as urinary tract infection (UTI), pneumonia, and wound and bloodstream infections (*Escherichia coli*, *Klebsiella pneumoniae* and *Staphylococcus aureus*), as well as increasing anti-HIV drug resistance among patients starting anti-retroviral treatments.

The exceptional resistance profile of MBL, their quick global spread, the lack of available inhibitors and the existence of yet other concurrent resistance mechanisms prompts a thorough search of compound databases for molecules with inhibitory properties, that, to the best of our knowledge, hasn't been done on the full set of the NCI, ZINC, and DrugBank databases, despite the several studies on MBL inhibitors reported on Section 1.7.2.3 that focus on specific molecule families, exploring a restricted chemical space. Thus, in this study we aimed to screen the NCI, ZINC and DrugBank databases for compounds with affinity for the IMP-I MBL and to select the best candidates for development into inhibitors with clinical value.

The active site of IMP-I was explored for pharmacophore properties, modelling a three-dimensional map of pharmacophoric points that was used to perform a first screening of the compound database, followed by two consecutive screenings with a docking protocol with increasing algorithm efficiency and separate configurations for thiol molecules given the extensive literature on the affinity of thiols as MBL inhibitors [104, 139–141, 204–207]. Finally, lipinski rules were applied to the resulting candidates, producing a final set of 212 molecules, plus 49 thiol molecules, a total of 261 compounds.

The final set of molecules presents, in general, *lead- or drug-like* properties, forced by the application of Lipinski's rule of 5, but it also presents features in line with the characteristics of the protein being studied: β -Lactam groups and peptidic bonds, that are perfectly in accordance with the protein function; bulky aromatic groups in rotatable parts of the molecule that allow orientation

for interaction with the flap that folds over the active site on ligand binding, and thiol moieties that have been reported in the literature as preferential binders with zinc ions.

In our study new chemotypes for IMP-I inhibition have been identified, broadening the chemical space for the exploitation of novel inhibitors. Specifically, phosphate and diphosphate nucleotide compounds (Figure 4.7), aminoacid derivatives bearing a free carboxylic acid group (Figures 4.9, 4.11, and 4.16), and catechin analogues (Figure 4.17) have been found to fit the active site of IMP-I and to attain good scores for further exploitation. Interestingly, the final set of molecules found some chemical families previously identified as potential inhibitors in the literature, such as thiophenes (Figure 1.48 [65] and Figure 4.16), the briefly cited thioureas (Table 1.16 [157] and Figure 4.24), diverse heterocyclic compounds (Figures 1.60, 1.61 [169], 1.64 [171], and 1.66 [172] and Figures 4.18 and 4.19), and sulfur containing β -lactams (Figures 1.43 [158] and 1.44 [161], and Figure 4.10).

The screening process allowed us to filter out 99.55 % of the initial database and keep only the top 0.45 % of the best fitting molecules, a number feasible to be tested *in vitro* at our lab.

As future perspectives, this final set of molecules will be either sourced or synthesized locally in our synthesis lab and then a *in vitro* methodology adequate for IMP-I inhibitor testing will be set-up and the available compounds will be tested, determining their affinity for the enzyme and their inhibitory potential, and exploring structure-activity relationships, improving the current pharmacophore model. Ideally this will lead to the identification of a few lead structures with promising properties as MBL inhibitors.

Bibliography

- [1] COMBACTE; 2016. Available from: www.combacte.com.
- [2] Mitsuhashi S. Drug resistance in bacteria: history, genetics and biochemistry. *The Journal of international medical research*. 1993;21(1):1–14.
- [3] Greenwood D, Finch R, Davey P, Wilcox M. *Antimicrobial Chemotherapy*. 5th ed. Greenwood D, editor. New York: Oxford University Press; 2007.
- [4] Chain E, Florey HW, Gardner AD, Heatley NG, Jennings MA, Orr-Ewing J, et al. PENICILLIN AS A CHEMOTHERAPEUTIC AGENT. *The Lancet*. 1940 aug;236(6104):226–228.
- [5] Domagk G. Ein Beitrag zur Chemotherapie der bakteriellen Infektionen. *DMW - Deutsche Medizinische Wochenschrift*. 1935 feb;61(07):250–253.
- [6] Trefouél J, Trefouél J, Nitti F, Bovet D. Activity of paminophenylsulfamide in the experimental streptococcal infections of the mouse and rabbit. *C R Seances Soc Biol Fil*. 1935;120:756.
- [7] Schatz A, Bugle E, Waksman SA. Streptomycin, a Substance Exhibiting Antibiotic Activity Against Gram-Positive and Gram-Negative Bacteria. *Experimental Biology and Medicine*. 1944 jan;55(1):66–69.
- [8] Hotchkiss D, Dubos R. The isolation of bactericidal substances from cultures of *Bacillus brevis*. *The Journal of Biological Chemistry*. 1941;141:155–162.
- [9] Lipsitch M, Singer RS, Levin BR. Antibiotics in agriculture: when is it time to close the barn door? *Proceedings of the National Academy of Sciences of the United States of America*. 2002 apr;99(9):5752–4.
- [10] Hughes VM, Datta N. Conjugative plasmids in bacteria of the ‘pre-antibiotic’ era. *Nature*. 1983 apr;302(5910):725–726.
- [11] Datta N, Hughes VM. Plasmids of the same Inc groups in Enterobacteria before and after the medical use of antibiotics. *Nature*. 1983;306(5943):616–617.
- [12] Abraham E. Selective reminiscences of beta-lactam antibiotics: early research on penicillin and cephalosporins. *BioEssays*. 1990 dec;12(12):601–6.
- [13] O’Brien TF. Resistance of bacteria to antibacterial agents: report of Task Force 2. *Reviews of infectious diseases*;9 Suppl 3:S244–60.

- [14] Martinez JL, Baquero F. Mutation frequencies and antibiotic resistance. *Antimicrobial agents and chemotherapy*. 2000 jul;44(7):1771–7.
- [15] Barlow M. What Antimicrobial Resistance Has Taught Us About Horizontal Gene Transfer. In: Fiedler L, editor. *Horizontal Gene Transfer*. vol. 1332 of *Methods in Molecular Biology*. New York, NY: Springer New York; 2009. p. 397–411.
- [16] Paterson DL. Resistance in Gram-Negative Bacteria: Enterobacteriaceae. *American Journal of Medicine*. 2006;119(6 SUPPL. 1):20–28.
- [17] Hopkins KL, Davies RH, Threlfall EJ. Mechanisms of quinolone resistance in *Escherichia coli* and *Salmonella*: Recent developments. *International Journal of Antimicrobial Agents*. 2005;25(5):358–373.
- [18] Nikaido H. Multidrug resistance in bacteria. *Annual Review of Biochemistry*. 2009;78:119–146.
- [19] Clancy J, Dib-Hajj F, Petitpas JW, Yuan W. Cloning and characterization of a novel macrolide efflux gene, *mreA*, from *Streptococcus agalactiae*. *Antimicrobial Agents and Chemotherapy*. 1997;41(12):2719–2723.
- [20] Medeiros AA. Recent increases in resistance: mechanisms and organisms. Evolution and Dissemination of β -Lactamases Accelerated by Generations of β -Lactam Antibiotics. *Clinical Infectious Diseases*. 1997;24(Suppl 1):19–45.
- [21] Barlow M, Reik RA, Jacobs SD, Medina M, Meyer MP, McGowan JE, et al. High rate of mobilization for *bla*_{CTX-MS}. *Emerging Infectious Diseases*. 2008;14(3):423–428.
- [22] Henriques Normark B, Normark S. Evolution and spread of antibiotic resistance. *Journal of Internal Medicine*. 2002;252(2):91–106.
- [23] Reynolds PE. Structure, Biochemistry and Mechanism of Action of Glycopeptide Antibiotics. *Eur J Clin Microbiol Infect Dis*. 1989;8(11):943–950.
- [24] Rice LB. Mechanisms of resistance and clinical relevance of resistance to β -lactams, glycopeptides, and fluoroquinolones. *Mayo Clinic proceedings*. 2012 feb;87(2):198–208.
- [25] Yarlaga V, Manjunath GB, Sarkar P, Akkapeddi P, Paramanandham K, Shome BR, et al. Glycopeptide Antibiotic To Overcome the Intrinsic Resistance of Gram-Negative Bacteria. *ACS Infectious Diseases*. 2015;p. acsinfecdis.5b00114.
- [26] Sieradzki K, Pinho MG, Tomasz A. Inactivated *pbp4* in highly glycopeptide-resistant laboratory mutants of *Staphylococcus aureus*. *The Journal of biological chemistry*. 1999 jul;274(27):18942–6.
- [27] Neu HC, Gootz TD. *Antimicrobial Chemotherapy*. In: Baron S, editor. *Medical Microbiology*. 4th ed. Galveston (TX): University of Texas Medical Branch at Galveston; 1996.

- [28] David HL. Resistance to D-cycloserine in the tubercle bacilli: mutation rate and transport of alanine in parental cells and drug-resistant mutants. *Applied microbiology*. 1971;21(5):888–92.
- [29] Cáceres NE, Harris NB, Wellehan JF, Feng Z, Kapur V, Barletta RG. Overexpression of the D-alanine racemase gene confers resistance to D-cycloserine in *Mycobacterium smegmatis*. *Journal of bacteriology*. 1997;179(16):5046–55.
- [30] Stone KJ, Strominger JL. Mechanism of Action of Bacitracin: Complexation with Metal Ion and C55-Isoprenyl Pyrophosphate. *Proceedings of the National Academy of Sciences of the United States of America*. 1971;68(12):3223–3227.
- [31] Podlesek Z, Comino A, Herzog-Velikonja B, Žgur-Bertok D, Komel R, Grabnar M. *Bacillus licheniformis* bacitracin-resistance ABC transporter: Relationship to mammalian multidrug resistance. *Molecular Microbiology*. 1995;16(5):969–976.
- [32] Cain BD, Norton PJ, Eubanks W, Nick HS, Allen CM. Amplification of the *bacA* gene confers bacitracin resistance to *Escherichia coli*. *Journal of Bacteriology*. 1993;175(12):3784–3789.
- [33] Jana S, Deb JK. Molecular understanding of aminoglycoside action and resistance. *Applied Microbiology and Biotechnology*. 2006;70(2):140–150.
- [34] Chopra I, Roberts M. Tetracycline Antibiotics: Mode of Action, Applications, Molecular Biology, and Epidemiology of Bacterial Resistance. *Microbiology and Molecular Biology Reviews*. 2001 jun;65(2):232–260.
- [35] Chopra I, Hawkey PM, Hinton M. Tetracyclines, molecular and clinical aspects. *Journal of Antimicrobial Chemotherapy*. 1992 mar;29(3):245–277.
- [36] Schnappinger D, Hillen W. Tetracyclines: antibiotic action, uptake, and resistance mechanisms. *Archives of microbiology*. 1996;165(6):359–369.
- [37] Buck MA, Cooperman BS. Single protein omission reconstitution studies of tetracycline binding to the 30S subunit of *Escherichia coli* ribosomes. *Biochemistry*. 1990 jun;29(22):5374–5379.
- [38] Speer BS, Salyers AA. Characterization of a novel tetracycline resistance that functions only in aerobically grown *Escherichia coli*. *Journal of bacteriology*. 1988 apr;170(4):1423–9.
- [39] Speer BS, Salyers AA. Novel aerobic tetracycline resistance gene that chemically modifies tetracycline. *Journal of bacteriology*. 1989 jan;171(1):148–53.
- [40] Speer BS, Salyers AA. A tetracycline efflux gene on *Bacteroides* transposon Tn4400 does not contribute to tetracycline resistance. *Journal of bacteriology*. 1990 jan;172(1):292–8.
- [41] Gaynor M, Mankin AS. Macrolide antibiotics: binding site, mechanism of action, resistance. *Current topics in medicinal chemistry*. 2003;3(9):949–61.

- [42] Johnston NJ, Mukhtar TA, Wright GD. Streptogramin antibiotics: mode of action and resistance. *Current drug targets*. 2002 aug;3(4):335–44.
- [43] Vazquez D. Inhibitors of protein synthesis. *FEBS letters*. 1974 mar;40(March):S63–84.
- [44] Cseplö A, Etzold T, Schell J, Schreier PH. Point mutations in the 23 S rRNA genes of four lincomycin resistant *Nicotiana plumbaginifolia* mutants could provide new selectable markers for chloroplast transformation. *Molecular & general genetics : MGG*. 1988 oct;214(2):295–9.
- [45] Douthwaite S. Functional interactions within 23S rRNA involving the peptidyltransferase center. *Journal of bacteriology*. 1992 feb;174(4):1333–8.
- [46] Douthwaite S. Interaction of the antibiotics clindamycin and lincomycin with *Escherichia coli* 23S ribosomal RNA. *Nucleic acids research*. 1992;20(18):4717–20.
- [47] Tran TT, Munita JM, Arias CA. Mechanisms of drug resistance: Daptomycin resistance. *Annals of the New York Academy of Sciences*. 2015;1354(1):32–53.
- [48] Kracht M, Rokos H, Ozel M, Kowall M, Pauli G, Vater J. Antiviral and hemolytic activities of surfactin isoforms and their methyl ester derivatives. *The Journal of antibiotics*. 1999;52(7):613–619.
- [49] Vollenbroich D, Ozel M, Vater J, Kamp RM, Pauli G. Mechanism of inactivation of enveloped viruses by the biosurfactant surfactin from *Bacillus subtilis*. *Biologicals : journal of the International Association of Biological Standardization*. 1997;25(3):289–97.
- [50] Béven L, Wróblewski H. Effect of natural amphiphatic peptides on viability, membrane potential, cell shape and motility of mollicutes. *Research in Microbiology*. 1997;148(2):163–175.
- [51] Vollenbroich D, Pauli G, Ozel M, Vater J. Antimycoplasma properties and application in cell culture of surfactin, a lipopeptide antibiotic from *Bacillus subtilis*. *Applied and environmental microbiology*. 1997 jan;63(1):44–9.
- [52] Kameda Y, Oira S, Matsui K, Kanatomo S, Hase T. Antitumor activity of bacillus natto. V. Isolation and characterization of surfactin in the culture medium of *Bacillus natto* KMD 2311. *Chemical & pharmaceutical bulletin*. 1974 apr;22(4):938–44.
- [53] Heerklotz H, Seelig J. Leakage and lysis of lipid membranes induced by the lipopeptide surfactin. *European Biophysics Journal*. 2007;36(4-5):305–314.
- [54] Hoefler BC, Gorzelnik KV, Yang JY, Hendricks N, Dorrestein PC, Straight PD. Enzymatic resistance to the lipopeptide surfactin as identified through imaging mass spectrometry of bacterial competition. *Proceedings of the National Academy of Sciences of the United States of America*. 2012;109(32):13082–7.

- [55] Bialvaei AZ, Samadi Kafil H. Colistin, mechanisms and prevalence of resistance. *Current Medical Research and Opinion*. 2015 apr;31(4):707–721.
- [56] Li J, Rayner CR, Nation RL, Owen RJ, Spelman D, Tan KE, et al. Heteroresistance to colistin in multidrug-resistant *Acinetobacter baumannii*. *Antimicrobial Agents and Chemotherapy*. 2006;50(9):2946–2950.
- [57] Hsueh PR, Tseng SP, Teng LJ, Ho SW. Pan-drug-resistant *Pseudomonas aeruginosa* causing nosocomial infection at a university hospital in Taiwan. *Clinical Microbiology and Infection*. 2005;11(8):670–673.
- [58] Liu YY, Wang Y, Walsh TR, Yi LX, Zhang R, Spencer J, et al. Emergence of plasmid-mediated colistin resistance mechanism MCR-1 in animals and human beings in China: a microbiological and molecular biological study. *The Lancet Infectious diseases*. 2016 feb;16(2):161–8.
- [59] Martis N, Leroy S, Blanc V. Colistin in multi-drug resistant *Pseudomonas aeruginosa* bloodstream infections: A narrative review for the clinician. *Journal of Infection*. 2014;69(1):1–12.
- [60] Then RL. Mechanisms of resistance to trimethoprim, the sulfonamides, and trimethoprim-sulfamethoxazole. *Reviews of infectious diseases*. 1982;4(2):261–9.
- [61] Ruiz J. Mechanisms of resistance to quinolones: Target alterations, decreased accumulation and DNA gyrase protection. *Journal of Antimicrobial Chemotherapy*. 2003;51(5):1109–1117.
- [62] Fisher JF, Meroueh SO, Mobashery S. Bacterial resistance to beta-lactam antibiotics: compelling opportunism, compelling opportunity. *Chemical reviews*. 2005 mar;105(2):395–424.
- [63] Brown L, Wolf JM, Prados-Rosales R, Casadevall A. Through the wall: extracellular vesicles in Gram-positive bacteria, mycobacteria and fungi. *Nature Reviews Microbiology*. 2015 sep;13(10):620–630.
- [64] Walsh TR, Toleman Ma, Poirel L, Nordmann P. Metallo-beta-lactamases: the quiet before the storm? [Review]. *CLINICAL MICROBIOLOGY REVIEWS*. 2005 apr;18(2):306+.
- [65] Shen B, Yu Y, Chen H, Cao X, Lao X, Fang Y, et al. Inhibitor Discovery of Full-Length New Delhi Metallo- β -Lactamase-1 (NDM-1). *PLoS ONE*. 2013;8(5):4–10.
- [66] Franceschini N, Caravelli B, Galleni M, Frère Jm, Rossolini GM. Purification and Biochemical Characterization of the VIM-1 Metallo-b-Lactamase. *Antimicrobial agents and chemotherapy*. 2000;44(11):3003.
- [67] Livermore DM. Acquired carbapenemases. *The Journal of antimicrobial chemotherapy*. 1997 jun;39(6):673–6.
- [68] Ambler RP. The Structure of beta-Lactamases. *Philosophical Transactions of the Royal Society B: Biological Sciences*. 1980 may;289(1036):321–331.

- [69] Bush K. Characterization of beta-lactamases. *Antimicrobial agents and chemotherapy*. 1989 mar;33(3):259–63.
- [70] Bush K, Jacoby GA, Medeiros AA. A functional classification scheme for beta-lactamases and its correlation with molecular structure. *Antimicrobial agents and chemotherapy*. 1995 jun;39(6):1211–33.
- [71] Bush K, Jacoby Ga. Updated functional classification of beta-lactamases. *Antimicrobial agents and chemotherapy*. 2010 mar;54(3):969–76.
- [72] Oelschlaeger P, Ai N, Duprez KT, Welsh WJ, Toney JH. Evolving carbapenemases: can medicinal chemists advance one step ahead of the coming storm? *Journal of medicinal chemistry*. 2010 apr;53(8):3013–27.
- [73] Drawz SM, Bonomo Ra. Three decades of beta-lactamase inhibitors. [Review]. *Clinical microbiology reviews*. 2010 jan;23(1):160–201.
- [74] Bush K. Beta-lactamase inhibitors from laboratory to clinic. *Clinical microbiology reviews*. 1988;1(1):109–23.
- [75] Buynak JD. Understanding the longevity of the beta-lactam antibiotics and of antibiotic/beta-lactamase inhibitor combinations. *Biochemical pharmacology*. 2006 mar;71(7):930–40.
- [76] Cantón R, Coque TM. The CTX-M beta-lactamase pandemic. *Current opinion in microbiology*. 2006 oct;9(5):466–75.
- [77] Philippon A, Labia R, Jacoby G. MINIREVIEW Extended-Spectrum Beta-Lactamases. *Antimicrobial agents and chemotherapy*. 1989;33(8):1131–1136.
- [78] Zhanel G, Lawson C, Adam H, Schweizer F, Zelenitsky S, Lagacé-Wiens PS, et al. Ceftazidime-Avibactam: a Novel Cephalosporin/ β -lactamase Inhibitor Combination. *Drugs*. 2013;73(2):159–177.
- [79] Drawz SM, Papp-Wallace KM, Bonomo Ra. New β -lactamase inhibitors: a therapeutic renaissance in an MDR world. *Antimicrobial agents and chemotherapy*. 2014 apr;58(4):1835–46.
- [80] Blizzard TA, Chen H, Kim S, Wu J, Bodner R, Gude C, et al. Discovery of MK-7655, a β -lactamase inhibitor for combination with Primaxin®. *Bioorganic & medicinal chemistry letters*. 2014 feb;24(3):780–5.
- [81] Livermore DM, Mushtaq S. Activity of biapenem (RPX2003) combined with the boronate β -lactamase inhibitor RPX7009 against carbapenem-resistant Enterobacteriaceae. *The Journal of antimicrobial chemotherapy*. 2013 aug;68(8):1825–31.
- [82] Wyrembak PN, Babaoglu K, Pelto RB, Shoichet BK, Pratt RF. O-aryloxycarbonyl hydroxamates: new beta-lactamase inhibitors that cross-link the active site. *Journal of the American Chemical Society*. 2007 aug;129(31):9548–9.

- [83] Tilwawala R, Pratt RF. Covalent inhibition of serine β -lactamases by novel hydroxamic acid derivatives. *Biochemistry*. 2013 may;52(21):3712–20.
- [84] Schneider KD, Ortega CJ, Renck Na, Bonomo Ra, Powers Ra, Leonard Da. Structures of the class D carbapenemase OXA-24 from *Acinetobacter baumannii* in complex with doripenem. *Journal of molecular biology*. 2011 mar;406(4):583–94.
- [85] Poirel L, Potron A, Nordmann P. OXA-48-like carbapenemases: the phantom menace. *The Journal of antimicrobial chemotherapy*. 2012 jul;67(7):1597–606.
- [86] Osano E, Arakawa Y, Wacharotayankun R, Ohta M, Horii T, Ito H, et al. Molecular characterization of an enterobacterial metallo beta-lactamase found in a clinical isolate of *Serratia marcescens* that shows imipenem resistance. *Antimicrobial agents and chemotherapy*. 1994 jan;38(1):71–8.
- [87] Vella P, Hussein WM, Leung EWW, Clayton D, Ollis DL, Mitić N, et al. The identification of new metallo- β -lactamase inhibitor leads from fragment-based screening. *Bioorganic and Medicinal Chemistry Letters*. 2011 jun;21(11):3282–3285.
- [88] Fukigai S, Alba J, Kimura S, Iida T, Nishikura N, Ishii Y, et al. Nosocomial outbreak of genetically related IMP-1 β -lactamase-producing *Klebsiella pneumoniae* in a general hospital in Japan. *International Journal of Antimicrobial Agents*. 2007 mar;29(3):306–310.
- [89] Kerr KG, Snelling AM. *Pseudomonas aeruginosa*: a formidable and ever-present adversary. *Journal of Hospital Infection*. 2009 dec;73(4):338–344.
- [90] Penteado AP, Castanheira M, Pignatari ACC, Guimarães T, Mamizuka EM, Gales AC. Dissemination of blaIMP-1-carrying integron In86 among *Klebsiella pneumoniae* isolates harboring a new trimethoprim resistance gene dfr23. *Diagnostic Microbiology and Infectious Disease*. 2009 jan;63(1):87–91.
- [91] Arakawa Y, Murakami M, Suzuki K, Ito H, Wacharotayankun R, Ohsuka S, et al. A novel integron-like element carrying the metallo-beta-lactamase gene blaIMP. *Antimicrobial agents and chemotherapy*. 1995;39(7):1612–5.
- [92] Laraki N, Franceschini N, Rossolini GM, Santucci P, Meunier C, de Pauw E, et al. Biochemical characterization of the *Pseudomonas aeruginosa* 101/1477 metallo-beta-lactamase IMP-1 produced by *Escherichia coli*. *Antimicrobial agents and chemotherapy*. 1999;43(4):902–6.
- [93] Marumo K, Takeda A, Nakamura Y, Nakaya K. Purification and Characterization of Metallo- β -Lactamase from *Serratia marcescens*. *Microbiology and Immunology*. 1995 jan;39(1):27–33.
- [94] Poirel L, Naas T, Nicolas D, Collet L, Bellais S, Cavallo JD, et al. Characterization of VIM-2, a carbapenem-hydrolyzing metallo-beta-lactamase and its plasmid- and integron-borne gene from a *Pseudomonas aeruginosa* clinical isolate in France. *Antimicrobial agents and chemotherapy*. 2000 apr;44(4):891–7.

- [95] Tsakris A, Pournaras S, Woodford N, Palepou MF, Babini GS, Douboyas J, et al. Outbreak of infections caused by *Pseudomonas aeruginosa* producing VIM-1 carbapenemase in Greece. *Journal of clinical microbiology*. 2000 mar;38(3):1290–2.
- [96] Watanabe M, Iyobe S, Inoue M, Mitsuhashi S. Transferable imipenem resistance in *Pseudomonas aeruginosa*. *Antimicrobial agents and chemotherapy*. 1991 jan;35(1):147–51.
- [97] Ito H, Arakawa Y, Ohsuka S, Wacharotayankun R, Kato N, Ohta M. Plasmid-mediated dissemination of the metallo-beta-lactamase gene blaIMP among clinically isolated strains of *Serratia marcescens*. *Antimicrobial agents and chemotherapy*. 1995 apr;39(4):824–9.
- [98] Concha NO, Janson Ca, Rowling P, Pearson S, Cheever Ca, Clarke BP, et al. Crystal Structure of the IMP-1 Metallo-beta-lactamase from *Pseudomonas aeruginosa* and Its Complex with a Mecarptocarboxylate Inhibitor: Binding Determinants of a Potent, Broad-Spectrum Inhibitor. *Biochemistry*. 2000;39:4288–4298.
- [99] Toney JH, Hammond GG, Fitzgerald PM, Sharma N, Balkovec JM, Rouen GP, et al. Succinic acids as potent inhibitors of plasmid-borne IMP-1 metallo-beta-lactamase. *The Journal of biological chemistry*. 2001 aug;276(34):31913–8.
- [100] Hiraiwa Y, Saito J, Watanabe T, Yamada M, Morinaka A, Fukushima T, et al. X-ray crystallographic analysis of IMP-1 metallo- β -lactamase complexed with a 3-aminophthalic acid derivative, structure-based drug design, and synthesis of 3,6-disubstituted phthalic acid derivative inhibitors. *Bioorganic & medicinal chemistry letters*. 2014 oct;24(20):4891–4.
- [101] Brem J, van Berkel SS, Zollman D, Lee SY, Gileadi O, McHugh PJ, et al. Structural Basis of Metallo- β -Lactamase Inhibition by Captopril Stereoisomers. *Antimicrobial agents and chemotherapy*. 2016 jan;60(1):142–50.
- [102] Galleni M, Lamotte-Brasseur J, Rossolini GM, Spencer J, Dideberg O, Frère JM, et al. Standard numbering scheme for class B beta-lactamases. *Antimicrobial agents and chemotherapy*. 2001 mar;45(3):660–3.
- [103] Garau G, García-Sáez I, Bebrone C, Anne C, Mercuri P, Galleni M, et al. Update of the standard numbering scheme for class B beta-lactamases. *Antimicrobial agents and chemotherapy*. 2004 jul;48(7):2347–9.
- [104] Liénard BMR, Garau G, Horsfall L, Karsisiotis AI, Damblon C, Lassaux P, et al. Structural basis for the broad-spectrum inhibition of metallo-beta-lactamases by thiols. [Article]. *Organic & biomolecular chemistry*. 2008 jul;6(13):2282–94.
- [105] Page MI, Badarau A. The mechanisms of catalysis by metallo beta-lactamases. *Bioinorganic chemistry and applications*. 2008;2008(5):576297.
- [106] Palzkill T. Metallo- β -lactamase structure and function. *Annals of the New York Academy of Sciences*. 2013 jan;1277(1):91–104.

- [107] Bebrone C. Metallo-beta-lactamases (classification, activity, genetic organization, structure, zinc coordination) and their superfamily. *Biochemical pharmacology*. 2007 dec;74(12):1686–701.
- [108] Ullah JH, Walsh TR, Taylor IA, Emery DC, Verma CS, Gamblin SJ, et al. The crystal structure of the LI metallo-beta-lactamase from *Stenotrophomonas maltophilia* at 1.7 Å resolution. *Journal of molecular biology*. 1998 nov;284(1):125–36.
- [109] Concha NO, Rasmussen BA, Bush K, Herzberg O. Crystal structure of the wide-spectrum binuclear zinc beta-lactamase from *Bacteroides fragilis*. *Structure*. 1996 jul;4(7):823–36.
- [110] Borra PS, Leiros HKS, Ahmad R, Spencer J, Leiros I, Walsh TR, et al. Structural and computational investigations of VIM-7: insights into the substrate specificity of vim metallo- β -lactamases. [Article]. *Journal of molecular biology*. 2011 aug;411(1):174–89.
- [111] Carfi A, Duée E, Galleni M, Frère JM, Dideberg O. 1.85 Å resolution structure of the zinc (II) beta-lactamase from *Bacillus cereus*. *Acta crystallographica Section D, Biological crystallography*. 1998 may;54(Pt 3):313–23.
- [112] Docquier JD, Benvenuti M, Calderone V, Stoczko M, Menciassi N, Rossolini GM, et al. High-resolution crystal structure of the subclass B3 metallo-beta-lactamase BJP-1: rational basis for substrate specificity and interaction with sulfonamides. *Antimicrobial agents and chemotherapy*. 2010 oct;54(10):4343–51.
- [113] Fabiane SM, Sohi MK, Wan T, Payne DJ, Bateson JH, Mitchell T, et al. Crystal structure of the zinc-dependent beta-lactamase from *Bacillus cereus* at 1.9 Å resolution: binuclear active site with features of a mononuclear enzyme. *Biochemistry*. 1998 sep;37(36):12404–11.
- [114] Garau G, Bebrone C, Anne C, Galleni M, Frère JM, Dideberg O. A metallo- β -lactamase enzyme in action: Crystal structures of the monozinc carbapenemase CphA and its complex with biapenem. *Journal of Molecular Biology*. 2005;345(4):785–795.
- [115] Garcia-Saez I, Hopkins J, Papamicael C, Franceschini N, Amicosante G, Rossolini GM, et al. The 1.5-angstrom structure of *Chryseobacterium meningosepticum* zinc beta-lactamase in complex with the inhibitor, D-captopril [Article]. *JOURNAL OF BIOLOGICAL CHEMISTRY*. 2003 jun;278(26):23868–23873.
- [116] Garcia-Saez I, Mercuri PS, Papamicael C, Kahn R, Frere JM, Galleni M, et al. Three-dimensional structure of FEZ-1, a monomeric subclass B3 metallo-beta-lactamase from *Fluoribacter gormanii*, in native form and in complex with D-captopril [Article]. *JOURNAL OF MOLECULAR BIOLOGY*. 2003 jan;325(4):651–660.
- [117] Garcia-Saez I, Docquier JD, Rossolini GM, Dideberg O. The three-dimensional structure of VIM-2, a Zn-beta-lactamase from *Pseudomonas aeruginosa* in its reduced and oxidised form. *Journal of molecular biology*. 2008 jan;375(3):604–11.

- [118] Murphy TA, Catto LE, Halford SE, Hadfield AT, Minor W, Walsh TR, et al. Crystal structure of *Pseudomonas aeruginosa* SPM-I provides insights into variable zinc affinity of metallo-beta-lactamases. *Journal of molecular biology*. 2006 mar;357(3):890–903.
- [119] Zhang H, Hao Q. Crystal structure of NDM-I reveals a common β -lactam hydrolysis mechanism. *FASEB Journal*. 2011;25(8):2574–2582.
- [120] Yang Y, Keeney D, Tang X, Canfield N, Rasmussen BA. Kinetic properties and metal content of the metallo-beta-lactamase CcrA harboring selective amino acid substitutions. *The Journal of biological chemistry*. 1999;274(22):15706–15711.
- [121] Yanchak MP, Taylor Ra, Crowder MW. Mutational analysis of metallo-beta-lactamase CcrA from *Bacteroides fragilis*. *Biochemistry*. 2000;39(37):11330–9.
- [122] de Seny D, Prosperi-Meys C, Bebrone C, Rossolini GM, Page MI, Noel P, et al. Mutational analysis of the two zinc-binding sites of the *Bacillus cereus* 569/H/9 metallo-beta-lactamase. *The Biochemical Journal*. 2002 may;363(Pt 3):687–96.
- [123] Garrity JD, Carenbauer AL, Herron LR, Crowder MW. Metal binding Asp-120 in metallo-beta-lactamase LI from *Stenotrophomonas maltophilia* plays a crucial role in catalysis [Article]. *JOURNAL OF BIOLOGICAL CHEMISTRY*. 2004 jan;279(2):920–927.
- [124] Wang Z, Fast W, Valentine AM, Benkovic SJ. Metallo- β -lactamase: structure and mechanism. *Current Opinion in Chemical Biology*. 1999 oct;3(5):614–622.
- [125] Wang Z, Fast W, Benkovic SJ. On the mechanism of the metallo-beta-lactamase from *Bacteroides fragilis*. *Biochemistry*. 1999 aug;38(31):10013–23.
- [126] Park H, Brothers EN, Merz KM. Hybrid QM/MM and DFT investigations of the catalytic mechanism and inhibition of the dinuclear zinc metallo-beta-lactamase CcrA from *Bacteroides fragilis* [Article]. *JOURNAL OF THE AMERICAN CHEMICAL SOCIETY*. 2005 mar;127(12):4232–4241.
- [127] Crowder MW, Spencer J, Vila AJ. Metallo-beta-lactamases: Novel weaponry for antibiotic resistance in bacteria [Review]. *Accounts of chemical research*. 2006 oct;39(10):721–728.
- [128] Hu Z, Periyannan G, Bennett B, Crowder MW. Role of the Zn1 and Zn2 sites in metallo-beta-lactamase LI. *Journal of the American Chemical Society*. 2008 oct;130(43):14207–16.
- [129] Garrity JD, Bennett B, Crowder MW. Direct evidence that the reaction intermediate of metallo-beta-lactamase LI is metal bound. [Article]. *Biochemistry*. 2005 jan;44(3):1078–87.
- [130] Llarrull LI, Fabiane SM, Kowalski JM, Bennett B, Sutton BJ, Vila AJ. Asp-120 Locates Zn2 for Optimal Metallo-beta-lactamase Activity [Article]. *Journal of Biological Chemistry*. 2007 apr;282(25):18276–18285.
- [131] Rasia R, Vila A. Mechanistic study of the hydrolysis of nitrocefin mediated by *B. cereus* metallo- β -lactamase. *Arkivoc*. 2003;2003(x):507–516.

- [132] Yang H, Aitha M, Hetrick AM, Richmond TK, Tierney DL, Crowder MW. Mechanistic and spectroscopic studies of metallo- β -lactamase NDM-1. *Biochemistry*. 2012 may;51(18):3839–47.
- [133] Griffin DH, Richmond TK, Sanchez C, Moller AJ, Breece RM, Tierney DL, et al. Structural and kinetic studies on metallo- β -lactamase IMP-1. [Article]. *Biochemistry*. 2011 oct;50(42):9125–34.
- [134] Moali C, Anne C, Lamotte-Brasseur J, Gros Lambert S, Devreese B, Van Beeumen J, et al. Analysis of the importance of the metallo-beta-lactamase active site loop in substrate binding and catalysis. *Chemistry & biology*. 2003 apr;10(4):319–29.
- [135] Yamaguchi Y, Kuroki T, Yasuzawa H, Higashi T, Jin W, Kawanami A, et al. Probing the role of Asp-120(81) of metallo-beta-lactamase (IMP-1) by site-directed mutagenesis, kinetic studies, and X-ray crystallography. [Article]. *The Journal of biological chemistry*. 2005 may;280(21):20824–32.
- [136] Tioni MF, Llarrull LI, Poeylout-Palena AA, Martí MA, Saggiu M, Periyannan GR, et al. Trapping and characterization of a reaction intermediate in carbapenem hydrolysis by *B. cereus* metallo-beta-lactamase. *Journal of the American Chemical Society*. 2008 nov;130(47):15852–63.
- [137] Mojica MF, Bonomo RA, Fast W. *BI-Metallo-beta-Lactamases : Where Do We Stand ? Current Drug Targets*. 2016;17(9):1029–50.
- [138] Herzberg O, Fitzgerald PM. Metallo Beta-Lactamases. In: *Handbook of Metalloproteins*. Chichester, UK: John Wiley & Sons, Ltd; 2006. .
- [139] Payne DJ, Bateson JH, Gasson BC, Proctor D, Khushi T, Farmer TH, et al. Inhibition of metallo-beta-lactamases by a series of mercaptoacetic acid thiol ester derivatives. *Antimicrobial agents and chemotherapy*. 1997 jan;41(1):135–40.
- [140] Payne DJ, Bateson JH, Gasson BC, Khushi T, Proctor D, Pearson SC, et al. Inhibition of metallo-beta-lactamases by a series of thiol ester derivatives of mercaptophenylacetic acid. *FEMS microbiology letters*. 1997 dec;157(1):171–5.
- [141] Goto M, Takahashi T, Yamashita F, Koreeda A, Mori H, Ohta M, et al. Inhibition of the metallo-beta-lactamase produced from *Serratia marcescens* by thiol compounds. *Biological & pharmaceutical bulletin*. 1997;20(11):1136–1140.
- [142] Hammond GG, Huber JL, Greenlee ML, Laub JB, Young K, Silver LL, et al. Inhibition of IMP-1 Metallo-beta-lactamase and Sensitization of IMP-1-producing Bacteria by Thioster Derivatives. *FEMS Microbiol Lett*. 1999;459(1999):289–296.
- [143] Mollard C, Moali C, Papamicael C, Damblon C, Vessilier S, Amicosante G, et al. Thiomandelic acid, a broad spectrum inhibitor of zinc β -lactamases. Kinetic and spectroscopic studies. *Journal of Biological Chemistry*. 2001;276(48):45015–45023.

- [144] Karsisiotis AI, Damblon CF, Roberts GCK. Solution structures of the *Bacillus cereus* metallo-beta-lactamase BclI and its complex with the broad spectrum inhibitor R-thiomandelic acid [Article]. *BIOCHEMICAL JOURNAL*. 2013 dec;456(3):397–407.
- [145] Olsen L, Pettersson I, Hemmingsen L, Adolph Hw, Jørgensen FS. Docking and scoring of metallo- β -lactamases inhibitors. *Journal of Computer-Aided Molecular Design*. 2004 apr;18(4):287–302.
- [146] Wang C, Guo H. Inhibitor binding by metallo-beta-lactamase IMP-I from *Pseudomonas aeruginosa*: Quantum Mechanical/Molecular mechanical simulations [Article]. *JOURNAL OF PHYSICAL CHEMISTRY B*. 2007 aug;111(33):9986–9992.
- [147] Antony J, Gresh N, Olsen L, Hemmingsen L, Schofield CJ, Bauer R. Binding of D- and L-captopril inhibitors to metallo-beta-lactamase studied by polarizable molecular mechanics and quantum mechanics. *Journal of Computational Chemistry*. 2002;23(13):1281–1296.
- [148] Selevsek N, Tholey A, Heinzle E, Liénard BMR, Oldham NJ, Schofield CJ, et al. Studies on ternary metallo-beta lactamase-inhibitor complexes using electrospray ionization mass spectrometry. [Article]. *Journal of the American Society for Mass Spectrometry*. 2006 jul;17(7):1000–4.
- [149] Damblon C, Jensen M, Ababou A, Barsukov I, Papamicael C, Schofield CJ, et al. The inhibitor thiomandelic acid binds to both metal ions in metallo- β -lactamase and induces positive cooperativity in metal binding. *Journal of Biological Chemistry*. 2003;278(31):29240–29251.
- [150] Heinz U, Bauer R, Wommer S, Meyer-Klaucke W, Papamichaels C, Bateson J, et al. Coordination geometries of metal ions in d- or l-captopril-inhibited metallo-beta-lactamases. *The Journal of biological chemistry*. 2003 jun;278(23):20659–66.
- [151] Rydzik AM, Brem J, van Berkel SS, Pfeffer I, Makena A, Claridge TDW, et al. Monitoring conformational changes in the NDM-I metallo- β -lactamase by 19F NMR spectroscopy. *Angewandte Chemie (International ed in English)*. 2014 mar;53(12):3129–33.
- [152] Li N, Xu Y, Xia Q, Bai C, Wang T, Wang L, et al. Simplified captopril analogues as NDM-I inhibitors. *Bioorganic and Medicinal Chemistry Letters*. 2014 jan;24(1):386–389.
- [153] Nauton L, Kahn R, Garau G, Hernandez JF, Dideberg O. Structural insights into the design of inhibitors for the LI metallo-beta-lactamase from *Stenotrophomonas maltophilia*. [Article]. *Journal of molecular biology*. 2008 jan;375(1):257–69.
- [154] Lassaux P, Hamel M, Gulea M, Delbrück H, Mercuri PS, Horsfall L, et al. Mercaptophosphate compounds as broad-spectrum inhibitors of the metallo- β -lactamases [Article]. *Journal of Medicinal Chemistry*. 2010 jul;53(13):4862–4876.
- [155] Puerta DT, Lewis JA, Cohen SM. New beginnings for matrix metalloproteinase inhibitors: Identification of high-affinity zinc-binding groups. *Journal of the American Chemical Society*. 2004;126(27):8388–8389.

- [156] Schlesinger SR, Bruner B, Farmer PJ, Kim SK. Kinetic characterization of a slow-binding inhibitor of Bla2: thiomaltol. *Journal of enzyme inhibition and medicinal chemistry*. 2013 feb;28(1):137–42.
- [157] Faridoon, Hussein WM, Vella P, Islam NU, Ollis DL, Schenk G, et al. 3-Mercapto-1,2,4-triazoles and N-acylated thiosemicarbazides as metallo- β -lactamase inhibitors. *Bioorganic & Medicinal Chemistry Letters*. 2012 jan;22(1):380–386.
- [158] Nagano R, Adachi Y, Imamura H, Yamada K, Hashizume T, Morishima H. Carbapenem derivatives as potential inhibitors of various beta-lactamases, including class B metallo-beta-lactamases. *Antimicrobial agents and chemotherapy*. 1999;43(10):2497–2503.
- [159] Nagano R, Adachi Y, Hashizume T, Morishima H. In vitro antibacterial activity and mechanism of action of J-111,225, a novel 1beta-methylcarbapenem, against transferable IMP-I metallo-beta-lactamase producers. *The Journal of antimicrobial chemotherapy*. 2000 mar;45(3):271–6.
- [160] Murphy BP, Pratt RF. A thiono-beta-lactam substrate for the beta-lactamase II of *Bacillus cereus*. Evidence for direct interaction between the essential metal ion and substrate. *The Biochemical journal*. 1989;258(3):765–768.
- [161] Tsang WY, Dhanda A, Schofield CJ, Frère JM, Galleni M, Page MI. The inhibition of metallo- β -lactamase by thioxo-cephalosporin derivatives. *Bioorganic & Medicinal Chemistry Letters*. 2004 apr;14(7):1737–1739.
- [162] Siemann S, Evanoff DP, Marrone L, Clarke AJ, Viswanatha T, Dmitrienko GI. N-Arylsulfonyl Hydrazones as Inhibitors of IMP-I Metallo- -Lactamase [Article]. *Antimicrobial Agents and Chemotherapy*. 2002 aug;46(8):2450–2457.
- [163] Moloughney JG, Thomas JD, Toney JH, D Thomas J. Novel IMP-I metallo-beta-lactamase inhibitors can reverse meropenem resistance in *Escherichia coli* expressing IMP-I. [Article]. *FEMS microbiology letters*. 2005 feb;243(1):65–71.
- [164] Ishii Y, Eto M, Mano Y, Tateda K, Yamaguchi K. In vitro potentiation of carbapenems with ME1071, a novel metallo-beta-lactamase inhibitor, against metallo-beta-lactamase-producing *Pseudomonas aeruginosa* clinical isolates. *Antimicrobial agents and chemotherapy*. 2010 sep;54(9):3625–9.
- [165] Livermore DM, Mushtaq S, Morinaka A, Ida T, Maebashi K, Hope R. Activity of carbapenems with ME1071 (disodium 2,3-diethylmaleate) against Enterobacteriaceae and *Acinetobacter* spp. with carbapenemases, including NDM enzymes. [Article]. *The Journal of antimicrobial chemotherapy*. 2013 jan;68(1):153–8.
- [166] Hiraiwa Y, Morinaka A, Fukushima T, Kudo T. Metallo- β -lactamase inhibitory activity of phthalic acid derivatives. *Bioorganic & Medicinal Chemistry Letters*. 2009 sep;19(17):5162–5165.

- [167] Hiraiwa Y, Morinaka A, Fukushima T, Kudo T. Metallo- β -lactamase inhibitory activity of 3-alkyloxy and 3-amino phthalic acid derivatives and their combination effect with carbapenem. *Bioorganic & medicinal chemistry*. 2013 sep;21(18):5841–50.
- [168] Mohamed MS, Hussein WM, McGeary RP, Vella P, Schenk G, Abd El-hameed RH. Synthesis and kinetic testing of new inhibitors for a metallo- β -lactamase from *Klebsiella pneumonia* and *Pseudomonas aeruginosa* [Article]. *European Journal of Medicinal Chemistry*. 2011 dec;46(12):6075–6082.
- [169] Toney JH, Fitzgerald PM, Grover-Sharma N, Olson SH, May WJ, Sundelof JG, et al. Antibiotic sensitization using biphenyl tetrazoles as potent inhibitors of *Bacteroides fragilis* metallo-beta-lactamase. *Chemistry & biology*. 1998;5(4):185–96.
- [170] Toney JH, Cleary KA, Hammond GG, Yuan X, May WJ, Hutchins SM, et al. Structure-activity relationships of biphenyl tetrazoles as metallo- β -lactamase inhibitors. *Bioorganic & Medicinal Chemistry Letters*. 1999 sep;9(18):2741–2746.
- [171] Feng L, Yang KW, Zhou LS, Xiao JM, Yang X, Zhai L, et al. N-Heterocyclic dicarboxylic acids: Broad-spectrum inhibitors of metallo- β -lactamases with co-antibacterial effect against antibiotic-resistant bacteria. *Bioorganic and Medicinal Chemistry Letters*. 2012;22(16):5185–5189.
- [172] Hussein WM, Fatahala SS, Mohamed ZM, McGeary RP, Schenk G, Ollis DL, et al. Synthesis and kinetic testing of tetrahydropyrimidine-2-thione and pyrrole derivatives as inhibitors of the metallo- β -lactamase from *Klebsiella pneumonia* and *Pseudomonas aeruginosa*. [Article]. *Chemical biology & drug design*. 2012 oct;80(4):500–15.
- [173] Jones G, Willett P, Glen RC, Leach AR, Taylor R. Development and validation of a genetic algorithm for flexible docking. *Journal of molecular biology*. 1997;267(3):727–48.
- [174] Jain AN. Scoring functions for protein-ligand docking. *Current protein & peptide science*. 2006 oct;7(5):407–20.
- [175] GOLD scoring function performance against the DUD decoy/active set. *Cambridge Crystallographic Data Centre*; 2011.
- [176] Wermuth CG, Ganellin CR, Lindberg P, Mitscher La. Glossary of Terms Used in Medicinal Chemistry (IUPAC recommendations 1998). *Pure and Applied Chemistry*. 1998;70(5):1129–1143.
- [177] Van Drie JH. Strategies for the determination of pharmacophoric 3D database queries. *Journal of computer-aided molecular design*. 1997;11(1):39–52.
- [178] Irwin JJ, Sterling T, Mysinger MM, Bolstad ES, Coleman RG. ZINC: A free tool to discover chemistry for biology. *Journal of Chemical Information and Modeling*. 2012;52(7):1757–1768.

- [179] Wishart DS, Knox C, Guo AC, Shrivastava S, Hassanali M, Stothard P, et al. DrugBank: a comprehensive resource for in silico drug discovery and exploration. *Nucleic acids research*. 2006;34(Database issue):D668–72.
- [180] Halgren Ta. Merck molecular force field. I. Basis, form, scope, parameterization, and performance of MMFF94. *Journal of Computational Chemistry*. 1996 apr;17(5-6):520–552.
- [181] Kurosaki H, Yamaguchi Y, Yasuzawa H, Jin W, Yamagata Y, Arakawa Y. Probing, inhibition, and crystallographic characterization of metallo- β -lactamase (IMP-1) with fluorescent agents containing dansyl and thiol groups. *ChemMedChem*. 2006;1(9):969–972.
- [182] Navarro PG, Osso BQ, Ortiz RG, Martinez de las Parras PJ, Martinez Puentedura MI, Cabeza Gonzalez MC. Inhibition of Beta-Lactamase II of *Bacillus cereus* by Penamaldic Derivatives of Penicillins. *Antimicrobial Agents and Chemotherapy*. 2004 mar;48(3):1058–1060.
- [183] Yamaguchi Y, Jin W, Matsunaga K, Ikemizu S, Yamagata Y, Wachino Ji, et al. Crystallographic investigation of the inhibition mode of a VIM-2 metallo-beta-lactamase from *Pseudomonas aeruginosa* by a mercaptocarboxylate inhibitor [Article]. *JOURNAL OF MEDICINAL CHEMISTRY*. 2007 dec;50(26):6647–6653.
- [184] Liénard BMR, Hüting R, Lassaux P, Galleni M, Frère JM, Schofield CJ. Dynamic Combinatorial Mass Spectrometry Leads to Metallo- β -lactamase Inhibitors. *Journal of Medicinal Chemistry*. 2008 feb;51(3):684–688.
- [185] Wachino JI, Yamaguchi Y, Mori S, Kurosaki H, Arakawa Y, Shibayama K. Structural insights into the subclass B3 metallo- β -lactamase SMB-1 and the mode of inhibition by the common metallo- β -lactamase inhibitor mercaptoacetate. *Antimicrobial agents and chemotherapy*. 2013 jan;57(1):101–9.
- [186] Badarau A, Llinás A, Laws AP, Damblon C, Page MI. Inhibitors of metallo-beta-lactamase generated from beta-lactam antibiotics. *Biochemistry*. 2005;44(24):8578–8589.
- [187] Olsen L, Jost S, Adolph HW, Pettersson I, Hemmingsen L, Jørgensen FS. New leads of metallo-beta-lactamase inhibitors from structure-based pharmacophore design. *Bioorganic & medicinal chemistry*. 2006 apr;14(8):2627–35.
- [188] Horsfall L, Garau G, Liénard BMR, Dideberg O, Schofield CJ, Frère JM, et al. Competitive inhibitors of the CphA metallo- β -lactamase from *Aeromonas hydrophila*. *Antimicrobial Agents and Chemotherapy*. 2007;51(6):2136–2142.
- [189] Liénard BMR, Horsfall L, Galleni M, Frère JM, Schofield CJ. Inhibitors of the FEZ-1 metallo- β -lactamase. *Bioorganic and Medicinal Chemistry Letters*. 2007;17(4):964–968.
- [190] Ganta SR, Perumal S, Pagadala SRR, Samuelsen Ø, Spencer J, Pratt RF, et al. Approaches to the simultaneous inactivation of metallo- and serine- β -lactamases. *Bioorganic and Medicinal Chemistry Letters*. 2009;19(6):1618–1622.

- [191] Walter MW, Felici A, Galleni M, Paul R, Robert M. Trifluoromethyl alcohol and ketone inhibitors of metallo- β -lactamases. *Bioorganic and Medicinal Chemistry Letters*. 1996;6(20):2455–2458.
- [192] Walter MW, Adlington RM, Baldwin JE, Schofield CJ. Synthesis of metallo- β -lactamase inhibitors. *Tetrahedron*. 1997 may;53(21):7275–7290.
- [193] Payne D], Hueso-Rodríguez JA, Boyd H, Concha NO, Janson Ca, Gilpin M, et al. Identification of a series of tricyclic natural products as potent broad-spectrum inhibitors of metallo-beta-lactamases. *Antimicrobial agents and chemotherapy*. 2002 jun;46(6):1880–6.
- [194] Denny BJ, Lambert PA, West PWJ. The flavonoid galangin inhibits the LI metallo-beta-lactamase from *Stenotrophomonas maltophilia*. *FEMS Microbiology Letters*. 2002;208(1):21–24.
- [195] Chen P, Horton LB, Mikulski RL, Deng L, Sundriyal S, Palzkill T, et al. 2-Substituted 4,5-dihydrothiazole-4-carboxylic acids are novel inhibitors of metallo- β -lactamases. *Bioorganic & medicinal chemistry letters*. 2012 oct;22(19):6229–32.
- [196] Fitzgerald PM, Wu JK, Toney JH. Unanticipated inhibition of the metallo-beta-lactamase from *Bacteroides fragilis* by 4-morpholineethanesulfonic acid (MES): a crystallographic study at 1.85-Å resolution. *Biochemistry*. 1998;37(19):6791–800.
- [197] Zervosen A, Valladares MH, Devreese B, Prosperi-Meys C, Adolph HW, Mercuri PS, et al. Inactivation of *Aeromonas hydrophila* metallo-beta-lactamase by cephamycins and moxalactam. *European journal of biochemistry / FEBS*. 2001 jul;268(13):3840–50.
- [198] Mercuri PS, García-Sáez I, De Vriendt K, Thamm I, Devreese B, Van Beeumen J, et al. Probing the specificity of the subclass B3 FEZ-I metallo- β -lactamase by site-directed mutagenesis. *Journal of Biological Chemistry*. 2004;279(32):33630–33638.
- [199] Kurosaki H, Yamaguchi Y, Higashi T, Soga K, Matsueda S, Yumoto H, et al. Irreversible inhibition of metallo-beta-lactamase (IMP-I) by 3-(3-mercaptopropionylsulfanyl)propionic acid pentafluorophenyl ester. *Angewandte Chemie (International ed in English)*. 2005 jun;44(25):3861–4.
- [200] Thomas PW, Spicer T, Cammarata M, Brodbelt JS, Hodder P, Fast W. An altered zinc-binding site confers resistance to a covalent inactivator of New Delhi metallo-beta-lactamase-I (NDM-I) discovered by high-throughput screening. *Bioorganic and Medicinal Chemistry*. 2013;21(11):3138–3146.
- [201] Weide T, Saldanha SA, Minond D, Spicer TP, Fotsing JR, Spaargaren M, et al. NH-1,2,3-triazole inhibitors of the VIM-2 metallo- β -lactamase. *ACS Medicinal Chemistry Letters*. 2010;1(4):150–154.
- [202] Hartigan JA. *Wiley Series in Probability and Mathematical Statistics*. 1st ed. New York: John Wiley & Sons, Inc; 1975.

- [203] Antimicrobial resistance: Global Report on Surveillance. World Health Organization; 2014.
- [204] Greenlee ML, Laub JB, Balkovec JM, Hammond ML, Hammond GG, Pompliano DL, et al. Synthesis and SAR of thioester and thiol inhibitors of IMP-I metallo-beta-lactamase. *Bioorganic & medicinal chemistry letters*. 1999 sep;9(17):2549–54.
- [205] Siemann S, Clarke AJ, Viswanatha T, Dmitrienko GI. Thiols as classical and slow-binding inhibitors of IMP-I and other binuclear metallo-beta-lactamases. *Biochemistry*. 2003 feb;42(6):1673–83.
- [206] Jin W, Arakawa Y, Yasuzawa H, Taki T, Hashiguchi R, Mitsutani K, et al. Comparative Study of the Inhibition of Metallo- β -Lactamases (IMP-I and VIM-2) by Thiol Compounds That Contain a Hydrophobic Group. *Biological & Pharmaceutical Bulletin*. 2004;27(6):851–856.
- [207] Arjomandi OK, Hussein WM, Vella P, Yusof Y, Sidjabat HE, Schenk G, et al. Design, synthesis, and in vitro and biological evaluation of potent amino acid-derived thiol inhibitors of the metallo- β -lactamase IMP-I. *European Journal of Medicinal Chemistry*. 2016;114:318–327.

Appendices

Appendix A

Molecules excluded from the result set

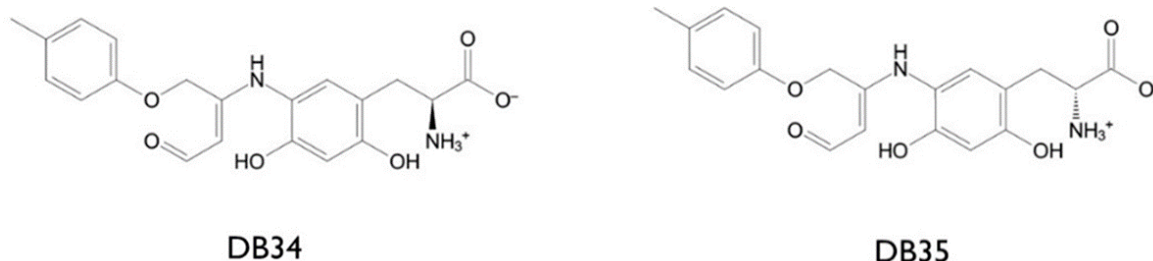


Figure A.1. Docking screening results: Aldehydes from the DrugBank subset.

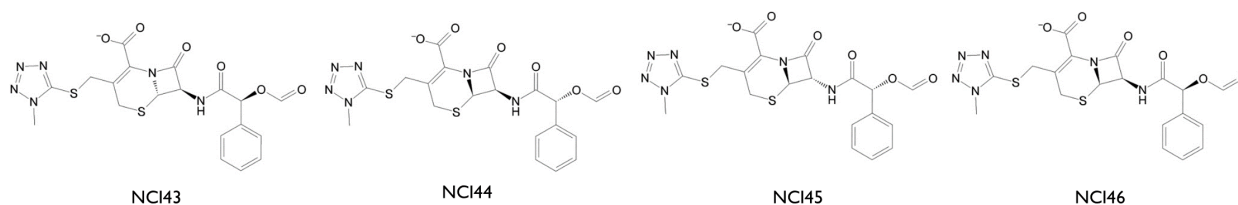


Figure A.2. Docking screening results: Aldehydes from the NCI subset.

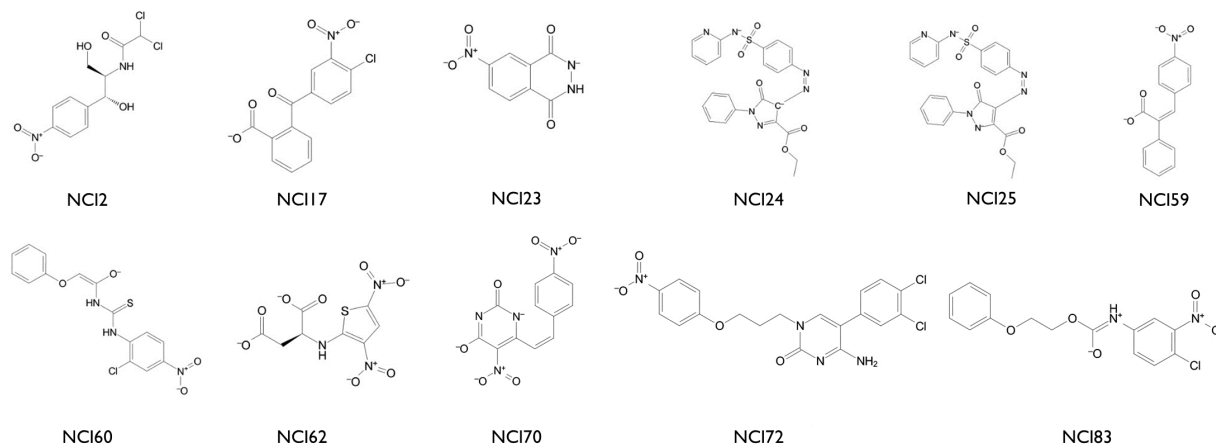


Figure A.3. Docking screening results: Compounds with nitro groups from the NCI subset.

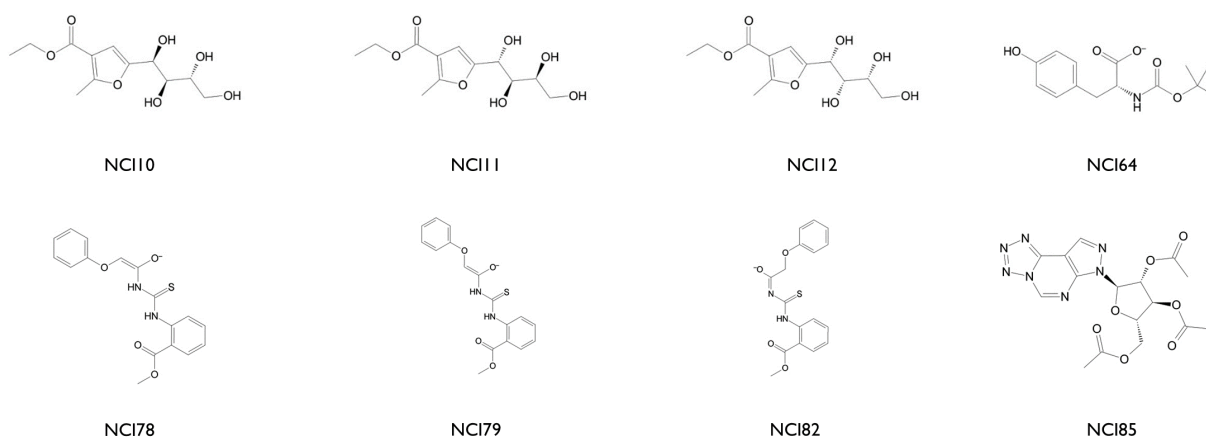


Figure A.4. Docking screening results: Esters from the NCI subset.

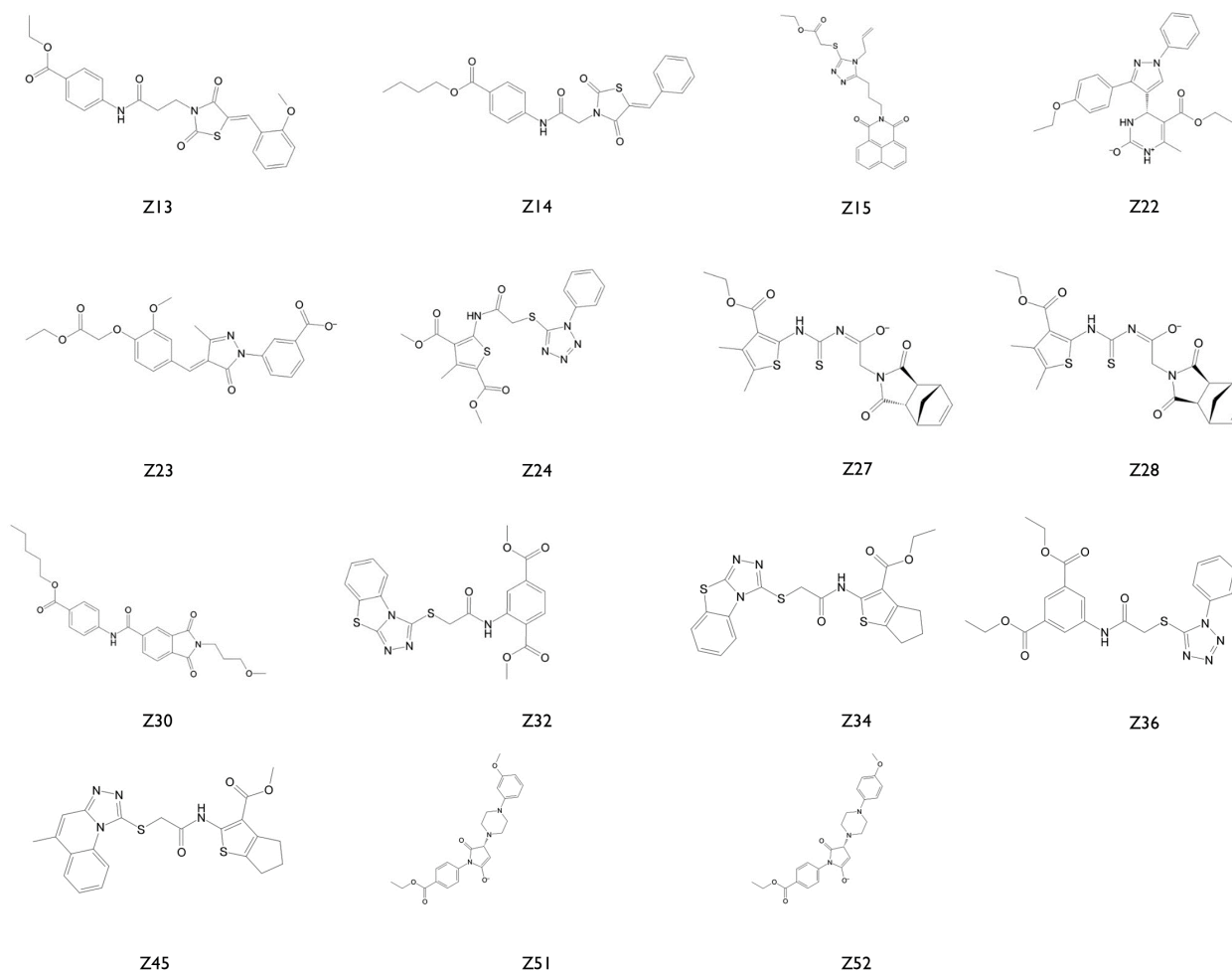


Figure A.5. Docking screening results: Esters from the ZINC subset.

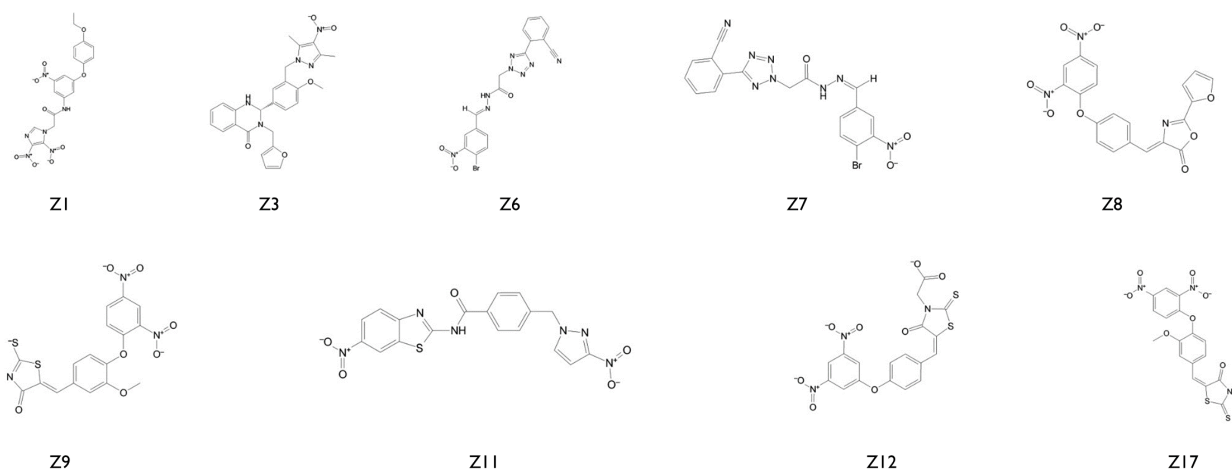


Figure A.6. Docking screening results: Compounds with nitro groups from the ZINC subset.

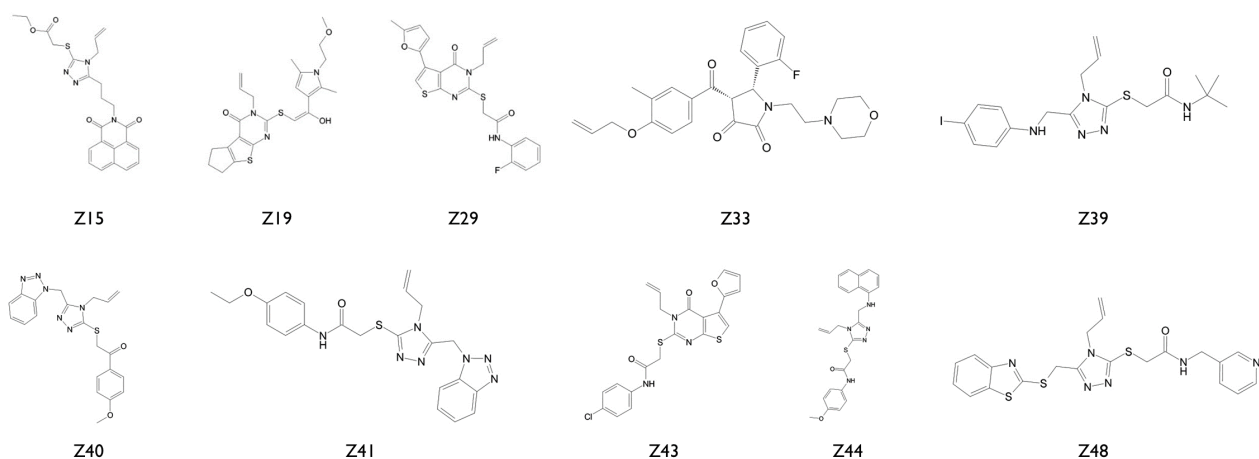


Figure A.7. Docking screening results: Compounds with terminal alkenes from the ZINC subset.

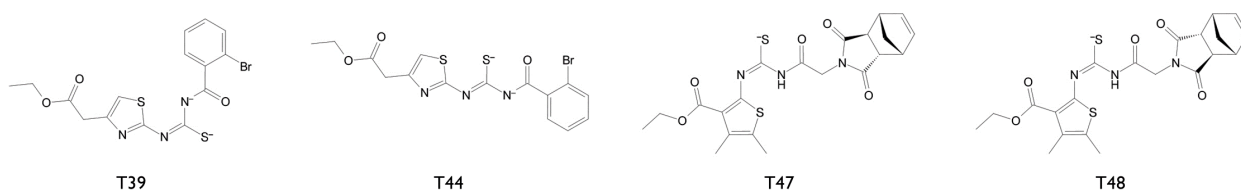


Figure A.8. Docking screening results: Ester from the Thiol subset.

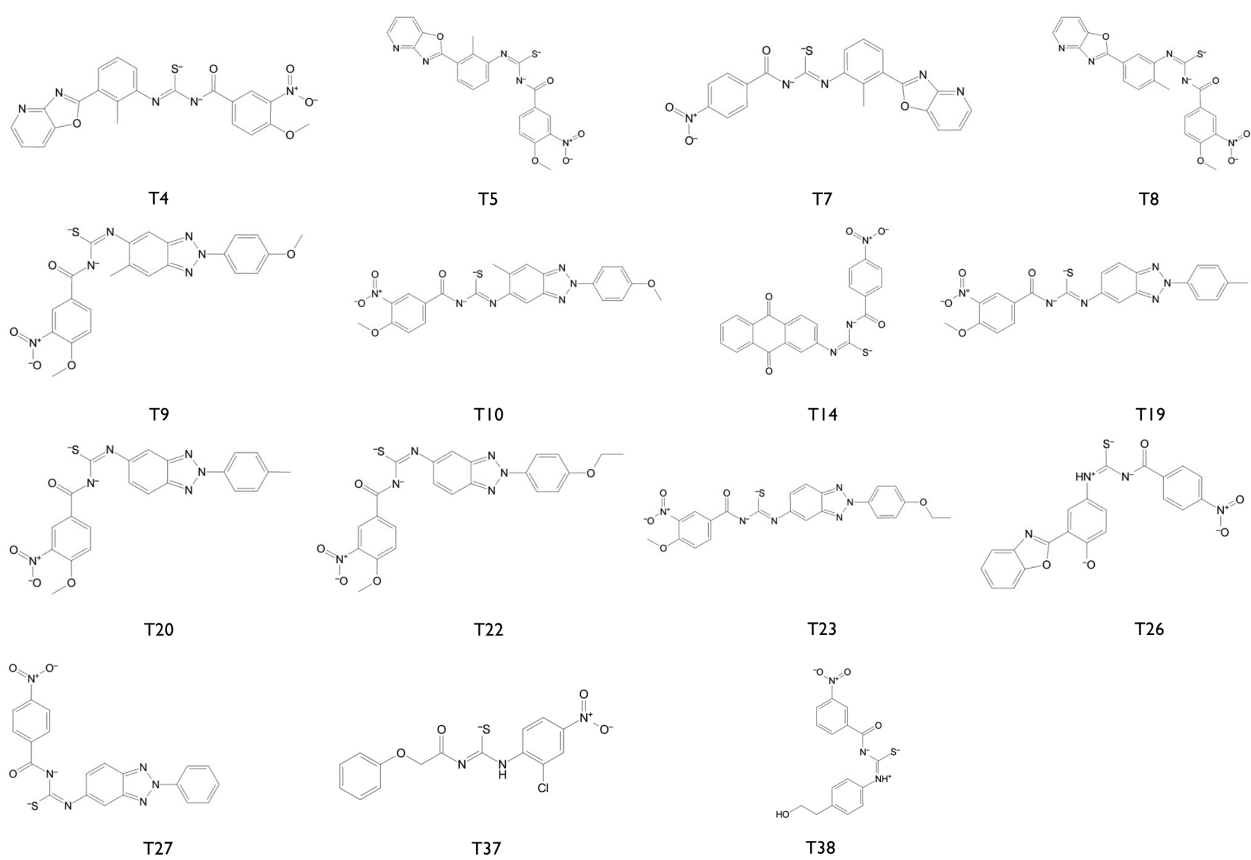


Figure A.9. Docking screening results: Compounds with nitro groups from the Thiol subset.

Appendix B

Molecule codes

Table B1. Molecule identifiers.

Study ID	Database ID	Gold PLP Fitness
DB1	DB00278	92.493
DB2	DB00118	93.009
DB3	DB00144	98.289
DB4	DB00225	101.362
DB5	DB00303	93.865
DB6	DB00319	100.334
DB7	DB00303	93.865
DB8	DB02030	95.223
DB9	DB02324	91.835
DB10	DB02569	91.534
DB11	DB02569	97.974
DB12	DB02569	92.792
DB13	DB02569	92.662
DB14	DB02511	97.026
DB15	DB02511	91.052
DB16	DB02569	101.901
DB17	DB02569	95.614
DB18	DB02569	91.010
DB19	DB02569	99.742
DB20	DB01903	92.742
DB21	DB01903	90.903
DB22	DB02324	94.758
DB23	DB02307	95.204
DB24	DB02677	91.332
DB25	DB02677	91.740

Study ID	Database ID	Gold PLP Fitness
DB26	DB02267	92.848
DB27	DB02635	91.159
DB28	DB02635	92.062
DB29	DB01961	90.698
DB30	DB01937	94.460
DB31	DB02480	91.578
DB32	DB02549	91.430
DB33	DB02549	103.696
DB34	DB02537	96.482
DB35	DB02537	91.190
DB36	DB00811	91.282
DB37	DB01799	91.337
DB38	DB02380	95.408
DB39	DB01834	91.085
DB40	DB01834	92.551
DB41	DB02549	97.924
DB42	DB02380	91.548
DB43	DB02380	100.767
DB44	DB02443	93.766
DB45	DB02443	90.873
DB46	DB02025	94.069
DB47	DB02549	90.991
DB48	DB02519	95.392
DB49	DB01814	125.428
NCI1	NSC3620	91.183
NCI2	NSC3069	91.199
NCI3	NSC115916	92.050
NCI4	NSC112530	91.405
NCI5	NSC105571	90.930
NCI6	NSC227190	100.836
NCI7	NSC227190	91.732
NCI8	NSC227190	91.390
NCI9	NSC9600	99.659
NCI10	NSC5569	94.121
NCI11	NSC5569	93.781
NCI12	NSC5569	97.259
NCI13	NSC4467	99.845

Study ID	Database ID	Gold PLP Fitness
NCI14	NSC16773	96.046
NCI15	NSC21923	95.435
NCI16	NSC17124	91.720
NCI17	NSC15366	90.964
NCI18	NSC24628	93.941
NCI19	NSC24628	93.282
NCI20	NSC16764	111.503
NCI21	NSC12353	90.863
NCI22	NSC41579	91.246
NCI23	NSC524676	91.738
NCI24	NSC114375	93.948
NCI25	NSC114375	97.386
NCI26	NSC17153	100.782
NCI27	NSC17153	105.227
NCI28	NSC116651	110.193
NCI29	NSC89636	95.777
NCI30	NSC99559	103.185
NCI31	NSC89647	98.005
NCI32	NSC88478	104.598
NCI33	NSC89632	95.628
NCI34	NSC89632	93.671
NCI35	NSC81512	98.959
NCI36	NSC47083	90.696
NCI37	NSC111081	93.649
NCI38	NSC84339	97.052
NCI39	NSC260704	93.484
NCI40	NSC310036	98.623
NCI41	NSC310036	92.514
NCI42	NSC334044	94.301
NCI43	NSC299588	96.779
NCI44	NSC299588	95.476
NCI45	NSC299588	91.996
NCI46	NSC299588	95.593
NCI47	NSC257868	94.697
NCI48	NSC295275	90.944
NCI49	NSC334044	95.242
NCI50	NSC334044	91.850

Study ID	Database ID	Gold PLP Fitness
NCI51	NSC234506	92.497
NCI52	NSC332882	92.464
NCI53	NSC342731	91.139
NCI54	NSC342731	92.894
NCI55	NSC257868	95.853
NCI56	NSC203787	102.072
NCI57	NSC203787	96.703
NCI58	NSC257868	92.734
NCI59	NSC133920	95.263
NCI60	NSC216348	92.796
NCI61	NSC257868	92.268
NCI62	NSC245216	92.587
NCI63	NSC164035	100.221
NCI64	NSC334307	94.003
NCI65	NSC231438	96.635
NCI66	NSC205442	96.379
NCI67	NSC205442	91.153
NCI68	NSC305269	93.995
NCI69	NSC251195	92.038
NCI70	NSC260398	92.855
NCI71	NSC211823	99.632
NCI72	NSC211293	103.914
NCI73	NSC323892	93.048
NCI74	NSC299132	91.066
NCI75	NSC328171	92.089
NCI76	NSC298162	91.823
NCI77	NSC331806	107.621
NCI78	NSC220153	93.329
NCI79	NSC220153	94.665
NCI80	NSC282109	92.402
NCI81	NSC240662	95.216
NCI82	NSC220153	98.194
NCI83	NSC205918	96.058
NCI84	NSC338102	94.313
NCI85	NSC304114	92.320
NCI86	NSC287041	92.493
Z1	8434995	93.286

Study ID	Database ID	Gold PLP Fitness
Z2	8434865	91.371
Z3	8432213	95.295
Z4	8722520	91.733
Z5	8432853	91.124
Z6	3211127	99.724
Z7	3211127	97.432
Z8	8435024	96.681
Z9	2067674	93.007
Z10	1854373	94.138
Z11	13570155	99.358
Z12	2067837	99.879
Z13	8432980	92.554
Z14	8432975	94.416
Z15	8432993	99.183
Z16	8432760	91.399
Z17	15011501	91.037
Z18	8432850	91.155
Z19	1803301	98.537
Z20	670452	94.525
Z21	1019683	91.556
Z22	730344	93.317
Z23	8432652	93.700
Z24	1895120	103.545
Z25	8432462	94.490
Z26	8432865	92.079
Z27	8432859	107.118
Z28	8432859	103.779
Z29	719594	103.009
Z30	8432848	92.968
Z31	8433148	92.184
Z32	1801756	96.177
Z33	8433244	97.444
Z34	1895861	94.002
Z35	1016328	90.849
Z36	1895156	99.751
Z37	214478	104.789
Z38	1162829	92.613

Study ID	Database ID	Gold PLP Fitness
Z39	998343	100.730
Z40	998405	104.544
Z41	998304	96.397
Z42	710393	92.541
Z43	723896	91.386
Z44	670566	94.639
Z45	723995	97.833
Z46	34782204	98.321
Z47	1162829	91.613
Z48	6154177	97.060
Z49	710201	95.970
Z50	986282	94.573
Z51	8432754	91.207
Z52	8432754	92.467
Z53	8432745	91.112
Z54	8432748	91.670
